Genetic and functional analysis of the Rcs phosphorelay in the Enterobacteriaceae

Huang, Ya-hui

Award date:
2006

Awarding institution:
University of Bath

Genetic and Functional Analysis of the Rcs Phosphorelay in the *Enterobacteriaceae*

Submitted by

Ya-hui Huang

For the degree of PhD of the University of BATH

2006

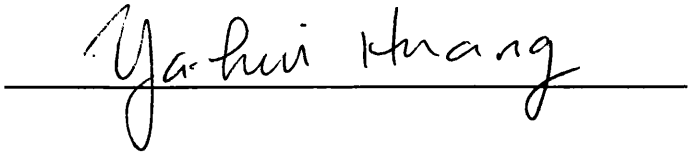

ProQuest LLC
789 East Eisenhower Parkway
P.O. Box 1346
Ann Arbor, MI 48106-1346

Acknowledgements

I would like to thank my supervisor Dr. David Clarke for providing me with the opportunity, guidance, and patience throughout the lab work and write-up.

I would like to give my thanks to Dr. Lionel Ferrières for his encouragement and advice. Thanks to Rob Watson, and all the members of "Team Clarke" (Susie, Jane, Helen, Hilton, and Catherine) for their help and discussions in the lab. I am also grateful to all my friends in Bath for being my surrogate family during the years of stay. I would particularly like to thank Paul for his love and support, especially during the write-up period.

I also thank my parents for their constant love and support over the years. I would like to acknowledge the Ministry of Education of Taiwan for the studentship, without which this study would not have been possible.

Abstract

The Rcs phosphorelay controls a variety of important cellular processes and has been implicated in virulence and biofilm formation. The phosphorelay involves two membrane-associated proteins, RcsC and RcsD, a soluble response regulator, RcsB and other proteins that modulate the output of the signalling pathway. The aim of this study was to determine the interactions between different components in the Rcs phosphorelay and investigate the role of the phosphorelay in the *Enterobacteriaceae*. Initially a comparative approach was undertaken and by comparing the sequences and functions of *rcs* homologues in different *Enterobacteriaceae*, the conserved nature of this phosphorelay was revealed. However, certain species-specific characteristics were also observed. The role of the Rcs phosphorelay in biofilm formation was of most interest because of the implications for industry and medicine. Genetic manipulations such as domain swapping, deletion and mutagenesis were used to identify regions and residues that are important in normal RcsC function. In this way, the input domain of RcsC in *E. coli* was identified to be important in biofilm formation. Two domains involved in independent signal perception were identified within the input domain. In addition, a novel domain with a potential role in biofilm formation, called the Q domain, was identified in this study. The role of the Rcs phosphorelay in *Photorhabdus* strains was investigated by constructing gene knockout mutants. The biofilm formation process of *Photorhabdus* strains was monitored using the flowcell chamber system, revealing a role for the Rcs phosphorelay at the early stages of biofilm formation. The findings of this study provide insight into the signal transduction mechanisms mediated by the RcsC protein and the understanding of the biological role of the Rcs phosphorelay in bacteria.

Abbreviations

°C	Degree Celcius
2CP	Two component pathway
Amp	Ampicillin
c-di-GMP	Cyclic-diguanylic acid
CA	Catalytic and ATP binding domain
CFU	Colony forming unit
CLSM	Confocal laser scanning microscope
Cm	Chloramphenicol
CTAB	Cetyl trimethyl ammonium bromide
D1	Receiver domain
dH_2O	Distilled water
DHp	Dimerization and histidine containing domain
DNA	Deoxyribosenucleic acid
dNTP	Deoxynucleotide 5'-triphosphate
EPS	Extracellular polysaccharides
FAD	Flavin adenine dinucleotide
Fig.	Figure
g	Gram
GFP	Green fluorescent protein
h	Hour
H1	Trasmitter domain
HK	Histidine kinase
HPt	Histidine-containing phosphotransfer domain
IJ	Infective juvenile
Kan	Kanamycin
LB	Luria-Bertani medium
LPS	Lipopolysaccharide
M	Molar
MCP	Methylated chemotaxis protein
MDO	membrane-derived oligosaccharides
mg	Milligram
mL	Millilitre
mM	Millimolar

mm	Millimetre
OD	Optical density
ONPG	*o*-nitro-phenyl-β-D-galactoside
PAGE	Polyacrylamide gel electrophoresis
PAS	Per-Arnt-Sim
PBS	Phosphate buffered saline
PCR	Polymerase chain reaction
PG	Peptidoglycan
pH	$-\log_{10}[H^+]$
PP	Polypropylene
PVC	Polyvinyl chloride
QS	Quorum sensing
Rif	Rifampicin
RLU	Relative luminescence unit
SDS	Sodium dodecyl sulphate
Tet	Tetracycline
TM	Transmembrane domain
TTSS	type III secretion system
U	Unit
Un-P	Undecaprenyl phosphate
Un-PP	Undecaprenyl pyrophosphate

Contents

Chapter 1
Introduction

1.1 Two-component pathway

1.1.1 Two-component pathway

Two-component pathways (2CPs) are signalling systems with a wide distribution in prokaryotes. Using these sophisticated signalling systems, bacteria are able to sense and respond to changes in the environment. The prototypical pathway is composed of two signal transducers, the sensor histidine kinase (HK) and the response regulator (RR). The transducer proteins are characterised by two conserved domains, the transmitter domain (H1), normally found in the HK, and the receiver domain (D1), normally found in the RR. These domains contain well-conserved amino acid residues, histidine and aspartate, respectively, that are essential for the function of the 2CP. HKs are known to function as a dimer, and in response to a stimulus, the conserved His residue in the H1 domain of the HK is phoshorylated via a *trans*-autophosphorylation mechanism whereby one HK monomer phosphorylates the His residue of the second monomer within the HK dimer. The phosophoryl group is then transferred from the H1 domain to the conserved Asp in the D1 domain of the RR. The phosphorelay between His and Asp residues is the basis of all two-component pathways (Robinson *et al.*, 2000; Stock *et al.*, 2000) (Fig. 1.1).

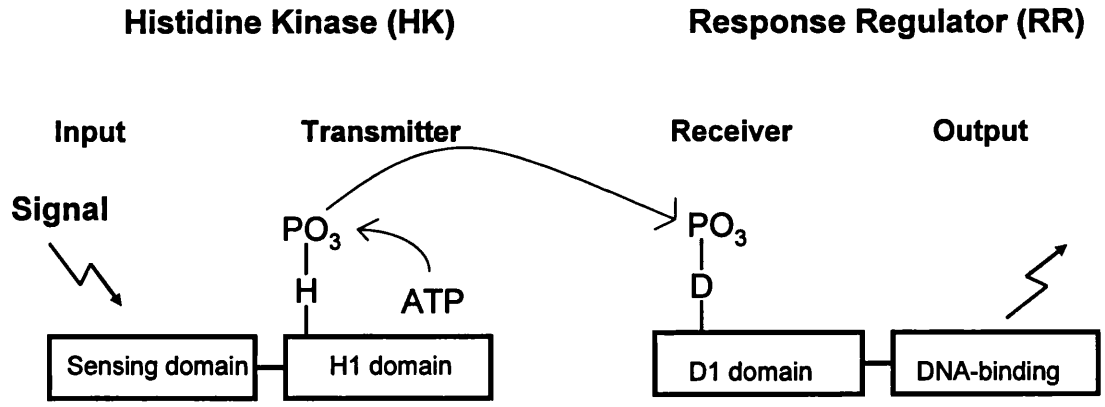

Figure 1.1. Schematic presentation of prototypical two-component signal transduction. The prototypical pathway is composed of two signal transducers, the sensor histidine kinase (HK) and the response regulator (RR). The HK contains conserved domain transmitter domain (H1), and the RR contains the receiver domain (D1). These domains contain well-conserved amino acid residues, histidine and

aspartate, respectively. In response to a stimulus, the conserved His (H) residue in the H1 domain of the HK is phosphorylated. The phosphoryl group is then transferred from the H1 domain to the conserved Asp (D) in the D1 domain of the RR. The phosphorelay between His and Asp residues is the basis of all two-component pathways

Two-component pathways enable bacteria to respond to the changing environment and often these pathways play key roles in controlling complex bacterial behaviours, such as chemotaxis, sporulation, differentiation, virulence or metabolism (Piggot and Hilbert, 2004; Szurmant and Ordal, 2004). 2CPs are widely distributed in Archaea and Bacteria and the availability of complete genome sequences has allowed the definitive assessment of their prevalence in prokaryotes. The number of two-component pathways varies among different species, for example, 2CPs are absent from the genomes of mycoplasma and *Buchnera* sp., while *Streptomyces* is predicted to have more than 85 HKs (Bentley *et al.*, 2002; Sebaihia *et al.*, 2002). In silico analysis also reveals a correlation between the complexity of a prokaryotic lifestyle and the average number of genes encoding potential RR present in a genome. Pathogens and enteric bacteria live in more constant environments while the environment of the soil is more variable and it is expected that more control of gene expression will be required in the complex lifestyle of bacteria. Therefore, pathogens and enteric bacteria have a lower average number of RRs, while plant pathogens and soil bacteria have more RRs (Ashby, 2004) (Table1.1).

The soil-dwelling, filamentous bacteria, *Streptomyces coelicolor* has the largest number of genes so far discovered in a bacterium, and has an unprecedented number of genes predicted to encode 2CPs i.e. 85 HKs and 79 RRs. Pseudomonads are also found in a variety of environmental niches, ranging from soil and water to plants and animals, and genomic analysis has revealed that the complete genome of *Pseudomonas aeruginosa* is predicted to have 63 HKs and 64 RRs (Rodrigue *et al.*, 2000). Therefore, there does appear to be a clear correlation between the number of genes encoding 2CPs and the complexity of the life-cycle of a particular prokaryote.

Habitat/lifestyle	Average number of RRs
Pathogen	16.5
Enteric	20.0
Plant pathogen	54.0
Aqueous	43.9
Soil	48.1
Complex	51.6

Table 1.1 The average number of potential response regulator genes sorted by hatitat/life style (Ashby, 2004).

1.1.2 The histidine kinase

Generally, when activated by environmental signals, the HK undergoes ATP-dependent auto-phosphorylation on the conserved His residue. The γ-phosphoryl group in ATP is transferred to the N3 position of the imidazole ring in the His side chain. The high-energy phosphoramidate N~P bond is ideally suited for phosphoryl transfer and participates in signal transduction and other physiological functions. For example, the phospho-His occurs as a phosphoenzyme intermediate in succinyl-CoA synthetase, pyruvate phosphate dikinase and nucleoside diphosphate kinase, and it is also used in the sugar phosphotransfer system. The phosphoramidate bond is chemically different to the phosphoesters created by Ser/Thr/Tyr protein kinases although catalytically HKs and proteins kinases are similar (Stock *et al.*, 2000).

All HKs are identified by unique signature sequences, called H, N, G1, F and G2 boxes, found within the transmitter domain. Furthermore, based on the arrangement of these sequences within the transmitter domain, HKs can be grouped into two classes, Class I and Class II (Dutta *et al.*, 1999) (Fig. 1.2). In class I HKs, the H box-containing region is contiguous with the other four conserved boxes. For example, EnvZ is a well-studied, orthodox class I HK with typical domain architecture. In class II HKs the H box-containing region is not contiguous with the CA domain and can be separated from the CA domain by other structural domains. To date, the chemotaxis HK, CheA, is the only representative of the class II category (Mizuno, 1997).

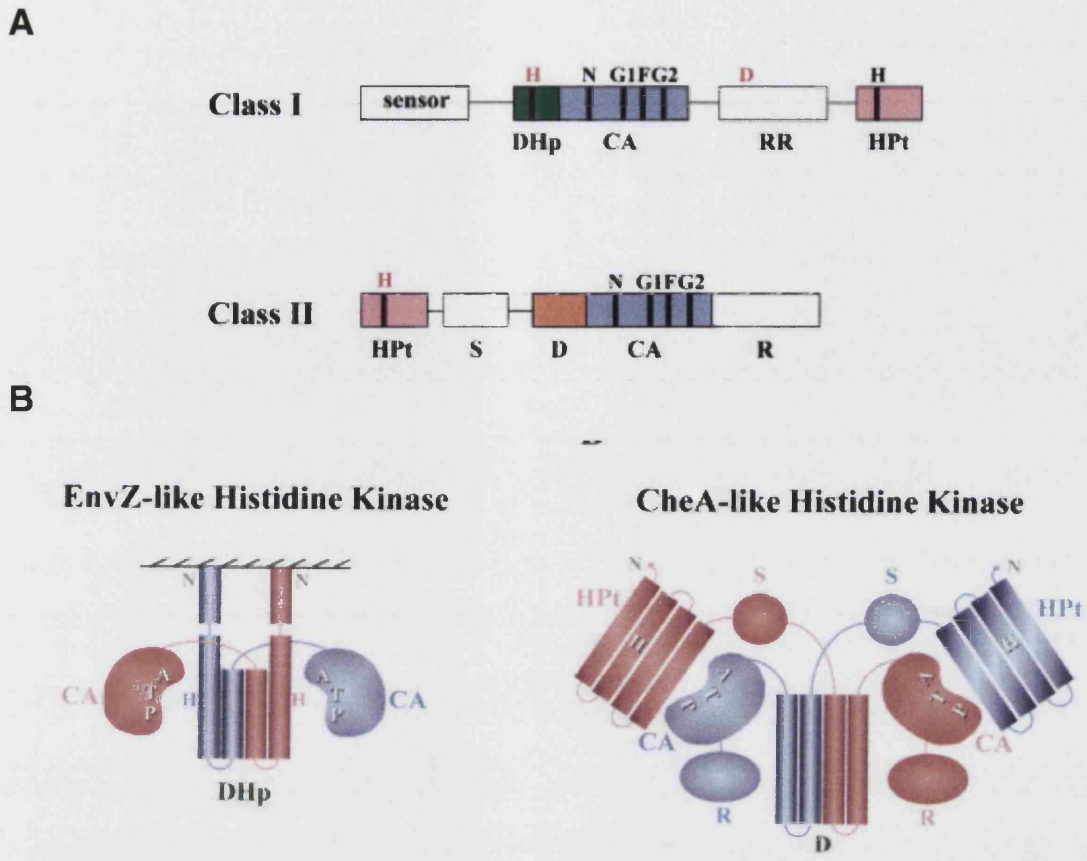

Figure1.2. (A) Domain organisation of Class I and Class II histidine kinases. Based on the position of the conserved histidine-containing region and conserved signature sequences (N, G1, F, G2 boxes), HKs can be grouped into two classes, Class I and Class II HKs. In class I HKs, the H box-containing region is contiguous with the other four conserved boxes and the H residue in DHp domain is the primary phosphorylation site. The phosphoryl group is then transferred to the conserved Asp residue (D) in response regulator domain (RR). In a hybrid HK, the RR is found in the HK, thus phosphoryl group is then sequentially transferred to the H box of a HPt domain. In Class II HKs, the conserved His residue is in the HPt domain. CA, catalytic and ATP binding domain, D, dimerization domain, DHp, dimerization and histidine containing domain; S, substrate-binding domain; R, regulatory domain (Dutta *et al.*, 1999).

(B) Models of domain organisation of class I (EnvZ-like) and class II (CheA-like) histidine kinases. The monomers in each dimer are represented as different colours (pink and blue) In the EnvZ-like HK, only the cytoplasmic catalytic region is shown. Shaded line denote the cytoplasmic membrane. The DHp domain of class I histidine kinase forms the dimerization core. In a HK dimer, the DHp form a four-helix bundle. It is also the trans-autophosphorylation site. The catalytic domain functions as a phosphodonor and contains an ATP-binding pocket. In class II histidine kinase, trans-autophosphorylation of occurs on the HPt domain and dimerization is through a separate dimerization domain. CA, catalytic and ATP binding domain, D, dimerization domain, DHp, dimerization and histidine containing domain. (Pictures taken from Dutta *et al.*, 1999)

1.1.3 Domains associated with 2CPs

Deletion analysis suggests that the transmitter (H1) domain of EnvZ contains at least two separate sub-domains, a dimerization domain and a catalytic domain (Fig. 1.3). The structure of both domains of EnvZ had been determined by NMR (Park *et al.*, 1998; Tanaka *et al.*, 1998; Tomomori *et al.*, 1999). The catalytic domain functions as a phosphodonor and contains an ATP-binding pocket located in a series of flexible loops (Fig. 1.3). This domain is also called the catalytic and ATP binding (CA) domain and encompasses the N, G1, F and G2 boxes mentioned above. The dimerization domain contains the H box and is also known as the dimerization and histidine containing (DHp) domain.

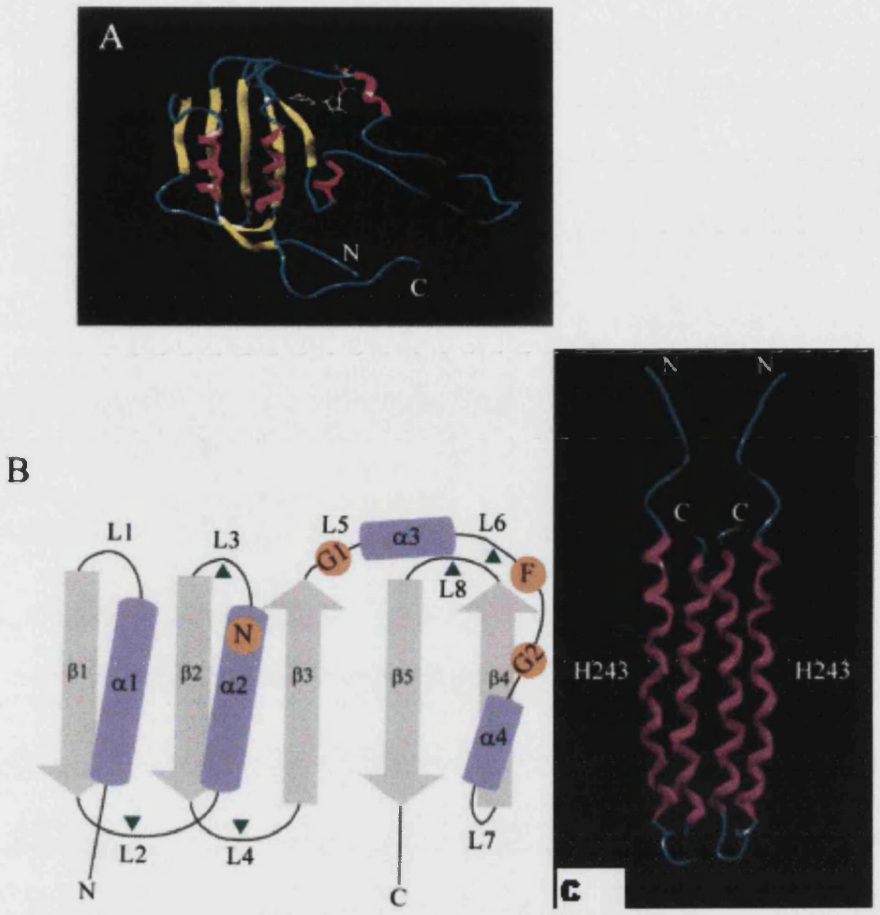

Figure 1.3. The structure of a typical Class I HK, EnvZ. (A) The CA domain of EnvZ, The catalytic domain functions as a phosphodonor and contains an ATP-binding pocket located in a series of flexible loops. (B) The schematic presentation of CA domain of EnvZ. (C) The dimeric DHp domains of EnvZ. The DHp domain of EnvZ, the DHp domain of EnvZ forms the dimerization core and consists of two helices where conserved His phosphorylation site on helix I. In the dimer, the four helices are parallel to each other, form a four-helix bundle. (Pictures taken from Dutta *et al.*, 1999)

Chemotaxis is one of the best understood signal transduction systems, although it is also considered as atypical. The CheA HK has no transmembrane domain but associates with membrane-spanning chemoreceptors, called methylated chemotaxis proteins (MCPs) (Fig.1.4). The conserved His residue is in the H box of the HPt domain in CheA (Fig. 1.2). CheA can be divided into five domains, P1-P5, and the phosphorylation site is in the P1 domain. The P4 domain is

where ATP binds and catalysis occurs. The P3 domain is the dimerization domain and the P2 domain is where CheY and CheB interact with CheA to receive phosphoryl groups (Baker *et al.*, 2006). *E. coli* has five MCPs that share highly conserved signaling and methylation domains: Tsr (serine chemoreceptor), Tar (aspartate and maltose chemoreceptor), Trg (ribose and galactose chemoreceptor), Tap (dipeptide chemoreceptor) and Aer (receptor for oxygen and redox taxis). The MCPs are composed of highly variable periplasmic sensing domains that interact with ligands in the environment, and conserved cytoplasimc domains that provide a scaffold for CheW and CheA binding. Ligand binding induces conformational changes in the MCPs and these changes modulate CheA activity. In *E. coli*, ligand binding inhibits the kinase activity of CheA, whereas in *B. subtilis*, ligand binding stimulates the CheA kinase activity (Baker *et al.*, 2006; Szurmant and Ordal, 2004).

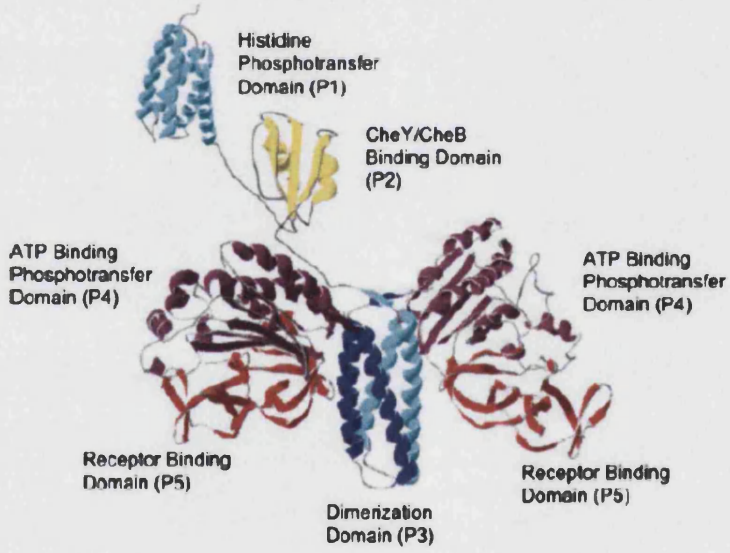

Figure 1.4. A molecular model of the chemotaxis kinase CheA. The five domains associated with CheA are labelled P1 through P5. The structure and functions of each domains are depicted within a CheA dimer (Picture taken from Baker *et al.*, 2006)

1.1.4 The input domain of HKs

The signal sensing or input domains of HKs are diverse in sequence and this possibly reflects the employment of different sensing mechanisms. Typically, HKs function as periplasmic membrane receptors, and therefore transverse the cytoplasmic cell membrane. In addition to ligand binding, transmembrane signalling will also require the transduction of the signal to the cytoplasmic signalling domains and it is likely that the transmembrane (TM) helices will be involved in this signal transduction. In principle, signal transduction could be achieved by conformational changes within the HK dimer resulting from TM helix sliding, tilting or rotation or altered helix dynamics. Although some cytoplasmic region of HKs have shown to be enough for normal signalling function, membrane anchoring may also be required to keep the sensor protein close to the signal (Chang and Winans, 1992).

Given their localisation, it is likely that the periplasmic domain of the HK is an important signal-sensing region for extracellular signals. The PhoPQ 2CP is important in the regulation of virulence in many bacteria, such as controlling the intramacrophage type three secretion system (TTSS) of *Salmonella* (Bijlsma and Groisman, 2005). It has been shown that the PhoQ HK contains a periplasmic domain of 146 amino acid residues that binds Mg^{2+} *in vitro* and is required for Mg^{2+}-mediated repression of gene expression *in vivo* (Chamnongpol *et al.*, 2003; Regelmann *et al.*, 2002). A single residue substitution in the periplasmic domain of PhoQ altered the response of the HK to Mg^{2+}, suggesting that this residue contributes to a conformational switch between signalling states (Sanowar *et al.*, 2003). CitA is a citrate receptor that is required for induction of citrate fermentation in *Klebsiella pneumoniae*. The periplasmic domain of this protein binds citrate and this results in the activation of the CitA/CitB system (Kaspar *et al.*, 1999). The structure of the periplasmic domain of CitA has been solved and this revealed as a PAS fold (Pappalardo *et al.*, 2003; Reinelt *et al.*, 2003). The structure and function of PAS domain will be discussed in a later section.

The well-studied *E. coli* EnvZ HK is a membrane-spanning osmosensor that has two TM domains, however, the EnvZ of *Xenorhabdus* does not have a

periplasmic domain, but does respond to change in osmolarity in *E.coli* (Tabatabai and Forst, 1995). In addition, it has been shown that replacement of the periplasmic domain (Met56 to Val147) of EnvZ with the PhoR periplasmic domain did not affect its ablity to sense osmolarity signals in *E. coli* (Leonardo and Forst, 1996). This suggests that the periplasmic domain of EnvZ is not involved in sensing osmolarity. Despite this, mutations in a conserved region within the periplasmic domain (Pro41 to Glu53) called I box, did impair osmosensing, suggesting that the I box and, therefore, the periplamic domain is involved in the signal transduction mechanism of EnvZ (Waukau and Forst, 1999).

Some HKs have multiple TM domains, e.g. KdpD has four TM domains (Fig. 1.5). In *E. coli* KdpD regulates the expression of a high-affinity K^+ transport system. However, a KdpD protein lacking all four transmembrane domains was still able to sense low K^+ concentrations (Heermann *et al.*, 2003). Therefore the transmembrane domains of KdpD are not essential for sensing K^+ limitation and KdpD might consist of a cytoplasmic sensing domain. It has been shown that substitution of a group of clustered arginine residues adjacent to TM4 affects the activity of KdpD (Jung and Altendorf, 1998). Moreover, the ArcB kinase of the Arc (anoxic redox control) system has a very short periplasmic sequence. The transmembrane domain of ArcB does not participate in signalling but only serves as an anchor that keeps the protein close to the source of signal. ArcB responds to O_2 levels by sensing the redox state through a cytoplasmic PAS domain (Kwon *et al.*, 2000).

HKs can therefore sense multiple signals through different domains suggesting that signal processing can occur in parallel e.g. the extracytoplasmic domain senses a signal, and the cytoplasmic region receives another signal. This has been shown to occur with the VirA-VirG two-component system of *Agrobacterium tumefaciens*. This 2CP responds to host signals and regulates expression of the *vir* regulon encoding the proteins that stimulte crown gall formation in plants. The periplasmic domain of the VirA HK detects sugars while the linker region detects phenolic compounds and pH. These signals also appear to act synergistically (Chang and Winans, 1992).

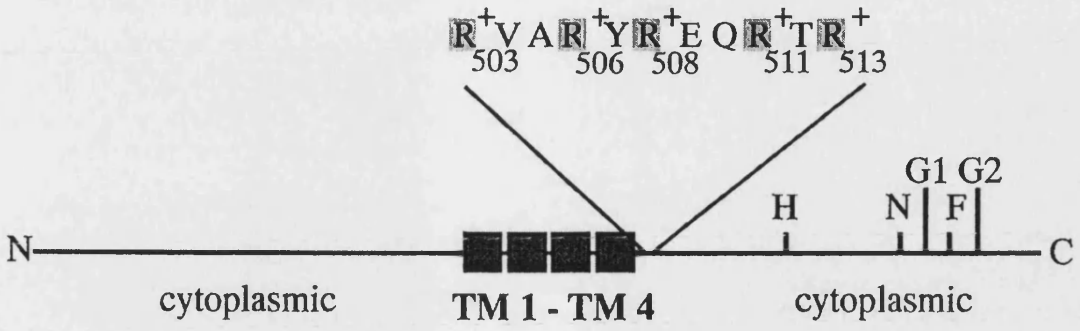

Figure 1.5.Schematic representation of tugor senosr KdpD. The KdpD protein consists of a long N-terminal cyoplasmic region, followed by four transmembrane domains (TM1- TM4). A cluster of charged residues are adjacent to TM4. The conserved H residue and kinase domains lie in the C-terminal cytoplasmic region (Image taken from Jung & Altendorf, 1998).

1.1.5 The PAS domain

The PAS (Per-Arnt-Sim) domains are known to be important in signal sensing and have been identified in both prokaryotic and eukaryotic proteins. PAS domains have low similarity at the primary amino acid sequence level and, thus, based upon structural predictions, the PAS domain was redefined as the PAS fold. The PAS fold represents an important sensory domain present in all kingdoms of life, some proteins appear to have more than one PAS fold, and multiple PAS folds are possibly used to integrate different environment signals (Hefti *et al.*, 2004).

The PAS fold is typically a cytoplasmic sensing domain and it has been shown to be involved in monitoring changes in light, redox potential, oxygen and small ligands (Taylor and Zhulin, 1999). Many HKs have been predicted to contain PAS folds and the best-studied is perhaps FixL, which is required for nitrogen fixation in response to oxygen limitation. The oxygen-detecting domain of FixL is a heme-binding region that contains a PAS structural motif. The binding of oxygen or other ligands to heme inhibits the kinase activity of FixL. The 3D

structure of the FixL heme binding domain has been determined by crystallography (Gong *et al.*, 1998). The dominant structural feature of the PAS domain is a five-stranded anti-parallel β barrel which is connected to a helical motif by loops (Fig. 1.6A). The secondary structure elements can be lablled as Aβ, Bβ, Cα, Dα, Eα, Fα, Gβ, Hβ and Iβ as in Fig. 1.6A. The flexible loop between Fα and Gβ, namely the FG loop, plays an important role in signal propagation by converting local conformational changes into subunit interaction.

In addition to the structure of FixL, the periplasmic PAS fold of CitA of *Klebsiella pneumoniae* and the fumarate sensor DcuS of *E. coli* have also been solved by NMR (Pappalardo *et al.*, 2003; Reinelt *et al.*, 2003). The secondary structure elements are clearly conserved among the members of PAS superfamily (Fig. 1.6B).

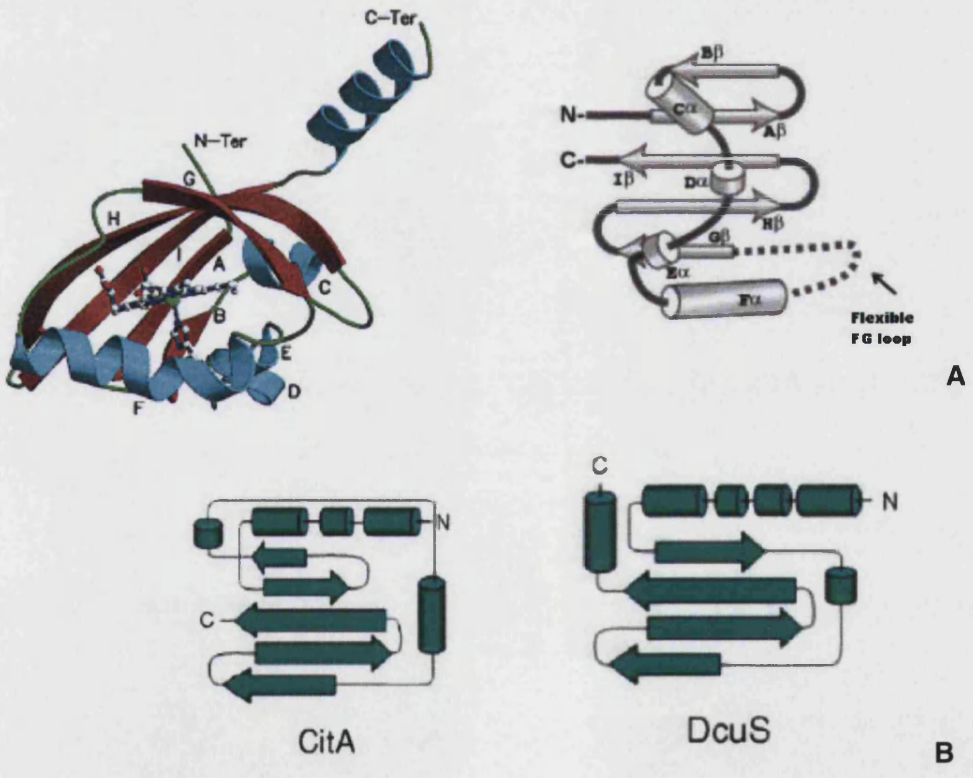

Figure 1.6. Representative secondary and ribbon diagrams of sensor PAS fold. (A) Ribbons diagram of FixL. The secondary structure elements are color-coded with α-helices as blue, β-sheets as red, and random coils as green. The heme cofactor is shown as ball-and-stick

model. (Images taken from Gong, 1998) (B) Schematic representation of the secondary structure of CitA and DcuS (Images taken from Khorchid & Ikura, 2006).

1.1.6 The linker HAMP domain

In transmembrane HKs, the input/sensing domain and the cytoplasmic signalling domain are connected by a linker region that plays an important role in signal propagation. The linker region can either serve as a structural joint that regulates the kinase/phosphatase activity of the HK by modulating the conformation of the signaling domains, or the linker region may actively contribute to signal sensing. Although the linker regions of different HKs share low primary sequence homology, many have been shown to have a similar helix-turn-helix fold based on secondary structure prediction. This kind of structure is called a HAMP domain (histidine kinases, adenylyl cyclases, methyl-accepting chemotaxis proteins, and phosphatases) or P-linker (Periplasmic signal transducing) (Aravind and Ponting, 1999; Whitfield and Roberts, 1999). This membrane-adjacent and conserved signal transduction domain has been shown to be important for normal signal transduction (Park and Inouye, 1997).

Despite the low homology of the primary amino acid sequence, the secondary structures of HAMP linkers are predicted to show similar topology (Williams and Stewart, 1999). The HAMP domain is represented by a conserved helix-turn-helix motif spanning approximately 50 amino acids. The two helices in the HAMP domain can be modeled as amphipathic helices (AS-I and AS-II). The exact mechanism of signal propagation via the HAMP domain remains unknown and two models have been postulated. In the first model, the two helices of the HAMP domain are coupled with the helical DHp domain of HKs and together they form a four-helix bundle. The intramolecular association between the HAMP and DHp domains would prevent spontaneous signaling in the absence of signals (Aravind and Ponting, 1999). The second model is the helix interaction model which hypothesizes that the AS-I lies parallel to the cytoplasmic membrane and embeds its hydrophobic surface within the membrane surface and the movement of the helices modulates the subsequent enzymatic activities. Upon stimulation, the movement of TM2 causes the reorientation of ASI and

ASII and ASII moves toward ASI resulting in conformational changes within the protein (Fig. 1.7) (Williams and Stewart, 1999). Both models propose that activating signals alter the conformation of HKs and release the catalytic domain from the HAMP domain for signaling. The HAMP domain structure was recently resolved by NMR, and it was shown that the dimeric HAMP domains form a parallel, four-helical coiled coil, with unusual interhelical packing. The rotation of helices causes conversion between two packing forms, and the rotary mechanism could account for the role of HAMP domains in signalling (Hulko *et al.*, 2006).

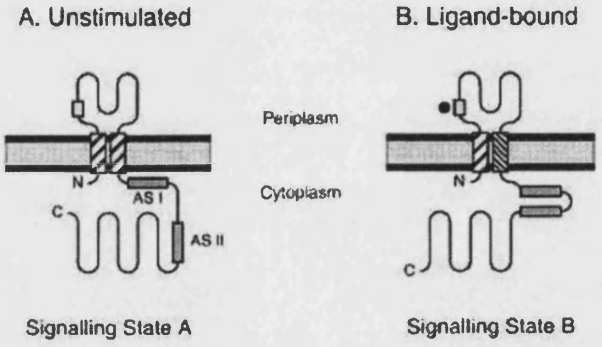

Figure1.7. The HAMP two helical model. The HAMP domain is represented by a conserved helix-turn-helix motif spanning approximately 50 amino acids. The two helices in the HAMP domain can be modeled as amphipathic helices (AS-I and AS-II). It is hypothesized that the AS-I lies parallel to the cytoplasmic membrane and embeds its hydrophobic surface within the membrane surface and the movement of the helices modulates the subsequent enzymatic activities. Upon stimulation, the movement of TM2 causes the reorientation of ASI and ASII and ASII moves toward ASI resulting in conformational changes within the protein. (Images taken from Williams & Stewart, 1999)

Therefore the linker region modulates the signal output by changing the conformation of the HKs and a key role for HAMP linkers in signal transduction has been supported by genetic evidence. Most HAMP mutants bias receptor signalling towards the stimulated signalling status (Zhu and Inouye, 2003).

However mutations in the linker region of BarA result in a dominant-negative phenotype i.e., impaired kinase activity and a net dephosphorylating activity (Tomenius *et al.*, 2005).

1.1.7 The multiple-step phosphorelay

Some two-component pathways contain more than a single transmitter and receiver domain resulting in a more complex phosphorelay. In a multiple-step phosphorelay, a single transmitter domain (H1, located on the HK) and several receiver domains (D1, D2 etc) are generally connected by a phosphoryl-carrying domain called the histidine-containing phosphotransfer domain or HPt domain. There is considerable diversity in the modular architecture of proteins involved in multi-step phosphorelays. For instance, H1, D1 and the HPt domain, can all be in a single protein, as the BvgS sensor in the BvgS-BvgA system (Bock and Gross, 2002), or the HPt domain can also be located in a separate protein as in the sporulation cascade in *Bacillus* (Zhang and Shi, 2005) (Fig. 1.8).

Sensor kinases that contain more than one signalling domain are called hybrid kinases and a recent survey revealed that more than one third of the 156 complete prokaryotic genomes possessed hybrid-type HKs (Zhang and Shi, 2005). However, not every domain of hybrid kinases is directly involved in the multi-step phosphorelay. The receiver domain of VirA of *Agrobacterium tumefaciens* can be deleted without loss of function, but the deletion causes a kinase-constitutive phenotype i.e., high basal activity in the absence of phenolic signals. Therefore, the receiver domain is not directly involved in the phosphotransfer between VirA and VirB but rather this receiver domain serves as a negative regulator of VirA kinase activity (Chang *et al.*, 1996).

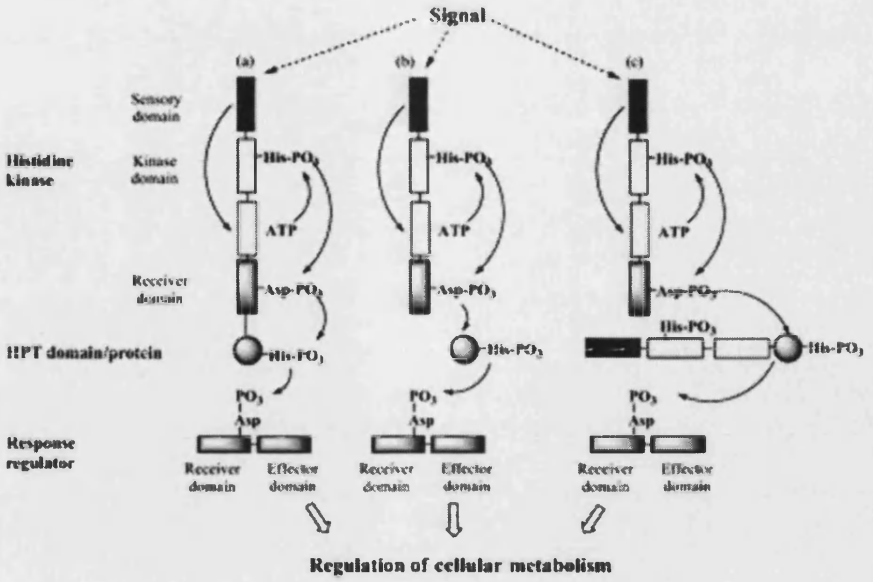

Figure 1.8. Schemes of multi-step phosphorelay signal transduction. In a multiple-step phosphorelay, a single kinase domain (shown as white rectangle boxes) and several receiver domains (shown as grey rectangle boxes) that are generally connected by a phosphoryl-carrying domain called the histidine-containing phosphotransfer domain (HPt) (shown as grey circles). There is considerable diversity in the modular architecture of proteins involved in multi-step phosphorelays. (a) H1, D1 and the HPt domain, can all be in a single protein, as the BvgS sensor in the BvgS-BvgA system. (b) Some hybrid kinase containing RR but lack HPt domain, and HPt domain resides in a separate protein. (C) The HPt domain can be located in another protein as in the case of Rcs phosphorelay of *E. coli*. (Image taken from Zhang and Shi, 2005)

The architecture of the phosphorelay cascade extends the fundamental His-Asp sequence into a four-step reaction. The complex multi-step phosphorelay of signal transduction will therefore allow different inputs to be integrated into a signaling pathway. The HPt domains are the convergent point of different signals. The HPt domains do not exhibit kinase or phosphotase activity, and act as specific cross-communication modules between different proteins. In a domain swapping analysis between BvgS and EvgS, the HPt domains define the

system specificity and mediate discrimination between heterologous two-component systems (Perraud *et al.*, 1998)

1.1.8 The sporulation in *Bacillus subtilis*

The regulation of sporulation in *Bacillus subtilis* is a well studied example of multi-step phosphorelay. The domains involved in this phosphorelay are found in four separate proteins. The initiation of sporulation is mainly controlled by the activity of KinA, although multiple HKs are involved in the regulation including KinB, KinC, KindD and KinE. KinA consists of three PAS domains at the N-terminal end and these domains are implicated in dimerizaion and ligand sensing. Upon autophosphorylation of the HKs, the phosphoryl group is transferred to Spo0F (D1), Spo0B (HPt) and finally the response regulator, Spo0A (D2) (Figure 1.9) (Stephenson and Hoch, 2002). Spo0A is the key transcriptional regulator of sporulation and has been shown to regulate the transcription of 121 genes. Phosphorylated Spo0A represses two thirds of the genes, and activates the expression of the remaining one-third. Many Spo0A regulon genes respond to Spo0A in a dose-dependent manner, and can be divided into four categories according to the threshold level of Spo0A~P and whether gene expression is activated or repressed (Fujita *et al.*, 2005). For example low levels of Spo0A~P represses the expression of some genes and the expression of sporulation genes requires higher levels of Spo0A~P, and in some cases, oligomerization of Spo0A~P (Piggot and Hilbert, 2004). Several independent phosphatases are also involved in the regulation of the level of Spo0A phosphorylation at different stages, providing the cell with the ability to fine tune the output of the phosphorelay (Fujita *et al.*, 2005) (Fig. 1.9).

1.1.9 The response regulator

Most response regulators (RRs) in prokaryotic systems are the terminal components of the 2CPs, functioning as phosphorlation-activated switches to affect the adaptive response. RRs often consist of two domains: a conserved N-terminal regulatory domain and a variable C-terminal output domain. The regulatory domain, containing the conserved receiver (D1) domain with the phosphoryl-accepting aspartate residue, is conserved in all RRs. The majority of experimentally characterized RRs act as transcription factors and, therefore,

have DNA-binding helix-turn-helix (HTH) output domains (Mizuno, 1997). Some RRs have enzymatic activity or interact with other proteins, for example the chemotaxis RR CheY interacts with the motility apparatus (Szurmant and Ordal, 2004).

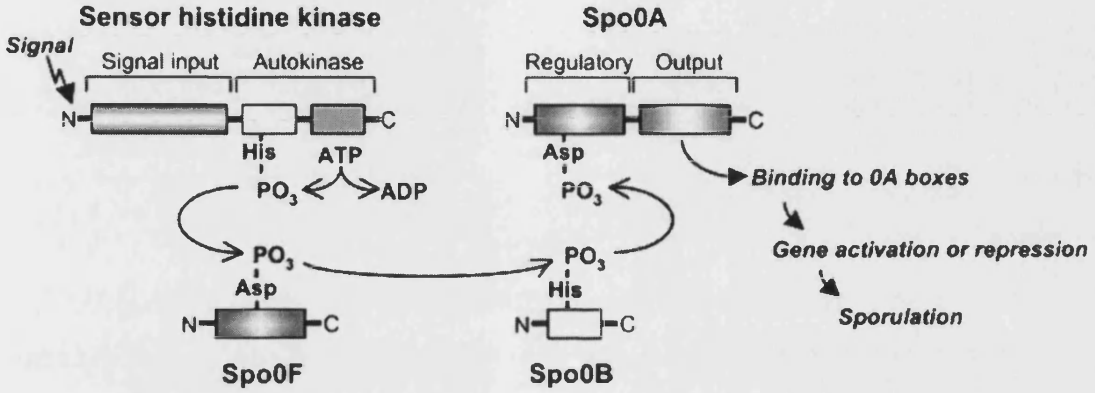

Figure 1.9. The *B. subtilis* sporulation phosphorelay. The domains associated with the sporulation phosphorelay are located in separate proteins. The initiation of sporulation is mainly controlled by the activity of multiple HKs, including KinA, KinB, KinC, KindD and KinE. The N-terminal of HK and these domains are implicated in dimerizaion and ligand sensing. Upon autophosphorylation of the HKs, the phosphoryl group is transferred to the Asp residue of Spo0F, then to the His residue of Spo0B, and finally to the RR, Spo0A (D2) (Image taken from Stephenson & Hoch, 2002).

Phosphorylation-induced dimerization is thought to play an important role in the DNA-binding ability of the RRs, dramatically improving their affinity for binding to their cognate DNA sequence. Dimerization may also have a relief-of-inhibition mechanism and promote enzymatic activity, such as the di-guanylate cyclase activity in the GGDEF domain (Galperin, 2006).

In some cases, the RR can be phoshorylated independently of its cognate HK, for example by cross-talk by non-cognate HKs or through the action of small

high energy phosphodonor molecules such as acetyl phosphate (Shin and Park, 1995). There are numerous documented examples of RRs being phosphorylated by acetylphosphate *in vitro*, including OmpR, PhoB, PhoR and UvrY (Tomenius *et al.*, 2005). However, *in vivo*, the evidence of direct phosphorylation is less certain, and most reports suggest that acetyl phosphate can influence RR activity only in strains that lack the cognate HK (Wolfe, 2005).

1.2 The Rcs phosphorelay in *Escherichia coli*

1.2.1 The Rcs phosphorelay

The Rcs phosphorelay in *E. coli* was originally described as a regulator of capsule synthesis. It controls the expression of the *cps* operon, encoding the proteins required for the production of the capsular polysaccharide, colanic acid (Gottesman *et al.*, 1985). The Rcs phosphorelay is more complex than a typical 2CP, as it is a multiple-component phosphorelay involving four signaling domains. The phosphorelay is unique in *E. coli* as the four signaling domains are situated in three separate proteins. The sensor kinase of this phosphorelay, RcsC, is a hybrid kinase, as the protein contains both a H1 and D1 domain (Stout and Gottesman, 1990). The conserved histidine and aspartate residues in these domains are involved in the phosphorelay (Clarke *et al.*, 2002). RcsB is the response regulator and contains a conserved receiver (D2) domain. In addition to the two main components, RcsC and RcsB, a third component, RcsD (previously called YojN), which contains a HPt domain, has been shown to be required in the phosphorelay (Takeda *et al.*, 2001). Therefore, when RcsC senses an environmental signal, it is activated by autophosphorylation of the histidine residue in the H1 domain followed by transfer of the phosphoryl group to the aspartate residue in the D1 domain. The phosphoryl group is then donated to the HPt domain of RcsD and finally to the D2 domain of RcsB. Once phosphorylated, phospho-RcsB is able to bind DNA and to regulate the transcription of its target genes (Huang *et al.*, 2006; Majdalani and Gottesman, 2005; Takeda *et al.*, 2001) (Fig. 1.10).

In addition to RcsC, RcsD and RcsB, there are several proteins involved in modulating the activity of the Rcs phosphorelay. In some cases, an auxiliary

protein, called RcsA, is involved in facilitating the binding of phospho-RcsB to DNA (Stout *et al.*, 1991). RcsA is a co-activator for *cps* expression, and it is a short-lived protein that is subject to degradation by the Lon and ClpYQ proteases (Kuo *et al.*, 2004; Stout *et al.*, 1991). The RcsA and RcsB proteins form a heterodimer that binds to a specific DNA sequence called the RcsAB box upstream from the *cps* operon and other RcsA-dependent genes (Wehland and Bernhard, 2000). However, RcsA is not required in all Rcs phosphorelay targets as the Rcs phosphorelay controls many genes in a RcsA-independent manner (Majdalani *et al.*, 2002; Mouslim *et al.*, 2003).

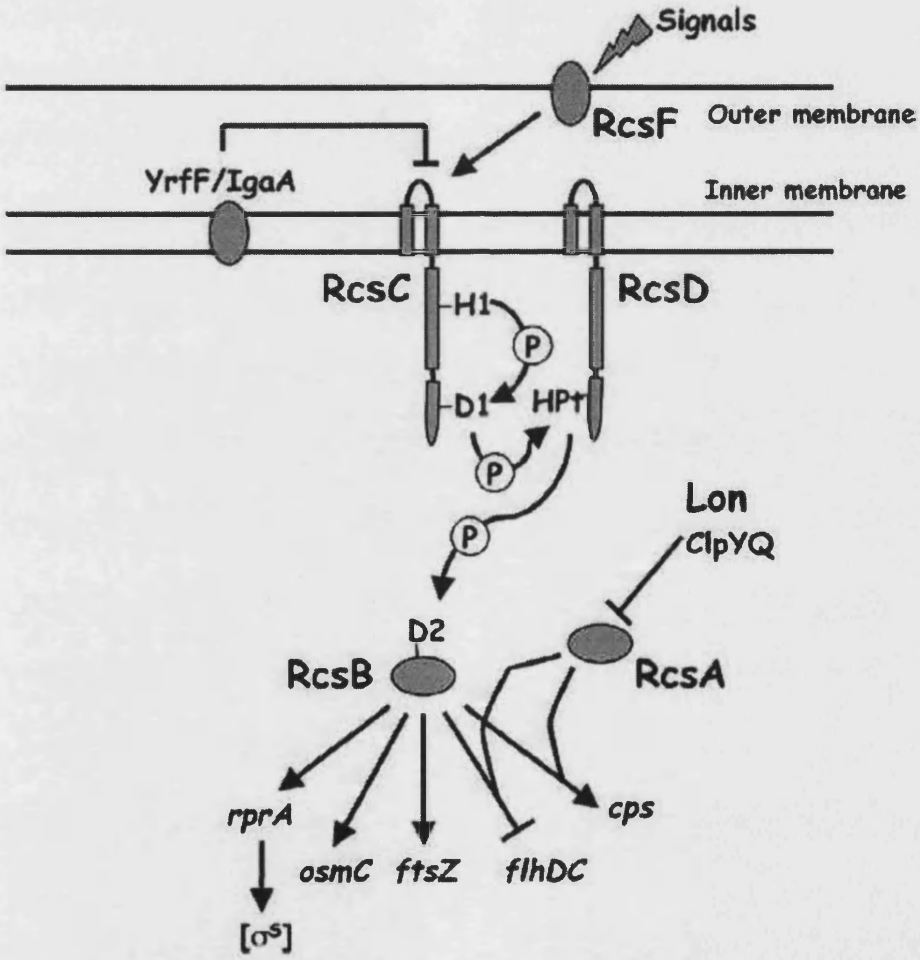

Figure 1.10. The communication model of the Rcs phosphorelay. The phosphorylation of RcsB involves a complex phosphorelay mediated by the RcsC and the RcsD proteins. The phosho-RcsB binds to DNA and regulates the expression of many genes (Huang *et al.*, 2006)

Another protein, called RcsF, is also involved in the Rcs-dependant expression induction of the *cps* operon. The protein was first identified as an activator of *cps* expression when expressed from a multiple-copy plasmid (Gervais and Drapeau, 1992). Although it was originally proposed that RcsF was capable of phosphorylating RcsB directly, the phosphorylation of RcsB by RcsF has not been demonstrated and seems unlikely considering recent results on RcsF localisation (Castanie-Cornet *et al.*, 2006). RcsF has now been shown to be a lipoprotein located in the outer membrane and therefore RcsF might be involved in sensing environment stimuli. Indeed in a recent epistasis study, it has been demonstrated that RcsF acts upstream of RcsC and it been shown that RcsF is required for the sensing of many of the signals that have previously been shown to activate the Rcs phosphorelay (Castanie-Cornet *et al.*, 2006; Majdalani and Gottesman, 2005)

Studies in *Salmonella enterica* serovar Typhimurium have shown that the Rcs phosphorelay is repressed by a membrane-localised protein called IgaA (the homologue in *E. coli* is called YrfF) and homologues of IgaA(YrfF) are found in all bacteria that have the Rcs phosphorelay. The Rcs phosphorelay can be activated by a mutation in *yrfF* in *E. coli* and *Salmonella*, suggesting IgaA/YrfF may also be part of the Rcs signaling network (Cano *et al.*, 2002; Dominguez-Bernal *et al.*, 2004; Tierrez and Garcia-del Portillo, 2004).

1.2.2 Rcs phosphorelay in other *Enterobacteriaceae*

Genes sharing homology with *rcsC, rcsB* and *rcsD* have been found in many *Enterobacteriaceae*, including *E. coli, Shigella flexneri, Salmonella enterica* serovar Typhi, *S. enterica* serovar Typhimurium, *Klebsiella pneumoniae, Photorhabdus luminescens, Proteus mirabilis, Yersinia* spp and *Erwinia* spp. Indeed the phosphorelay appears to be exclusive to the family *Enterobacteriaceae,* although the phosphorelay is not found in any of the enterobacterial endosymbiotic bacteria with reduced genome sizes, e.g. *Buchnera* spp., *Wigglesworthia* spp.

The genes encoding RcsC, RcsD and RcsB are located together and the gene arrangement within the *rcs* locus appears to be conserved. The *rcsB* and *rcsC* genes are adjacent to each other, but are transcribed in opposite directions. In addition, *rcsD* is upstream from *rcsB* and these two genes are transcribed in the same direction, suggesting they might be in the same operon. In *E. coli* the *ompC* gene, encoding the OmpC porin, is immediately upstream from the *rcs* locus and the occurrence of an *ompC*-like gene in the same position appears to be well conserved in other *Enterobacteriaceae*. In contrast, the genes downstream from the *rcs* locus appear to be variable. In *E. coli* K-12, the *atoSCDAEB* genes, which encode genes involved in the metabolism of acetoacetate, are immediately downstream of the *rcs* locus. The occurrence of the *ato* genes is conserved in uropathogenic *E.coli* (UPEC) and enteropathogenic *E. coli* (EPEC), but not enterohaemorrhagic *E. coli* (EHEC). The region downstream from the *rcs* locus in EHEC and *S. flexneri* are highly similar with a 98% DNA identity and this 9.4 kb of DNA is also conserved in in *E. coli* K-12, UPEC and EPEC, but located after the *ato* genes. Interestingly, in *S. enterica, Y. pestis* and *P. luminescens*, the *rcs* locus is immediately followed by the *gyrA* genes, while in other bacteria the *gyrA* gene is found downstream from the *ato* and other genes (Huang *et al.*, 2006) (Fig. 1.11).

Although the *rcs* locus is present in all sequenced *Yersinia* genomes it is noteworthy that the *rcsD* gene (YPO1219) of *Yersinia pestis* is a pseudogene by a frameshift within a homopolymeric tract of 7 T residues (Parkhill *et al.*, 2001). In contrast, the *rcsD* gene in *Y. pseudotuberculosis* and *Y. enterocolitica* is not a pseudogene (Achtman *et al.*, 1999; Chain *et al.*, 2004), suggesting a possible role for the Rcs phosphorelay in gut infections (Stewart Hinchliffe, London School of Hygiene and Tropical Medicine, London, personal communication).

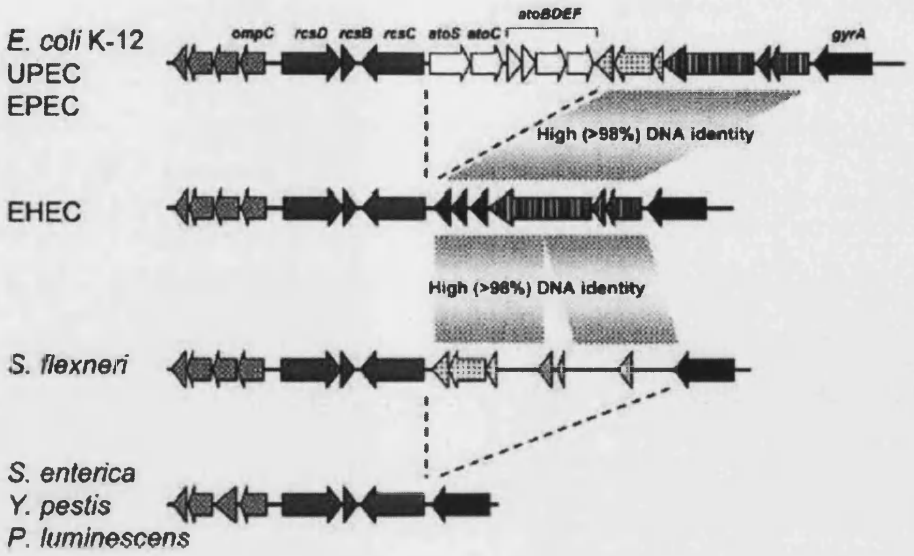

Figure 1.11. Comparative analysis of the *rcs* locus in *Enterobacteriaceae*. The *rcs* loci from various sequenced enterobacterial genomes were available at the ColiBase (http://www.colibase.bham.ac.uk) were collected and aligned using the MUMmer algorithm availale at ColiBase. Sequences shown are the *E. coli* K-12 MG1655, *E. coli* CFT073 (UPEC), *E.coli* E2348/69 (EPEC), *E. coli* O157:H7 EDL933 (EHEC), *Shigella flexneri* 2a 2457T, *S. enterica* serovar Typhimurium LT2, *Y. pestis* KIM and *P. luminescens* TT01. The *rcsBDC* genes are shaded in grey and ORFs encoding homologous proteins in the different genomes are given the same shading pattern (Huang *et al.*, 2006).

1.2.3 Activation of Rcs phosphorelay

Signaling through the Rcs phosphorelay is largely dependent on the RcsC HK. Environmental signals that activate the phosphorelay in a RcsC-dependent manner, but these signals can be either RcsF-dependent or independent (Majdalani *et al.*, 2005). It is possible that additional input signals may be sensed by other components of the phosphorelay, e.g. RcsD.

Although little is known about signals that activate the Rcs phosphorelay, previous studies have shown that osmotic shock transiently activates the

phosphorelay, as measured by expression of the *cps* operon (Sledjeski and Gottesman, 1996). Other environmental conditions such as growth at a low temperature (20°C) in the presence of glucose as a carbon source and high zinc concentrations also activates the phosphorelay (Hagiwara *et al.*, 2003). The presence of a cationic drug, chlorpromazine, disturbs membrane integrity and activates the Rcs phosphorelay (Conter *et al.*, 2002). Moreover, it has recently been shown that the Rcs phosphorelay is also induced by growth on a surface (Ferrieres and Clarke, 2003).

It has also been shown that the overproduction of DjlA, a membrane chaperone protein, can increase the expression of the *cps* operon in a *rcsC*-dependent manner and this response is not transient (Clarke *et al.*, 1997). DjlA overproduction appears to affect the integrity of the bacterial envelope although deletion of *djlA* also activates the Rcs phosphorelay, suggesting DjlA may normally regulate the phosphorelay negatively, and only act as an activator when overproduced (Bernard *et al.*, 1998; Shiba *et al.*, 2006)

Various mutations, for example *tolQRA, pgsA, rfa* and *mdoH,* that affect cell envelope integrity and/or composition also activate the Rcs phosphorelay (Clavel *et al.*, 1996; Conter *et al.*, 2002; Shiba *et al.*, 2004). A defect in the TAT (twin arginine translocation) secretion system also activates the expression of many genes controlled by the Rcs phosphorelay (Ize *et al.*, 2004).. It was shown that the Rcs-dependent TAT-minus phenotype was largely due to the mis-localisation of two substrates of the TAT system, the AmiA and AmiC amidases (Ize *et al.*, 2003). These enzymes are responsible for peptidoglygan metabolism and this suggests that the Rcs phosphorelay may be monitoring or responding to cellular peptidoglycan (PG). In support of this, the Rcs phosphorelay also responds to the presence of high concentrations of certain peptidoglycan-targeting β-lactam antibiotics. Bactericidal doses of ampicillin not only promote capsule synthesis but also changes the expression of many Rcs–regulated genes (Kaldalu *et al.*, 2004; Sailer *et al.*, 2003). There was a significant overlap in the regulons controlled by ampicilliin treatment and the Rcs phopshorelay and it has been shown that the ampicillin-dependent changes in the expression of

some genes was Rcs-dependent (Ferrieres and Clarke, 2003; Huang *et al.*, 2006)

The Rcs phosphorelay is also activated in response to a metabolic block in the glycolytic pathway (El-Kazzaz *et al.*, 2004). Phosphoglucose isomerase, encoded by *pgi,* catalyses the conversion of glucose-6-P to fructose-6-P and a mutation in *pgi* blocks the glycolytic pathway at an early stage and results in an accumulation of glucose-6-P. This excess of glucose-6-P is a metabolic stress that inhibits cell growth and activates the Rcs phosphorelay. The activation of the Rcs phosphorelay can be supressed by mutations in downstream pathways that can prevent synthesis of dTDP-glucose, a precursor of sugars found in the O-antigen and enterobacterial common antigen (ECA). The *pgi* mutation therefore might activate the Rcs phosphorelay by increasing dTDP-glucose and subsequently affecting the synthesis of ECA and O-antigen (El-Kazzaz *et al.*, 2004).

The conditions or mutations that lead to activation of the Rcs phosphorelay are all, in some way, related to envelope stress, suggesting that the Rcs phosphorelay is the 4th member of the group of envelope-stress sensors i.e., CpxAR, BaeSR and σ^E (Raffa and Raivio, 2002). The Rcs phosphorelay responds to perturbations in the production of cellular extracellular polysaccharides (EPSs) such as LPS, membrane-derived oligosaccharides (MDO) and PG. Although the biosynthesis of EPSs is initiated in the cytoplasm, these molecules are bound to the lipid carrier undecaprenyl phosphate (Un-P) then transported across the membrane (Fig. 1.12). During EPS biosynthesis, the undecaprenyl lipid carrier cycles between Un-P and undecaprenyl pyrophosphate (Un-PP) (Raetz and Whitfield, 2002). Therefore it is possible that the Rcs phosphorelay monitors polysaccharide production by sensing the ratio of Un-P and Un-PP in the membrane (Huang *et al.*, 2006). In support of this, the overproduction of UppP (undecaprenyl pyrophosphate phosphatase) which would lower the amount of Un-PP, appeared to cause mucoidy, indicating an increase in colanic production, thus presumably by activating the Rcs phosphorelay (El Ghachi *et al.*, 2004).

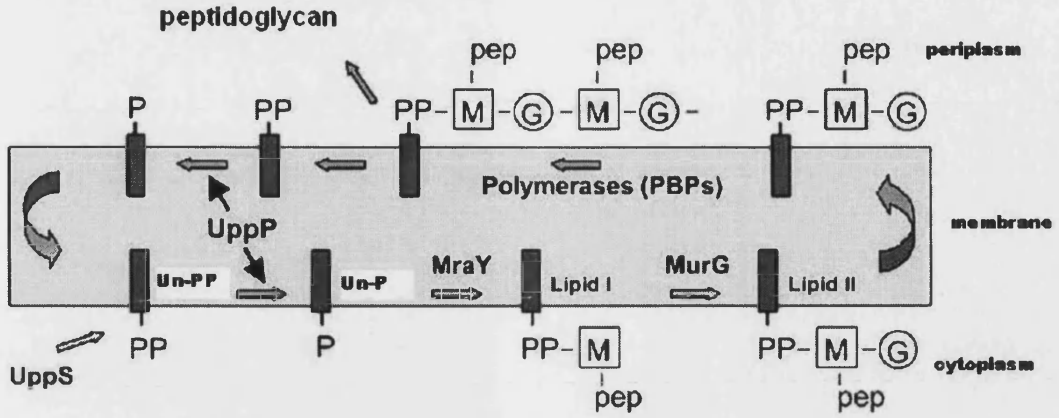

Figure 1.12. Biosynthesis of undecaprenyl phosphate (Un-P) and cell wall peptidoglycan synthesis. The lipid carrier precursor undecaprenyl (Un-PP) is synthesized by the synthetase UppS. The dephosphorylation of Un-PP to Un-P is catalyzed by undecaprenyl pyrophosphate phosphatase (UppP/BacA). The MraY and MurG enzymes catalyze the reaction generating the lipid I and lipid II intermediates, respectively. Lipid II is then translocated to the outer side of the membrane where polymerization reactions catalyzed by the penicillin-binding proteins (PBPs) to produce peptidoglycan or other cell wall components. During peptidoglycan biosynthesis, the undecaprenyl lipid carrier cycles between Un-P and Un-PP across the cell membrane (Image adapted from El Ghachi *et al.*, 2005).

1.2.4 RcsA

Overproduction of RcsA can activate the expression of the *cps* operon and this is dependent on RcsB but independent of RcsC (Brill *et al.*, 1988). The level of RcsA is regulated in different ways, it positively regulates its own expression with RcsB (Ebel and Trempy, 1999), and it is rapidly degraded by Lon and to lesser extent by ClpYQ (Kuo *et al.*, 2004; Stout *et al.*, 1991). In addition to RcsB, H-NS (a histone-like protein) and DsrA (a small RNA) are also involved in regulating *rcsA* expression. H-NS is a negative regulator of *rcsA* transcription while DsrA positively regulates *rcsA* expression by inhibiting the silencing effect of H-NS (Sledjeski and Gottesman, 1995). Signals that alter the transcription of

rcsA can also modulate the outputs of the Rcs phosphorelay. EsaR-mediated repression of the *rcsA* gene has been described in *Pantoea stewartii* (Minogue *et al.*, 2005). The LuxR-type quorum sensing (QS) transcription factor EsaR directly represses the transcription of the *rcsA* gene in the absence of AHL signal, therefore, at high cell densities, EsaR binds the AHL ligand and its affinity to the DNA target is reduced. The derepression of *rcsA* expression by QS promotes the expression of the *cps* operon at high cell density. Therefore, in some bacteria, there is an RcsA-dependent link between quorum sensing and the Rcs phosphorelay. High level of the global second messenger cyclic diguanylic acid (c-di-GMP) was also shown to upregulate RcsA transcription (Mendez-Ortiz *et al.*, 2006).

1.2.5 The Rcs regulon

Array studies have shown that the Rcs phosphorelay, either directly or indirectly, affects the expression of many genes. In one microarray study, using a combination of low temperature, glucose as sole carbon source and a high concentration of zinc as the activating signal, 32 genes were identified as being members of the Rcs regulon (Hagiwara *et al.*, 2003). In another study, using DjlA overproduction as the signal, 150 genes were identified as being regulated by the Rcs phosphorelay (Ferrieres and Clarke, 2003). In both studies many of the genes identified were predicted to have a function that was associated with the cell membrane, suggesting that the Rcs phosphorelay may contribute to the modification of the bacterial surface in response to the changes in the environment.

In addition to the regulation of colanic acid production, the Rcs phosphorelay regulates the synthesis of type I capsular polysaccharides in other bacteria, including Vi antigen in *S. enterica* serovar Typhi (Virlogeux *et al.*, 1996), and amylovoran in the plant pathogen *Erwinia amylovora* (Kelm *et al.*, 1997). The Rcs phosphorelay also participates in the regulation of the *Salmonella ugd* gene, a gene that is required for the production of L-aminoarabinose, an amino sugar that is added to the lipid A moiety of LPS to induce resistance to antimicrobial cationic peptides (Gunn *et al.*, 1998; Mouslim and Groisman, 2003).

The Rcs phosphorelay has been shown to be involved in the regulation of a variety of cellular processes. It positively regulates the expression of the cell division genes, *ftsA* and *ftsZ,* in *E. coli* (Carballes *et al.*, 1999). It has been recently shown that the Rcs phosphorelay negatively regulates flagella synthesis and motility in *E. coli* K-12, by repressing the expression of the *flhDC* operon which encodes the master regulators of flagella biosynthesis (Francez-Charlot *et al.*, 2003). Moreover, swarming behaviour in *Proteus mirabilis* and *S. enterica* seroar Typhimurium is also regulated by the Rcs phosphorelay. In *Proteus mirabilis,* a mutation in *rsbA* (a homologue of *rcsD*) results in precocious swarming, while a mutation in the same gene in *S. enterica* serovar Typhimurium results in a loss of swarming (Belas *et al.*, 1998; Toguchi *et al.*, 2000). The Rcs phosphorelay therefore regulates motility differently in these bacteria. The *tolQRA* genes, encoding proteins that are involved in membrane integrity, are regulated by the Rcs phosphorelay *in E. coli* (Clavel *et al.*, 1996), but in *Salmonella,* this phosphorelay does not appear to regulate the transcription of the *tolQRA* genes (Prouty *et al.*, 2002).

In *E. coli*, activation of the phosphorelay also leads to increased levels of the alternative sigma factor σ^S. The Rcs phosphorelay has been shown to regulate the expression of RprA, a 105-nt regulatory small RNA, that binds to the *rpoS* mRNA and increases the translatability of the message (Majdalani *et al.*, 2002). Therefore, the Rcs phosphorelay can activate RpoS-regulated genes indirectly. Interestingly, many Rcs-regulated genes are also subject to RpoS regulation. The significance of this type of complex regulation is unclear, however, two-component pathways can result in a faster response than sigma factor regulation. Using multiple regulatory systems to modulate the cellular activity can enable bacteria to respond appropriately to the changing environment.

1.2.6 The role of Rcs phosphorelay in biofilm formation

The Rcs phosphorelay is required for normal biofilm development in *E. coli* K-12, *S. enterica* serovar Typhimurium and *P. mirabilis* (Ferrieres and Clarke, 2003; Liaw *et al.*, 2004; Mireles *et al.*, 2001). The biofilm formation process can be divided into several stages, from initial attachment to the surface to the maturation of the biofilm into a three-dimensional structure, and genes involved

in different stages are subject to regulation by the Rcs phosphorelay. Therefore, genes encoding proteins involve in motility and attachment, such as flagella, antigen 43 and curli gene have been shown to be repressed by the Rcs phosphorelay whilst the production of colanic acid, important for the maturation of biofilm, is positively regulated by the RcsC phosphorelay (Danese *et al.*, 2000; Ferrieres and Clarke, 2003; Francez-Charlot *et al.*, 2003; Prigent-Combaret *et al.*, 2000; Vianney *et al.*, 2005). This leads to the possibility that the Rcs phosphorelay is regulating the temporal development of biofilm formation by controlling the transition from attached cells to mature biofilm (Huang *et al.*, 2006) (Fig. 1.13).

1.2.7 The Rcs phosphorelay in *Salmonella* pathogenicity

The Rcs phosphorelay is involved in the regulation of virulence in *S. enterica* serovar Typhi, the causative agent of human typhoid fever, and *S. enterica* serovar Typhimurium, the causative agent of either self-limited gastroenteritis or systemic infections in humans and other animal species (Tierrez and Garcia-del Portillo, 2005). Virulence-related genes shared by all *salmonellae* include the *Salmonella*-pathogenicity islands-1 (SPI-1) and -2 (SPI-2), which encode type III protein secretion systems (TTSS). SPI-1 is essential for invasion and SPI-2 is required for intracellular survival and proliferation (Guiney, 2005). The expression of invasion Sip proteins (encoded in SPI-1) and Vi antigen, a capsular polysaccharide, in *S. enterica* serovar Typhi is regulated by the Rcs phosphorelay (Arricau *et al.*, 1998; Virlogeux *et al.*, 1996). It has been shown that the Rcs phosphorelay is activated under conditions that mimic intracellular growth and a *rcsC* mutant was attenuated for systemic infection (Detweiler *et al.*, 2003). However other studies have shown that the Rcs phosphorelay must be tightly repressed during early stages of infection, indicating that shutdown of the Rcs phosphorelay is a requisite for *Salmonella* virulence (Dominguez-Bernal *et al.*, 2004; Mouslim *et al.*, 2004). Activation of the Rcs phosphorelay, either by a mutation in the *yrfF* gene or by constitutive *rcsC* alleles resulted in a significant attenuation in virulence (Dominguez-Bernal *et al.*, 2004; Garcia-Calderon *et al.*, 2005). Therefore, it appears that the Rcs phosphorelay must be inactive during the early stages of infection but must be activated at some stage during infection

to ensure cell survival during intracellular growth. This temporal response would be analogous to the proposed role of the Rcs phosphorelay during biofilm formation in *E. coli* where the Rcs phosphorelay is inactive during initial attachment stage, but must be activated in later stages to enable the maturation of the biofilm.

The Rcs phosphorelay is also involved in antibiotic resistance in *S. enterica* serovar Typhimurium. As already mentioned, a mutation in *yrfF* gene activates the Rcs phosphorelay and induces the expression of the *cps* operon, resulting in mucoidy. The *yrfF* mutant is also resistant to the beta-lactam antibiotic, mecillinam and this resistance requires the RcsB-mediated induction of the cell division genes *ftsA-ftsZ* (Costa and Anton, 2001). The Rcs phosphorelay also regulates the resistance to polymyxin B in *S. enterica* (Mouslim and Groisman, 2003).

1.2.8 Type III secretion system and other virulence factors in *Yersinia* and EHEC

The role of the Rcs phosphorelay in enterohaemorrhagic *E. coli* (EHEC) was recently investigated (Tobe *et al.*, 2005). The Rcs system can both positively and negatively regulate the expression of genes in the locus for enterocyte effacement (LEE). The LEE locus plays a role in bacterial adherence capacity and secretion and RcsB increases LEE expression through positive effects on both GrvA and Ler. Therefore, the overexpression of the RR, RcsB, led to increased production of the type III secretion apparatus (TTSS). However, deletion of *rcsB* increased the expression of *espB,* suggesting a negative effect of RcsB on LEE expression and this was shown to be due to RcsB-mediated repression of *pchA* expression. Therefore the Rcs phosphorelay regulates the expression of pathogenicity in EHEC through opposite effect on two regulators, PchA and GrvA (Tobe *et al.*, 2005).

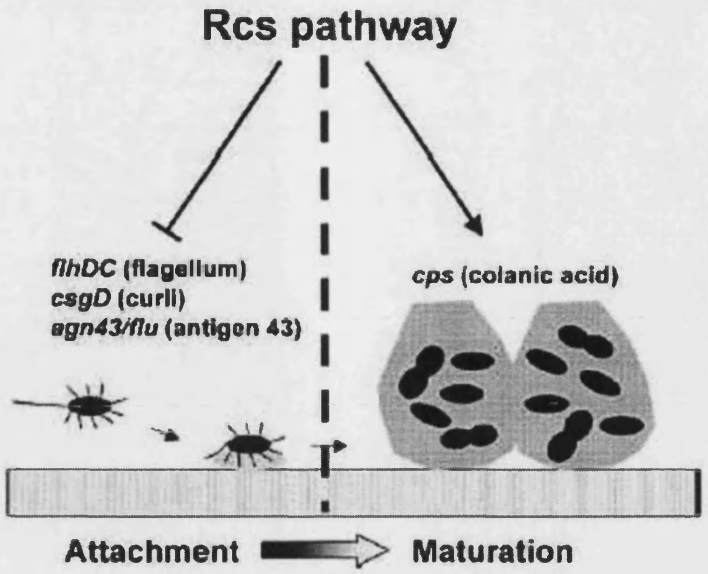

Figure 1.13. Model of the role of the Rcs phosphorelay in controlling the transition from attached cell to mature biofilm in *E. coli*. The Rcs phosphorelay is activated after the cells have attached to the surfaced (indicated by dashed line). Activation of the Rcs phosphorelay results in the repression of genes encoding surface structures required for bacterial attachment to a surface, e.g. flagella, curli and antigen 43. The activation induces the expression of genes responsible for the production of colanic acid/EPS, requires for biofilm maturation. The Rcs phosphorelay is involved in the regulation of a temporally important developmental checkpoint during biofilm formation in *E.coli*. (Image taken from Huang *et al.*, 2006)

A type III secretion system in *Yersinia enterocolitica* biovar 1B is also subject to regulation by the Rcs phosphorelay (Venecia and Young, 2005). In addition to virulence factors such as the plasmid-borne Ysc type III secretion system and urease that are found in all *Yersinia enterocolitica* biovars, a biovar-restricted virulence factor called *Yersinia* secretion apparatus pathogenicity island (YSA PI) was described in biovar 1B. The YSA PI encoded the Ysa TTSS, a secretion system distinct from the well-characterised Ysc TTSS (Foultier *et al.*, 2002). The Ysa TTSS is required for the export of a set of proteins called *Yersinia* secreted proteins (Ysps). A genetic analysis identified RcsB as a positive regulator of Ysp secretion. Interestingly, the Ysa TTSS system plays a role in the colonisation of

the terminal ileum, but does not contribute to colonisation of deep tissues during systemic infection. Thus, the Ysa TTSS system is important during the earliest stage of infection (Venecia and Young, 2005).

1.3 Conclusion

Bacteria utilize the 2CP signalling systems to sense and respond to extra- and intra-cellular changes. These pathways play important roles both in the bacteria-environment interaction and the bacteria-host interaction. The Rcs phosphorelay controls a variety of important cellular processes, e.g. motility, cell division, biofilm formation and pathogenicity. The biofilm formation phenotype was of particular interest as it has implications in both industry and medicine. The complex signalling mechanism and broad variety of target genes suggests that the Rcs phosphorelay acts as a global regulator controlling the remodelling of the cell surface of bacteria in response to the changing environment. Moreover, studies in *E. coli* and *S. enterica* have suggested that an important function of the Rcs phosphorelay is to temporally control the expression of genes during biofilm formation and pathogenicity. The understanding of the sensing and signalling mechanism of this phosphorelay will provide potential solutions for the control of biofilm formation.

1.4 Objectives of this work

The aim of this study was to analyse the sensing and signaling mechanisms of the Rcs phosphorelay, in particular the RcsC sensor kinase. Experiments carried out in this study attempted to identify the regions of RcsC which are involved in monitoring environmental signals. The primary amino acid sequence and predicted structure was used to try to understand how RcsC sense signals and what the interaction is between different components in the Rcs phosphorelay.

The role of Rcs in biofilm formation has been established in *E. coli.* In this study, I also investigated the role of the phosphorelay in other *Enterobacteriaceae*, i.e., *Photorhabdus*. The dynamics and developmental stages during biofilm formation

were studied in a flow chamber system using confocal scanning laser microscopy (CSLM), allowing a temporal examination of *Photorhabdus* biofilm formation *in situ*.

Chapter 2
Materials and Methods

2.1 Bacterial strains and plasmids and growth conditions

The bacterial strains and plasmids used in this study are listed in Table 2.1. Bacterial strains were routinely cultured in Luria-Bertani (LB) broth (1% [w/v] peptone, 0.5% [w/v] yeast extract and 1% [w/v] sodium chloride in water) or on LB agar (LB broth and 1.5% [w/v] agar) at 37°C for *E. coli* and 30°C for *P. luminescens*. When required, antibiotics were added at the following concentrations: ampicillin (Amp) 100 µg/mL, chloramphenicol (Cm) 20 µg/mL, kanamycin (Kan) 30 µg/mL, Tetracycline (Tet) 15 µg/mL and rifampicin (Rif) 100 µg/mL. Other culture media used in this study are listed in Table 2.2.

Unless otherwise stated, 'TT01' refers to a rifampicin resistant derivative of *P. luminescens* subsp *laumondii* TT01 (Bennett and Clarke, 2005).

Table2.1 Bacterial strains and plasmids used in this study.

Strain or plasmid	Relevant characteristics	source or reference
Strains		
Escherichia coli		
EC100	F⁻ *mcrA* Δ(*mrr-hsd*RMS-*mcr*BC) φ80d*lacZ*ΔM15 Δ*lacX74 recA1 endA1 araD*139 Δ(*ara, leu*)7697 *galU galK* λ⁻ *rpsL nupG*	Epicentre
EC100D *pir*⁺	EC100, *pir*⁺ (DHFR)	Epicentre
MC4100	*araD139* Δ(*argF-lac*)*205 flb-5301 pstF25 rpsL150 deoC1 relA1*	
PSG1031	MC4100 *cpsB-lacZ*	Clarke *et al.*, 1997
PSG1038	PSG1031 *rcsC52*::Tn10,Tet^r	Clarke *et al.*, 2002
S17-1	λ-*pir* lysogen; permissive host as conjugation donor	Lab stock
SG20907	*rcsC137, cps-lacZ*, Cm^r	Clarke *et al.*, 2002
ZK2686	W3110 Δ(*argF-lac*)*U169*	Takeda *et al.*, 2001
BMM520	ZK2686 *rcsC52*::Tn10 Tet^r	Ferriere and Clarke, 2003
BMM555	BMM520 *gmd*-λplacMu53	Ferriere, unpublished
Photorhabdus luminescens		
TT01-Rif	Rif^r	Bennett and Clarke, 2005

BMM601	TT01-Rif Δ*rcsC*	This study
BMM602	TT01-Rif Δ*rcsB*	This study
Plasmids		
pBMM101	pTrc99a derivative, *c-myc* epitope, Amp^r	Clarke *et al.*, 2002
pBMM102	$rcsC_{K12}$ in pBMM101	Clarke *et al.*, 2002
pBMM106	*envZ-rcsC* in pBMM101	Clarke, unpublished
pBMM107	$rcsC_{\Delta TM}$ in pBMM101	Clarke, unpublished
pBMM601	$rcsC_{O157}$ in pBMM101	This study
pBMM602	$rcsC_{LT2}$ in pBMM101	This study
pBMM603	$rcsC_{Yp}$ in pBMM101	This study
pBMM617	$rcsC_{\Delta PP}$ in pBMM101	This study
pBMM618	$rcsC_{\Delta PP\text{-}\Delta Linker}$ in pBMM101	This study
pBMM619	$rcsC_{\Delta INPUT}$ in pBMM101	This study
pBMM620	$rcsC_{\Delta Linker}$ in pBMM101	This study
pBMM621	$rcsC_{Q449H}$ in pBMM101	This study
pBMM622	$rcsC_{S282C}$ in pBMM101	This study
pBMM623	$rcsC_{L293V}$ in pBMM101	This study
pBMM624	$rcsC_{H339D}$ in pBMM101	This study
pBMM625	$rcsC_{R344S}$ in pBMM101	This study
pBMM626	$rcsC_{V422G}$ in pBMM101	This study
pBMM631	$rcsC_{K12\text{-}YP}$ in pBMM101	This study
pBMM639	$rcsC_{YP\text{-}K12}$ in pBMM101	This study
pBMM641	$rcsC_{YP(T->Q)}$ in pBMM101	This study
pBMM642	$rcsC_{K12(Q449H)\text{-}YP}$ in pBMM101	This study
pDS132	Cm^r, *sacB*	Philippe *et al.*, 2004
pBMM630	pDS132 containg flanking regions of $rcsC_{TT01}$	This study
pBMM633	pDS132 containg flanking regions of $rcsB_{TT01}$	This study
pBAD24	Expression vector, Amp^r, P_{araBAD}	Guzman *et al.*, 1995
pBMM640	*Photorhabdus rcsB* gene in pBAD24	This study
pBAD33	Expression vector, Cm^r, P_{araBAD}	Guzman *et al.*, 1995
pPSG961-31	*E. coli djlA* gene in pBAD33	Clarke *et al.*, 1997
pSU2007	Conjugative plasmid, GFP, Kan^r	Martinez ed de la Cruz, 1988

Table 2.2 List of agars, their composition and suppliers used in this study.

Media	Composition per litre dH_2O		Use
LB	Tryptone (BD)	10 g	General usage
	Bacto yeast extract (BD)	5 g	
	NaCl (BDH)	10 g	
	Agar (Merck)	15 g	
MgLB	Tryptone (BD)	10 g	Conjugation
	Bacto yeast extract (BD)	5 g	
	NaCl (BDH)	5 g	
	1 M $MgCl_2$ (Fisher)	1 mL	
	Agar (Merck)	15 g	
LB sucrose	Tryptone (BD)	10 g	Selection
	Bacto yeast extract (BD)	5 g	
	Sucrose (Fisher)	10 g	
	Agar (Merck)	15 g	
Motility agar	Tryptone (BD)	10 g	Motility assay
	Bacto yeast extract (BD)	5 g	
	NaCl (BDH)	10 g	
	Agar (Merck)	3 g	
EMB agar	Eosin methylene blue agar (Merck)	36 g	Dye uptake
MacConkey agar	MacConkey agar powder (Oxoid)	51.5 g	Dye uptake
NBTA	Nutrient agar (Oxoid)	28 g	Dye uptake
	Bromothymol blue (USB)	25 mg	
	2,3,5-Tetrazolium salt	30 mg	
LIA	Nutrient agar (Oxoid)	28 g	Lipase detection
	Tween 80 (BDH)	0.5% v/v	
PIA	Nutrient broth (Oxoid)	1 g	Protease detection
	Gelatine (Fisher)	20 g	
	D-Glucose (Fisher)	0.5 g	
	Agar (Merck)	15 g	
CAS agar	SolnA		Siderophore production
	Chrome Azurol S	60.5mg	
	H_2O	50 mL	
	SolnB		

	$FeCl_3$. $6H_2O$	1 mM	
	HCl	10 mM	
	H_2O	10 mL	
	SolnC		
	CTAB	72.9 mg	
	H_2O	40 mL	
Lipid agar	Nutrient agar (Oxoid)	25 g	Nematode development
	Bacto yeast extract (BD)	5 g	
	Corn syrup (Karo)	10 g	
	Cod liver oil (Seven seas)	5 mL	
	$MgCl_2 \cdot 6H_2O$ (Fischer)	2 g	

2.2 DNA extraction

2.2.1 Extraction of chromosomal DNA

Genomic DNA from the bacterial strain of interest was extracted using standard procedures. The bacterial strain of interest was grown overnight in LB and 4 mL of overnight culture was centrifuged at 13,000 rpm for two minutes. The pellet was resuspended in 567 µL of TE buffer (10 mM Tris, 1 mM EDTA, pH 8) by repeated pipetting. Sodium Dodecyl Sulfate (SDS) and proteinase K were added to give a final concentration of 100 µg/mL proteinase K in 0.5% (w/v) SDS. The sample was incubated for one hour at 37°C, then 100 µl of 5 M NaCl and 80 µL of preheated CTAB/NaCl solution (10% [w/v] CTAB in 0.7 M NaCl) was added. This mixture was mixed thoroughly and incubated at 65°C for 10 min. An equal volume of chloroform/isoamyl alcohol [24:1] was added and the sample was spun down at 10,000 rpm for 5 min in a microcentrifuge. The supernatant was transferred to a new tube and an equal volume of phenol/chloroform/isoamyl alcohol [25:24:1] was added. The sample was mixed thoroughly and centrifuged at 10,000 rpm for 5 min. The supernatant was transferred to a fresh tube and 0.6 volume isopropanol was added and the tube was left at -80°C to allow the nucleic acids to precipitate. DNA was pelleted by centrifugation at 13,200 rpm for 10 min. The supernatant was discarded and the pellet was washed with 70% ethanol. DNA was pelleted again by further centrifugation for 5 min and the

supernatant was discarded. The pellet was allowed to dry and the DNA was resuspended in 100 µL of sterile water.

2.2.2 Extraction of plasmid DNA

Plasmid DNA was extract with the Wizard Plus SV Minipreps DNA purification System (Promega®) and QIAprep Miniprep Kit (Qiagen®) according to the manufacturer's instructions

2.2.3 PCR clean-up

PCR products were purified with the Strataprep PCR purification Kit (Strategene®) according to the manufacturer's instructions.

2.2.4 Recovery of DNA from agarose gel

DNA fragments in agarose gel were recovered with the QIAQuick Gel extraction kit (Qiagen®) according to the manufacturer's instructions.

2.3 Cloning of *rcsC* genes

2.3.1 PCR amplification of *rcsC* genes

Genomic DNA from different strains of representative *Enterobacteriaceae* was isolated and used as template in PCR. Genomic DNA from *E. coli* O157 (gift from Dr. Brendan Kenny, University of Newcastle), *Salmonella enterica* serovar Typhimurium LT2 (gift from Charles Dorman, Trinity College) and *Yersinia pestis* (gift from Dr. Elisabeth Carniel, Institut Pasteur) was used for amplification. Genes of interest were amplified by PCR in a 50 µL reaction mix containing 1 µM of each specific primer. The amplification was performed as follows: 2 min at 92°C; 30 cycles: 30 s at 92°C, 30 s at 52°C, 7 min at 72°C; 14 min at 72°C.The specific primer pairs were designed to amplify the full length of the corresponding gene and to introduce *Xba*I and *Nco*I restriction sites at the 3' and 5' ends of the amplified DNA fragment respectively. Primer pairs used in this study are listed in Table 2.2.

2.3.2 Restriction digestion of DNA

The purified PCR products were cleaved with restriction endonucleases *Xba*I and *Nco*I (New England Biolabs®). The reaction mix was composed of 15 µL of purified DNA, 3 µL of 10X NEB Buffer (New England Biolabs®), 1.5 µL of each restriction endonuclease and 9 µL of sterile water. Restriction was carried out at 37°C for 2 hours and the digested product was then purified with Strataprep® PCR purification Kit (Stratagene®). The cloning vector pBMM101 (Clarke *et al.*, 2002) was digested with the same enzymes and the digested product was electrophoresed on a gel and recovered with QIAQuick Gel extraction kit (Qiagen®).

Table 2.3 Oligonucleotides used in this study.

Oligo	Sequence	Note
DC193	AGCCATGGTGTACGAGCGACGTATTTTCATTCC	5′ primer for *rcsC*$_{\Delta TM}$
DC194	AGCCATGGAAGAGTCGTTGCAGGAGATGG	5′ primer for *rcsC*$_{\Delta INPUT}$
DC212	TCGAGCCATGGTCAGAGCATTGGCGTTAGTGC	5′ primer for K12 *rcsC*
DC213	ATAGCTCTAGAGAATCCCGCGATTTCCTGACC	3′ primer for K12 *rcsC*
YH100	TCGAGCCATGGAATACCTTGCTTCCTTTCGAAC	5′ primer for LT2 *rcsC*
YH101	ATAGCTCTAGAGCCCGCGTTTTACGTACCCGC	3′ primer for LT2 *rcsC*
YH102	TCGAGCCATGGTTTTTCATGGTATCCGATTG	5′ primer for *Y. pestis rcsC*
YH103	ATAGCTCTAGACGTGATCGCCGTACTTGGTC	3′ primer for *Y. pestis rcsC*
YH104	TCGAGCCATGGTCAGAGCATTGGCGTTAGTGC	5′ primer for O157 rcsC
YH105	ATAGCTCTAGAGATTCCCGCGATTTCCTGACCCTC	3′ primer for *E. coli rcsC*
YH106	TCGAGCCATGGAATACCTTGCTTCTTTTCG	5′ primer for K12 *rcsC*
YH107	ATAGCTCTAGAGAATCCCGCGATTTCCTGACC	3′ primer for K12 *rcsC*
YH147	TTCCAGGAGCTCTTCTCGCTGATGTAACGC	PP deletion L
YH148	CGAGAAGAGCTCCTGGAACGCATTCGCATG	PP deletion R
YH149	TATTTAGCATGCGCGTAATGGTAACGTGATC	Primer 1 for *rcsC* K/O of TT01
YH150	GGGGTTTCAAATCATATATCTCAAAAGGTTACCTG	Primer 2 for *rcsC* K/O of TT01
YH151	CCTTTTGAGATATATGATTTGAAACCCCGGTACAA	Primer 3 for *rcsC* K/O of TT01
YH152	TAAAATAGAGCTCTGTATTAAAGCAAACGTACTG	Primer 4 for *rcsC* K/O

		of TT01
YH153	TATTTAGCATGCTGCATCATTATGGCGCGG	Primer 1 for *rcsB* K/O of TT01
YH154	GAACGGTATTTACATCTTATTAGTTACCCTGCTGC	Primer 2 for *rcsB* K/O of TT01
YH155	ACTAATAAGATGTAAATACCGTTCGTTATTTTAATA TG	Primer 3 for *rcsB* K/O of TT01
YH156	TAAAATAGAGCTCGACTATATTGGCTCACCGG	Primer 4 for *rcsB* K/O of TT01
YH162	TCGCACGGATGGAAGAGTCGTTGCAGGAGATG	Linker deletion L
YH163	CGACTCTTCCATCCGTGCGAGAGTAAACAATGC	Linker deletion R
YH166	CAGAAACATCGATTTTGATTGACTGGC	3′ primer for $rcsC_{YP}$ input
YH169	TCCGATCAAATCCCGTGC	Primer U for *rcsC* K/O
YH170	TAAGAATAGCATTAGCCG	Primer D for *rcsC* K/O
YH176	AACCTGGGTACGCACTATGC	Primer U for *rcsB* K/O
YH177	TCATCATGGCTTACCACACGG	Primer D for *rcsB* K/O
YH182	AAGGAACATCGATGTTTCTGGCTACCGTTAGTC	5′ primer for $rcsC_{YP}$ output
YH190	TCGAGCCATGGATAACCTTAACGTCATTATTGC	5′ primer for $rcsB_{TT01}$
YH191	TTGAATCTAGAGAATTTTCCTGTCAGG	3′ primer for $rcsB_{TT01}$
YH192	AAACATCGATTTTGATTGACTGGCTTGCTCTGCCGC TTGAGCCATTTCTTGTAGTGA	3′ primer for $rcsC_{YP}$ input

Underlined sequences indicate restriction sites, shaded sequences indicate complementary regions` in 3-step PCR.

2.3.3 Ligation

Restricted DNA fragments for ligation were denatured at 60°C for 5 minutes then place on ice before adding 2 μL T4 DNA ligase 10X Buffer (Promega®) and 1 U of T4 DNA ligase (Promega®) in a 20 μL reaction mixure. The reaction mixture was left at 16°C overnight. The ligation mixture was desalted by placing 20 μL of the ligation mixure on nitrocellulose filters (Millipore®) floating on sterile water for 20 minutes, then the mixture was recovered by pipetting to a new tube.

2.4 Construction of chimeric RcsC proteins

2.4.1 Construction of pBMM631

DNA sequence encoding the N-terminal region of $RcsC_{YP}$ (Met1-Ser481) was amplified by PCR using oligos YH102 and YH166, and the 1.4kb fragment of DNA was digested with *Nco*I and *Cla*I. Plasmid pBMM102 was also digested with *Nco*I and *Cla*I and ligated with digested $rcsC_{YP}$ PCR product, to generate pBMM631.

2.4.2 Construction of pBMM639

PCR primer pairs (YH192 and YH103) were designed to introduce a *Cla*I site into $rcsC_{YP}$ during amplification of the 3' end of $rcsC_{YP}$ (encoding the Met482-Arg958 of $RcsC_{Yp}$). Plasmid pBMM102 was digested with *Cla*I and *Xba*I. The $rcsC_{YP}$ PCR product was digested with *Cla*I and *Xba*I, and ligated with the restricted pBMM102, to give rise to pBMM639, encoding the N-terminal region of $RcsC_{K12}$ (Met1-Ser455) and the C-terminal region of $RcsC_{YP}$ (Met482-Arg958).

2.5 Construction of domain deletion RcsC variants

The domain deletion variants of $RcsC_{K12}$ were generated either by simple PCR or using a modified 3-step PCR method adapted from Ferrieres *et al.* (Fig. 2.1). (Ferrieres *et al.*, 2004).

$RcsC_{\Delta input}$ was generated by amplification of the 3' region of *rcsC* using primers YH194 and DC213. The PCR fragement was digested with *Nco*I and *Xba*I and ligated with pBMM101, resulting in pBMM619, encoding Met436 to Ser933 of $RcsC_{K12}$.

The periplasmic domain deletion ($RcsC_{\Delta PP}$) was constructed using a 3-step PCR. The upstream region of the periplasmic domain was amplified using oligo DC212 and YH147, and the downstream region was amplifed using YH148 and DC213. The primers YH147 and YH148 contain regions that are complementary to each other. Both PCR products were purified, mixed together and linked by 10 cycles of primer-free PCR. The linked mixture was then used as a template and amplified using DC212 and DC213, generating a periplasmic domain

deleted fragment (ΔPP). The fragment was digested with *Nco*I and *Xba*I and cloned into pBMM101, to yield pBMM617.

The linker domain deletion ($RcsC_{\Delta LInker}$) was also constructed using the 3-step PCR. The DNA region upstream from the linker domain of RcsC was amplified using DC212 and YH162, and the downstream region was amplified using YH163 and DC213. The complementary regions of YH162 and YH163 facilitate the linking of the two fragments, and the linked fragment was cloned into pBMM101, generating pBMM620. Moreover, using pBMM617 as template, the same primer sets were used to generate pBMM618, encoding $RcsC_{\Delta PP\text{-}\Delta LInker}$.

2.6 Random mutagenesis of input region

For introducing random mutations into the input region of $RcsC_{K12}$, mutagenic PCR was carried out using an error-prone DNA polymerase Mutazyme (Strategene®) according to the manufacturer's instructions. The DNA encoding the input region of $RcsC_{K12}$ was amplified using primers YH104 and YH144, and the mutagenised fragments were digested with *Nco*I and *Cla*I. Plasmid pBMM106 was digested with *Nco*I and *Cla*I, and ligated with the amplified mutagenised fragment.

2.7 Transformation

2.7.1 $CaCl_2$ method

An overnight culture of *E. coli* strain was inoculated into 50 mL of LB to an OD_{600}=0.01. The fresh culture was incubated at 37°C, with agitation, until an OD_{600}=0.4. The culture was transferred to a 50 mL polypropylene tube and placed on ice for 5 minutes. The cells were centrifuged at 4,000 rpm for ten minutes at 4°C. The pellet was resuspended in 15 mL of sterile ice cold 0.1 M $CaCl_2$. The suspension was placed on ice for 10 min, and the cells were pelleted by centrifugation. The pellet was finally resuspended in 1.5 mL sterile ice-cold 0.1 M $CaCl_2$ and stored on ice.

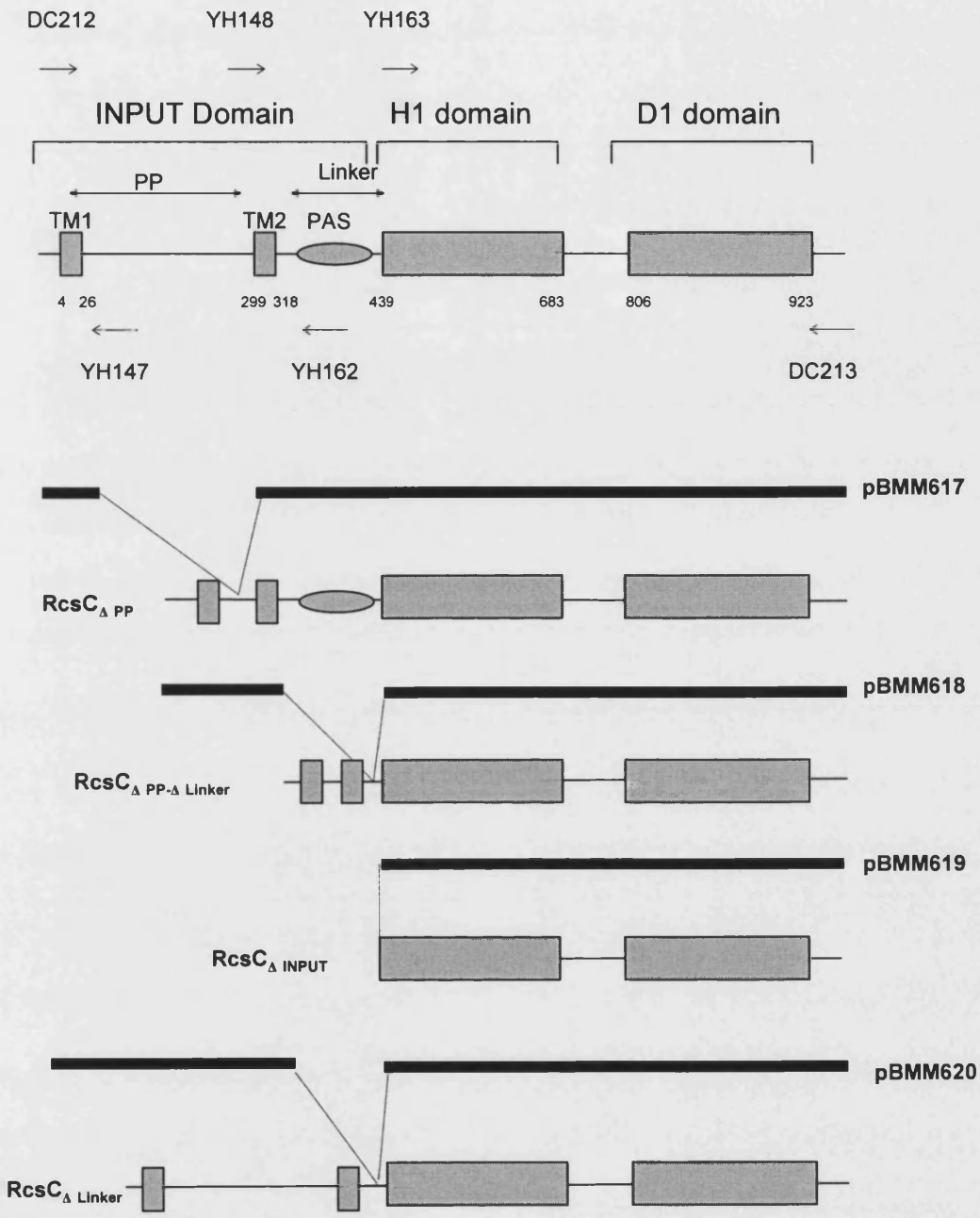

Figure 2.1 Schematic representation of deletion mutants constructed in this study. The domain structure of $RcsC_{K12}$ is presented at the top of the figure, two double arrows indicated the periplasmic domain (PP) and the linker region. PCR primers designed to amplify the upstream and downstream of the target regions (PP or linker) are presented by arrows. The DNA fragements amplified and cloned are presented by the bold lines, and the encoded proteins are depicted schematically.

For each transformation, 200 µL of suspension were transferred to a sterile tube and 2 µL of plasmid were added. The mixture was placed on ice for 30 minutes then the tubes were incubated at 42°C without agitation for 90 seconds. The samples were rapidly transferred to an ice bath for 2 min before 800 µL of LB were added and tubes were incubated at 37°C for 30 min before cells were spread onto plates with appropriate selective antibiotics.

2.7.2 Electroporation of *E. coli*

5 µL of desalted ligation reaction mixure was mixed with 50 µL of TransforMax® EC100 Electrocompetent *E. coli* (Epicentre®) and electroporated at 2.5 kV using 2 mm gap cuvettes. 950 µL of LB was added into the cuvette and the bacterial mixture was incubated at 37°C with agitation for 30 min before spreading onto plates with the appropriate selective antibiotics.

2.7.3 Electroporation of *Photorhabdus*

Electrocompetent *Photorhabdus* cells were prepared as follows: 200 mL of LB was inoculated with overnight culture of *Photorhabdus* and grown to an OD_{600}=0.2. The culture was then chilled on ice for 90 mins. The cells were harvested by centrifugation and the pellet was resuspend in 200 mL of ice cold SH buffer (5% [w/v] sucrose, 1 mM HEPES, pH 7). The cells were harvested and sequentially washed in 100 mL and 2 mL ice cold SH buffer and finally resuspended in 200 µL of SH buffer and stored on ice. the electroporation settings were the same as described for *E. coli* and 40 µL of cells and 2 µL of purified DNA were used in each reaction. 950 µL of LB was added into the cuvette and the bacterial mixture was incubated at 30°C with agitation for 3 hours before cells were spread onto plates with appropriate selective antibiotics.

2.8 Western Blotting

Cultures of PSG1038 containing the appropriate plasmids were grown overnight at 37°C and diluted 100-fold into fresh LB and incubated at 37°C for 2 hours before 1mM IPTG was added to the culture to induce the expression of *rcsC*. After incubation at 37°C for 2 hours, samples were taken for immuno detection.

Total cell proteins equivalent to 0.2 unit of OD_{600}, unless otherwise stated, were separated by SDS-PAGE, and transferred to a nitrocellulose membrane by electroblotting (4°C, 70 minutes, 80V). The proteins were fixed on the membrane and the transfer was checked by staining with Ponceau S (Sigma). The membranes were then blocked by incubation in PBS containing 5% (w/v) of skim milk powder for two hours at room temperature, with gentle shaking. The blocking solution was removed and the membrane was incubated overnight at 4°C, with gentle agitation, in PBS containing 0.5% (w/v) of skim milk powder and the primary antibody against RcsC (custom polyclonal anitbiodies, BioCarta) at a working dilution of 1:500. The membrane was washed 3 times with PBS, before hybridisation with peroxidase-labelled secondary antibody raised against rabbit. Detection was performed by chemiluminescence (ECL), according to the manufacturer's (Amersham) instructions.

2.9 β-Galactosidase assay

The β-galactosidase activity was estimated with *o*-nitro-phenyl-β-D-galactoside (ONPG) as a substrate in an assay modified after Miller (Miller, 1972). Bacteria were grown under appropriate condition overnight then collected and washed in 1x phosphate-buffered saline (PBS) before being resuspend in Z buffer (0.06 M Na_2HPO_4, 0.04 M NaH_2PO_4, 0.01 M KCl, 0.001 M $MgSO_4$, 0.05 M β-mercaptoethanol, pH 7). The cells were permeablized by adding 100 µL of chloroform and 50 µL of 0.1% (w/v) SDS, then 250 µL of ONPG (4 mg/mL) was added to the chloroform/SDS permeablized cells. The β-galactosidase reaction was stopped by the addition of 400 µL 1 M Na_2CO_3 when the reaction turned yellow, and the time between the start and the end of the reacton was recorded. After a centrifugation step, the OD_{420} and OD_{550} of the supernatant were deteremined immediately. Enzyme activities were calculated using the following formula:

$$(OD_{420}-1.75\times OD_{550}) \times 1000/OD_{600} \times \text{time (min)} \times \text{volume of culture (mL)}$$

2.10 Biofilm Assay

The capacity of *E. coli* strains to form a biofilm was assayed as described previously, with a few modifications (Ferrieres and Clarke, 2003). Briefly, bacteria containing the appropriate plasmids were grown overnight in LB at 30°C with agitation and diluted to an OD_{600}=0.01 in LB. Aliquots of 125 µL of the diluted culture were added into the wells of a polyvinylchloride (PVC) microtitre plate and the plate was incubated at 30°C without shaking. After 48h the planktonic bacteria were removed by aspiration and the wells were washed with PBS. To observe biofilm formation, 200 µL of 0.1% (w/v) crystal violet (CV) was added to each well and the wells were incubated at room temperature for 15 min before rinsing with PBS. To quantify biofilm formation the CV was dissolved into 200 µL of ethanol and CV concentration was determined by measuring the OD_{595} of a 100 µL of the sample in a new PVC plate by a plate reader (GENios, TECAN®).

The capacity of *Photorhabdus* to form a biofilm was performed as described above, except a polypropylene (PP) plate was used in stead of the PVC plate. Overnight culture was diluted to an OD_{600}=0.05, and 200 µL of the diluted culture was inoculated to each well of 96-well plate. To visualize the biofilm, 250 µL 0.1% (w/v) CV was added to the wells and the biofilm formation was quantified by dissolving CV by 250 µL ethanol and 100 µL of the sample was taken to a new plate for measurement by a plate reader as described above.

2.11 Motility Test

Bacterial strains of interest were grown overnight in a liquid culture, diluted to an OD_{600}=1 and 3 µL of the suspension was pipetted onto motility agar. The plates were incubated at 28°C and the motility of bacteria was assesseded by measuring the diameters of the halo formed after incubation.

2.12 Construction of *Photorhabdus* mutant strains

2.12.1 PCR amplification of knockout fragment

The *Photorhabdus rcsC/B* mutants were constructed using a modified 3-step PCR (Ferrieres *et al.*, 2004). In the first PCR step, about 600 bp of genomic fragments corresponding to the upstream regions of each gene to be knocked-

out were amplified using gene-specific primer 1 and primer 2 (Table 2.3), genomic DNA from *Photorhabdus luminescence* TT01, and KOD polymerase (Merck). Fragments corresponding to the downstream region of each gene were similarly amplified using the gene-specific primer 3 and primer 4 (Table 2.3). The complementary region in primer 2 and primer 3 facilitates the linking of the two fragments during a primer-free PCR step. In order to amplify the resulting knockout fragment, 10 µL of the reaction mixture was added to a 50 µL PCR mixture containing primer 1 and primer 4 (Fig. 2.2).

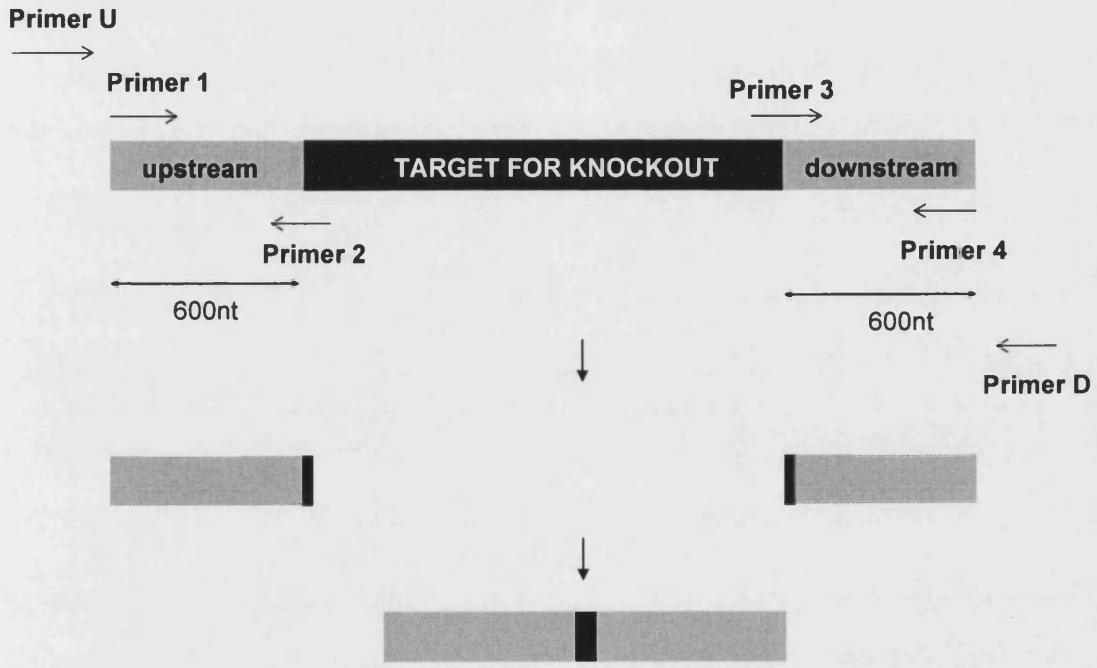

Figure 2.2 Schematic representation of constructing gene knockout clones. Approximately 600 nt of DNA upstream and downstream of the target genes are amplified separately with primer pairs. Primers 1 to 4 are designed to leave only stop and start codons of target gene after deletion. The complementary region in primer 2 and primer 3 facilitate the linking of the two fragments by a primer-free RCR. Primer 1 and primer 4 were used to amplify the knockout fragment, which was then cloned into appropriate vector. Primer U and Primer D are designed for PCR screening of mutants for the appropriate gene knockout.

2.12.2 Construction of knockout plasmid

The knockout fragment was purified and digested with *Sph*I and *Sac*I and cloned into the same site in pDS132 (Philippe *et al.*, 2004). The ligation mixture was electroporated into EC100D *pir*$^+$ (Epicentre®) and knockout plasmids were purified and moved to S17-1 λpir using the $CaCl_2$ method of transformation.

2.12.3 Conjugation

A single colony of S17-1 λpir with the desired plasmid was picked and grown overnight in LB/Cm broth; an overnight culture of TT01 cells was prepared at the same time. Both strains were inoculated into fresh MgLB before the cells were collected when the OD_{600}=0.5. The cells were pelleted and washed twice with equal volume of 4 mL of TT01 (recipient) and 1 mL of *E. coli* donor were spun down, mixed, and resupended in MgLB to a final volume of 200 μL. Conjugation was carried out by leaving the mixture on a MgLB agar at 30°C overnight. The conjugation mixture was recovered from the plate by adding 3 mL of MgLB and scraping the cells with a spreader. Appropriate volumes (10, 50, 100 μL) of the bacterial suspension were spread onto the selective LB/Rif/Cm agar plates and incubated at 30°C for 48h. The remaining mixture was frozen at -80°C in 20% glycerol.

Single colonies from the LB/Rif/Cm agar plates were inoculated into LB broth, and incubated at 30°C overnight. Serial dilution of the overnight culture was then spread onto LB/Sucrose plates. 100 colonies were picked and transferred to LB/Cm and LB/Sucrose plates to identify sucrose resistant and chloramphenicol sensitive colonies.

Colonies with the appropriate resistant profile (i.e., Cm^s, Suc^r) were checked by PCR using primers outside of the knockout target region (primer U and primer D). Successful gene knockouts were identified by the size difference of PCR products (Fig2.3). The PCR products were also sequenced to confirm the integrity of deletion.

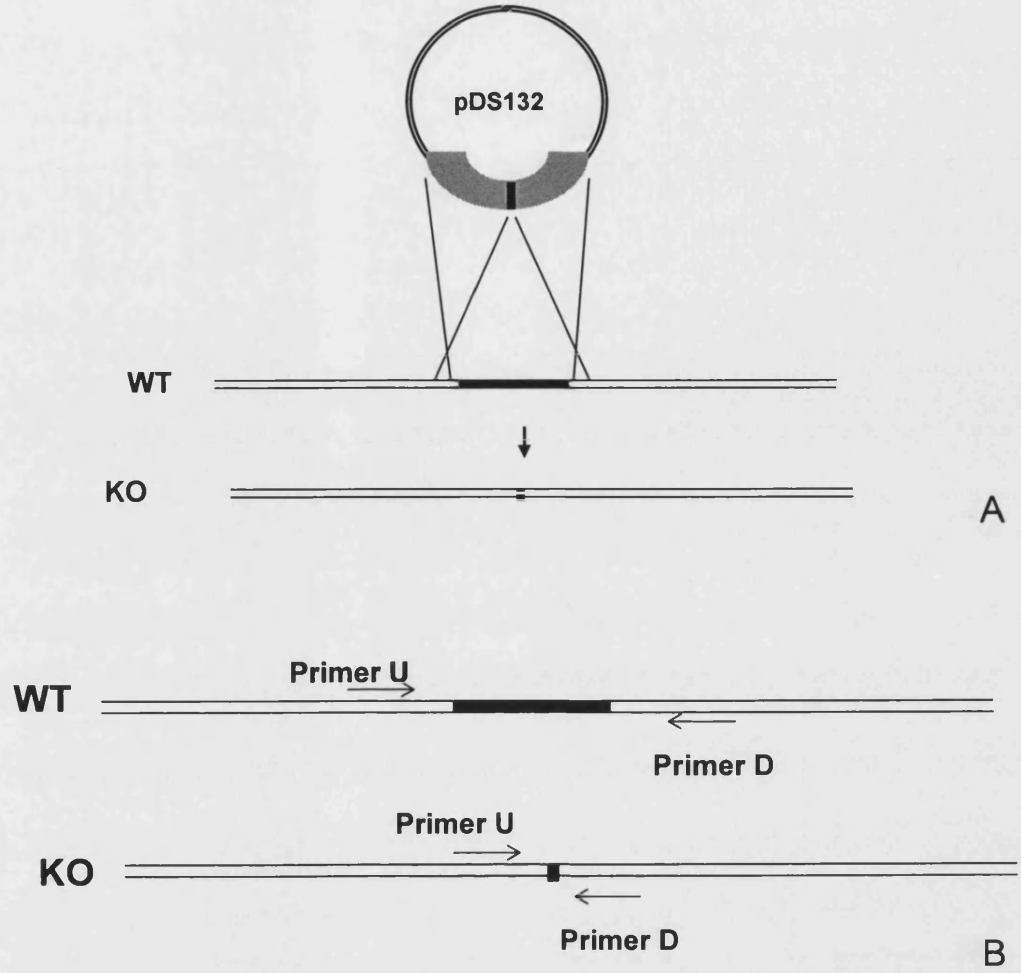

Figure 2.3 Schematic representation of constructing of gene knockout. (A) The DNA fragement flanking target gene is cloned into pDS132. The target gene was deleted from chromosome by allelic exchange between the recombinant plasmid and chromosome. (B) Wild type (WT) and gene knockout (KO) can be identified by the size difference of PCR products using primer U and D.

2.13 Phenotypic characterisation of *Photorhabdus*

2.13.1 Growth curve and bioluminescence measurements

Single colonies of *P. luminescens* strains of interest were inoculated into 3 mL LB cultures and grown overnight. Cultures were diluted to an OD_{600}=0.05 and incubated at 30°C, with shaking at 200 rpm. The OD_{600} was measured at appropriate time intervals and 100 μL of bacterial culture was taken to measure bioluminescence using a luminometer (GENios, TECAN®)

2.13.2 Dye uptake

Overnight cultures of *P. luminescens* strains were diluted with fresh LB to give an OD_{600} of 1.0 and 5μL was spotted onto the following agars: EMB (Eosin Methylene Blue lactose sucrose agar), MacConkey and NBTA (Nutrient agar, bromothymol blue, 2,3,5-tetrazolium chloride) and incubated at 30°C for 48 h to check for dye uptake (Table 2.2).

2.13.3 Siderophore, lipase and protease production

Overnight cultures of *P. luminescens* were diluted with fresh LB to give an OD_{600} of 1.0 and 5μL was spotted onto CAS, LIA and PIA plates. Siderophore production is apparent as an orange halo formed around bacterial colony on CAS agar. Lipase production was tested on LIA agar (Nutrient agar containing 0.5% [v/v] Tween 80) and protease production was tested on PIA agar (containing 2% [w/v] gelatine), respectively. The production of lipase and protease was indicated by a halo formed around the bacterial colony (Table 2.2).

2.13.4 Catalase Production

The *Photorhabdus* strains of interest were grown overnight and resuspend to an OD_{600} of 1.0, 10μL of suspension were pipetted onto a glass slide and 10μL of 3% (v/v) hydrogen peroxide were pipetted directly onto the suspension. Small bubbles and fizzing indicate catalase production.

2.13.5 Antibiotic production

Overnight cultures of *P. luminescens* were diluted with fresh LB to give an OD_{600} of 1.0 and 5μL was spotted on LB plates and incubated overnight. 1 mL of an overnight culture of *Micrococcus luteus* was mixed with 100 mL molten soft agar and poured over the colonies on the LB plates. Plates were incubated at 30°C for 48 h and antibiotic production was indicated by the inhibition of growth of *M. luteus* around the *Photorhabdus* colony.

2.14 Symbiosis assays

2.14.1 Surface sterilisation of nematode

Nematodes stocks were maintained by passage through final instar larvae of the Greater Waxmoth, *Galleria mellonella* (supplied by Livefood, UK). Nematodes were sterilised in 0.4% (w/v) hyamine for 15 min, and washed three times with sterile PBS. The nematodes were kept in PBS and stored at 4°C.

2.14.2 Growth and development of *Heterorhabditis* on *P. luminescens*

In vitro symbiosis assays were performed using lipid agar plates (Dunphy and Chadwick, 1989) inoculated with the *P. luminescens* strain of interest. Bacteria were grown overnight in LB broth and 50 µL were spread onto lipid agar in the form of a large "Z" and incubated for 72 h at 30°C. Approximately 50 surface sterile *H. bacterophora* TT01 infective juvenile (IJ) nematodes were added to the bacterial biomass and the plates were further incubated at 25°C. Development and reproduction of the nematodes was monitored over a period of weeks using a Nikon SMZ1500 stereo light microscope. IJs were collected from the lid of the Petri dish by washing with PBS and the collected IJs were stored at 4°C.

2.14.3 Retention of bacteria by nematodes

A single surface-sterilised IJ was homogenised in 100µL PBS using a pellet pestle. 50µL of the suspension was plated onto LB/Rif plate and incubated at 30°C for 48 h. The level of bacteria retention in the IJs was determined by counting the CFU.

2.15 Pathogenicity assay

2.15.1 Virulence of *P. luminescens* by injection

P. luminescens was grown overnight in LB broth and the bacteria were washed three times with PBS and adjusted to an OD_{600}=1 in PBS. The bacterial suspension was adjusted to a final cell density of 10^4 cells/mL, and 10µL of the suspension (equivalent to 100 cells) was directly injected into the hemocoel of Waxmoth larvae (*Galleria mellonella*) using a Hamilton syringe. The injection was repeated with 10 *Galleria* larvae for each strain used. The insects were incubated at 25°C and monitored over 72 h.

2.15.2 Reinfection of nematode carrying *P. luminescens*

Nematodes carrying *P. luminescens* strain of interest were surface sterilised as described. 10 *Galleria* larvae were placed between two 90 mm circular discs of Whatman filter paper in a 90 mm Petri dish. The bottom filter paper was moistened with approximately 600 IJs resuspended in 1 mL of PBS. The Petri dishes were incubated at 25°C and insect death was monitored over 72 h.

2.15.3 Recovery of nematodes

Nematodes were recovered from the infected *G. mellonella* cadavers using White traps (White, 1927). These were constructed in 90 mm Petri dish by position a 50 mm filter paper in a 50 mm dish as a platform. Insect cadavers were placed on the moistened filfter paper on the platform and 12 mL of PBS was added in the 90 mm Petri dish. Nematodes emerging from the insect cadavers were collected in the suspension PBS.

2.16 Biofilm assay of *Photorhabdus* in flowcell chamber system

The dynamic of biofilm formation by *Photorhabdus* was followed using flowcell. The flowcell chamber system was assembled with autoclaved silicon tubes connecting the chamber and bottles as shown in Figure 2.5. The flow in the system was generated by a Watson Marlow 250S peristaltic pump. The system was sterilised by pumping 0.5% (v/v) hydrochlorite through the system at 0.5 rmp for 2-3 hrs. After sterilisation, the system was saturated by pumping culture media (modified FAB medium supplemented with 2% LB) through the system at 1.75 rpm before inoculation. *Photorhabdus* strains were transformed with pSU2007 (Martinez and de la Cruz, 1988), which constitutively expresses GFP. *Photorhabdus* cultures containing pSU2007 were grown overnight at 30°C in LB then diluted to an OD_{600}=0.05 in PBS. The flowcell chambers were inoculated by direct injection of 250 µL of the diluted overnight culture with a small syringe. The injection area was immediately sealed with silicon sealant. The chambers were inverted and incubated without flow for 1 h. The pump was started 1 h after inoculation at 1.75 rpm. Microscopic observations and image acquisitions were performed on a Zeiss LSM 510 confocal laser scanning microscope at 12 h, 21, h, 36 h and 61 h.

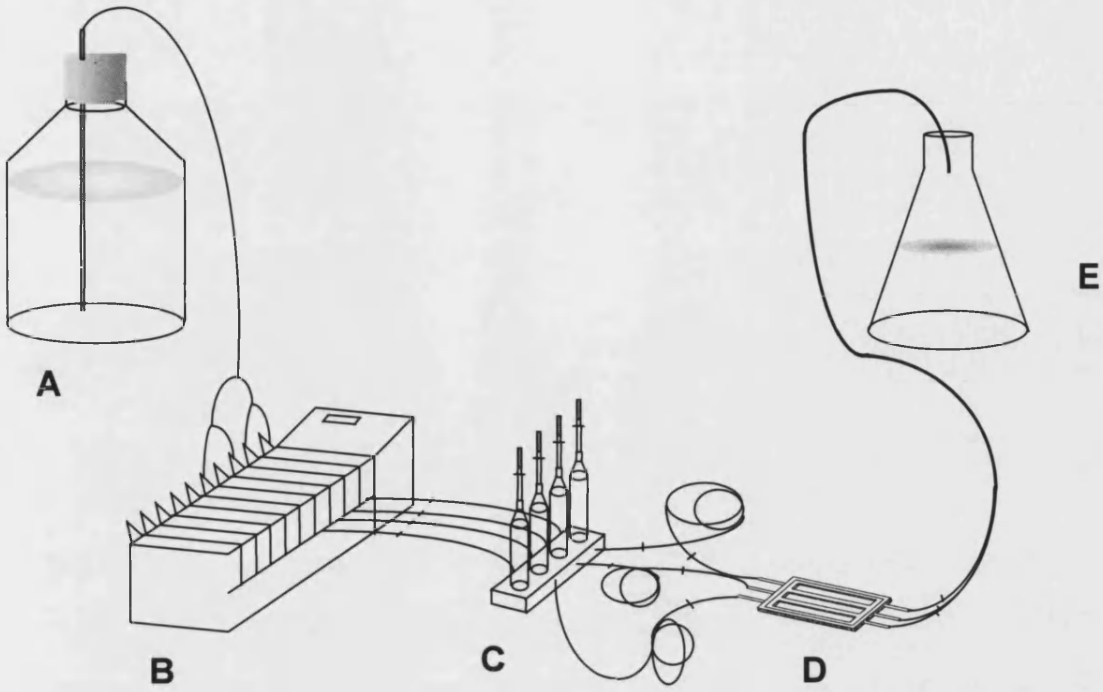

Figure 2.5 The flowcell chamber system for dynamic biofilm formation study. The flowcell chamber was made by mounting a coverglass to drilled Plexiglass. The system was assembled by connecting the media bottle, pump, bubble traps and flow cell by silicon tubings. Appropriate culture media were constantly running through the system .The flow channel media outlet is collect A: media bottle, B: Watson Marlow pump, C: bubble traps, D: flowcell chamber, E: waste bottle.

Chapter 3
Comparative Functional Analysis of RcsC from Different *Enterobacteriaceae*

3.1 Introduction

The Rcs phosphorelay controls many genes including those are involved in the production of capsule and has been implicated in biofilm formation in *E. coli* K-12 (Ferrieres and Clarke, 2003). The phosphorelay also controls virulence in the pathogenic strain *E. coli* O157 (Tobe *et al.*, 2005). The Rcs phosphorelay involves two membrane-associated proteins, RcsC, and RcsD, a soluble response regulator, RcsB, and two proteins that are presumed to modulate the activity of RcsC, RcsF and YrfF. An auxiliary protein, RcsA, is also involved in regulating target gene expression (Majdalani and Gottesman, 2005). In this study, the focus is on the RcsC sensor kinase in *E. coli* and other *Enterobacteriaceae*. In order to determine the interactions between RcsC and the other components of this system a comparative study was undertaken. Initially, the *rcsC* gene from different *Enterobacteriaceae* was tested for its ability to complement an *rcsC* mutation in *E. coli* K-12 in terms of activation of *cps* expression in response to DjlA overproduction, phosphatase activity and biofilm formation. The objective of these experiments was to combine this functional data with comparative sequence analysis so that regions important for RcsC signaling could be identified.

3.2 Results

3.2.1 Comparison and cloning of *rcsC* from other *Enterobacteriaceae*

3.2.1.1 RcsC proteins from other *Enterobacteriaceae*

The *rcs* loci are conserved in the genomes of the *Enterobacteriaceae*, however, they can be divided into at least three categories as seen in Figure 1.11. At least one example from each category was chosen for this comparative study. Full-length *rcsC* genes were cloned from *E. coli* K-12, *E. coli* O157, *Salmonella enterica* serovar Typhimurium LT2, and *Yersinia pestis*. Clones containing inserts of the correct size were identified by restriction digest analysis and purified plasmids were sequenced to confirm the integrity of the inserts. The plasmids carrying the *rcsC* gene from *E. coli* O157, *S. typhimurium* LT2, and *Y. pestis* (encoding $RcsC_{O157}$, $RcsC_{LT2}$ and $RcsC_{YP}$) were designated as pBMM601, pBMM602, and pBMM603, respectively. The plasmid carrying the *rcsC* gene from *E. coli* K-12 ($rcsC_{K12}$), pBMM102, was obtained from a previous study (Clarke *et al*., 2002). All the plasmids were constructed using pBMM101, a

pTRC99a-derived vector constructed in our laboratory to facilitate the C-terminal tagging of proteins with a *c-myc* epitope. In addition, expression of the cloned genes is under the control of the inducible P_{trc} promoter. An alignment of the predicted amino acid sequences of the different RcsC homologues is shown in Figure 3.1.

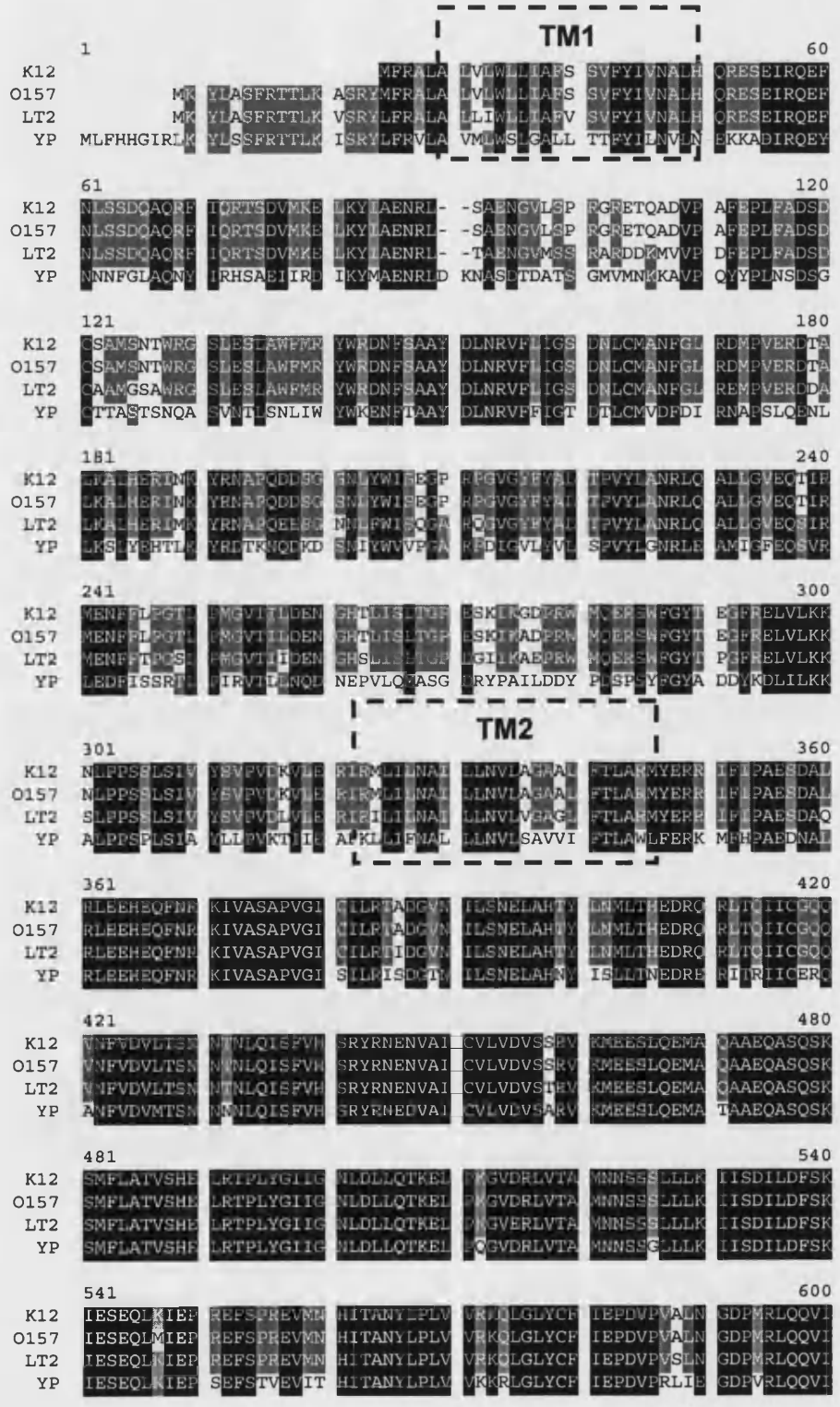

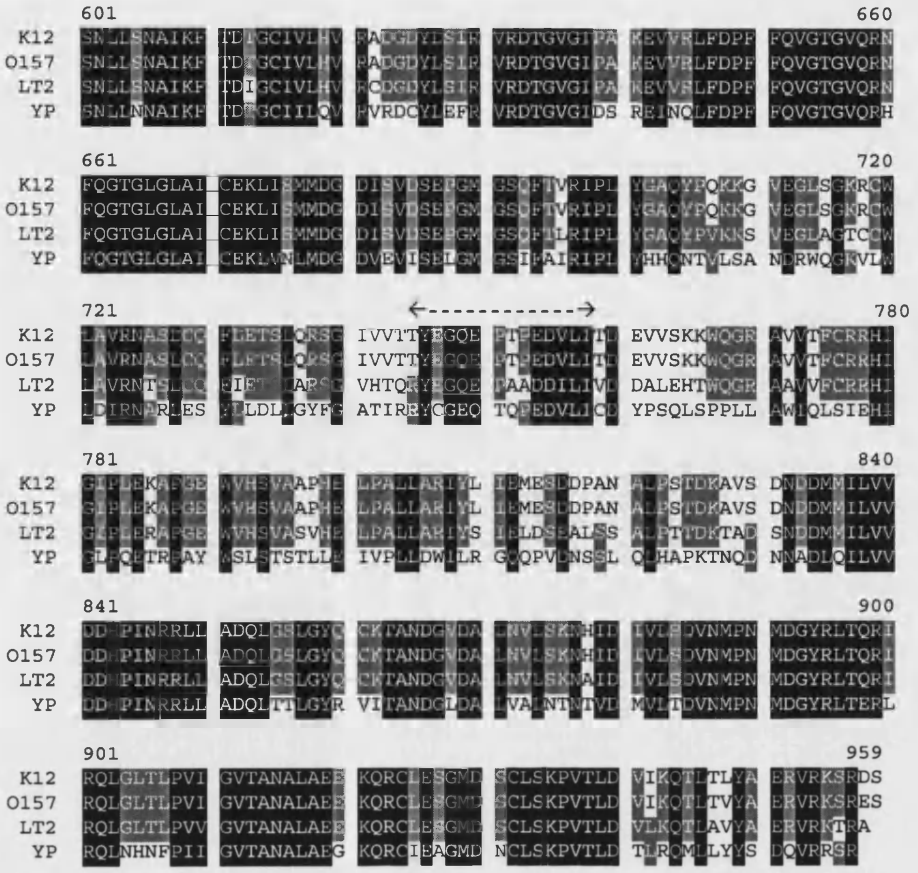

Figure 3.1 Multiple alignment of the RcsC proteins from *E. coli* K-12 (K12), EHEC O157 (O157), *S. enterica* serovar Typhimurium (LT2), and *Y. pestis* (YP). Alignment was generated using Multalin software (http://prodes.toulouse.inra.fr/multalin/multalin.html).

The predicted transmembrance domains (TM1 and TM2) are shown in boxes. The region used for generating peptide antibody is labelled by double arrow.

3.2.1.2 Immunoblot of the RcsC proteins

Although a *c-myc* epitope was added to the C-terminus of the different RcsC proteins, a monoclonal antibody against the *c-myc* epitope did not detect these proteins after immunoblotting. However, the antibody was able to detect the *c-myc* epitope of a truncated form of RcsC, consisting of the cytoplasmic region only, by the same immunoblotting procedure. Therefore, the *c-myc* antibody does not appear to be sensitive enough to detect the membrane-associated RcsC protein in total cell lysates (data not shown).

Alternatively, RcsC-specific antiserum was raised against the 13 amino acid peptide (TYEGQEPTPEDVL) located between the transmitter domain and the receiver domain (residue 719-731) of $RcsC_{K12}$. The polyclonal antibody was purified from this resulting antiserum by Protein G. The antibodies were tested against total cell extracts from *rcsC* mutant cells expressing the different plasmids and each showed specific binding to a protein that migrated with a molecular weight of approx 100kDa (the predicted MW of RcsC is 106kDa) in cells producing $RcsC_{K12}$ and $RcsC_{O157}$ (Fig. 3.2). This suggests that the *rcsC* gene is being expressed from pBMM102 and pBMM601. The $RcsC_{K12}$ and $RcsC_{O157}$ proteins can be clearly detected using RcsC-specific antibody when expression is induced by the addition of IPTG.

The region between the transmitter domain and receiver domain is divergent amongst the RcsC homologues in the different *Enterobacteriaceae* (see Figure 3.1) and the anti-RcsC antibody could not detect either $RcsC_{LT2}$ or $RcsC_{YP}$. However, as all of the *rcsC* genes in this study were expressed under the control of the same P_{trc} promoter it is likely that all genes are expressed at the same level.

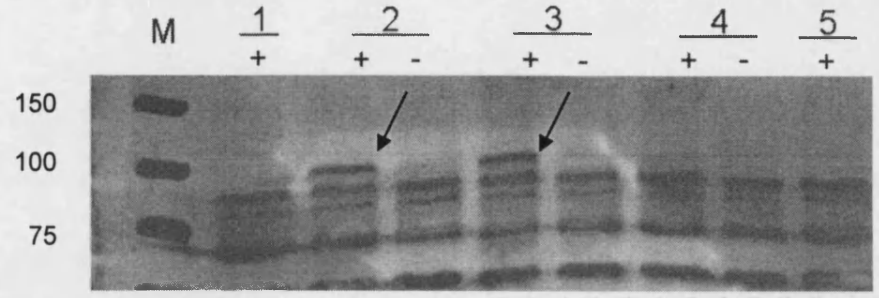

Figure 3.2. Western blotting of RcsC proteins. BMM520 (*rcsC52::Tn10*), carrying pBMM101 (vector), pBMM102, pBMM601, pBMM602, and pBMM603 (encoding $RcsC_{K12}$, $RcsC_{O157}$, $RcsC_{LT2}$ and $RcsC_{YP}$, respectively) were cultured overnight at 37°C in LB broth supplemented with 5 mM IPTG and collected by centrifugation. 0.4 OD_{600} equivalents were analysed by sodium dodecyl sulphate-polyacrylamide gel electrophoresis and immunoblotted with a polyclonal antibody raised against $RcsC_{K12}$.

The -/+ indicate the addition of IPTG. Sample 1-5, pBMM101 pBMM102 ($RcsC_{K12}$), pBMM601 ($RcsC_{O157}$), pBMM602 ($RcsC_{LT2}$), and pBMM603 ($RcsC_{YP}$). Arrows indicated the band that corresponds to RcsC protein.

3.2.2 Complementation of *rcsC* mutants by *rcsC* genes from other *Enterobacteriaceae*

3.2.2.1 RcsC proteins from other *Enterobacteriaceae* complement the induction of *cps-lacZ* expression by DjlA overproduction

One of the signals that activates the Rcs phosphorelay is DjlA overproduction (Clarke *et al.*, 1997). Therefore, when DjlA is overproduced, activation of the Rcs phosphorelay can be detected by an increase in *cpsB-lacZ* expression. Moreover, it has been shown that the induction of *cpsB-lacZ* expression by DjlA overproduction requires the RcsC protein (Clarke *et al.*, 2002). Therefore, to test whether the different enteric *rcsC* homologues could respond to DjlA overproduction, strain PSG1038 (*rcsC52::Tn10 cpsB-lacZ*), carrying the DjlA-overproducing plasmid pPSG961-31 (*djlA* expression is under the control of the

arabinose inducible P_{BAD} promoter) (Clarke *et al.*, 1997), was transformed with pBMM102, pBMM601, pBMM602, and pBMM603 and the strains were grown overnight at 30°C on LB agar or LB agar supplemented with 0.2% (w/v) arabinose. Interestingly, the PSG1038 strain, carrying the pBMM101 vector, had a significant basal expression of *cpsB-lacZ* of 64.1±14.7 Miller Units, indicating that RcsC has a function in the negative regulation of *cps* gene expression (see Figure 3.3). In the absence of arabinose the Rcs phosphorelay is not activated as DjlA production is not induced and, as expected, strains expressing $rcsC_{K12}$, $rcsC_{O157}$ and $rcsC_{LT2}$ expressed low levels of *cpsB-lacZ* (see Figure 3.3). However, cells carrying pBMM603, encoding $RcsC_{Yp}$, did express *cpsB-lacZ* at a level of 57.7±13.9 Miller Units even in the absence of the DjlA signal suggesting that the $RcsC_{YP}$ might be defective in the negative regulation of *cps* expression.

When arabinose was present in the LB agar plates, bacteria carrying pBMM601 and pBMM102 expressed similar levels of *cpsB-lacZ* suggesting that $RcsC_{O157}$ and $RcsC_{K12}$ function in a similar way. Similarly, $RcsC_{LT2}$ (encoded in pBMM602) also responded positively to the DjlA signal (as seen by an increase in *cpsB-lacZ* expression), although the level of *cpsB-lacZ* induction is less than that observed with $RcsC_{K12}$ or $RcsC_{O157}$. On the other hand, $RcsC_{YP}$ appeared more responsive to the DjlA signal and the level of *cpsB-lacZ* expression was 4-fold higher in cells producing $RcsC_{YP}$ compared to cells that producing either $RcsC_{K12}$ or $RcsC_{O157}$. These results suggested that all of the clones were producing RcsC proteins with kinase activity and all of these proteins were capable of responding to the DjlA signal. The differences in the levels of activity might be due to how the RcsC homologues interact with either DjlA or downstream components of the phosphorelay, i.e., RcsD.

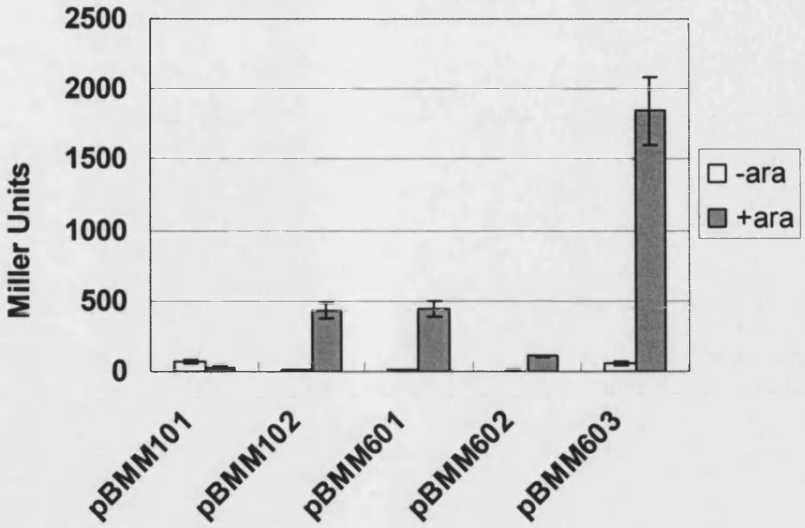

Figure 3.3. RcsC proteins from other *Enterobacteriaceae* complement the induction of *cps-lacZ* expression by DjlA overproduction. PSG1038 (*rcsC52*::Tn10 *cpsB-lacZ*) carrying a DjlA overproducing plasmid pPSG961-31 was transformed with plasmid pBMM101 (vector), pBMM102 ($RcsC_{K12}$), pBMM601 ($RcsC_{O157}$), pBMM602 ($RcsC_{LT2}$), and pBMM603 ($RcsC_{YP}$). Cells were cultured overnight at 30°C on LB agar plates in the absence (white column) or presence of 0.2% (w/v) L-arabinose (grey column). To determine the level of *cpsB-lacZ* expression, cells were harvested and assayed for β-galactosidase activity. The results shown are the mean of three independent biological replicates, and the error bars represent standard deviations.

3.2.2.2 $RcsC_{YP}$ is less sensitive to temperature and RcsA limitation

RcsA is required for the optimal expression of a sub-set of the Rcs-regulated genes and RcsA functions by modulating the DNA-binding ability of the RcsB response regulator by forming heterodimers with phosphorylated RcsB (Ebel and Trempy, 1999). The maximal induction of capsule synthesis and *cps* expression requires RcsA and the level of RcsA in the cell is limited by proteolysis, particularly at 37°C. Therefore, capsule synthesis is optimal at lower temperatures as this permits the accumulation of RcsA (Stout *et al.*, 1991). As seen in Figure 3.4, at 37°C in liquid culture the activation of *cpsB-lacZ* expression by DjlA overproduction in cells producing $RcsC_{K12}$, $RcsC_{O157}$, $RcsC_{LT2}$ and $RcsC_{YP}$ was significantly lower when compared to cells grown at 30°C. However, the level of *cpsB-lacZ* expression in cells producing $RcsC_{YP}$ still remained at a relatively high level at 37°C. The presence of high levels of active (i.e. phosphorylated) RcsB can make *cps* expression relatively independent of RcsA (Stout *et al.*, 1991). Therefore it appears that $RcsC_{YP}$ is more sensitive to DjlA overproduction and is capable of producing significantly higher levels of active RcsB in the cell than the other RcsC homologues.

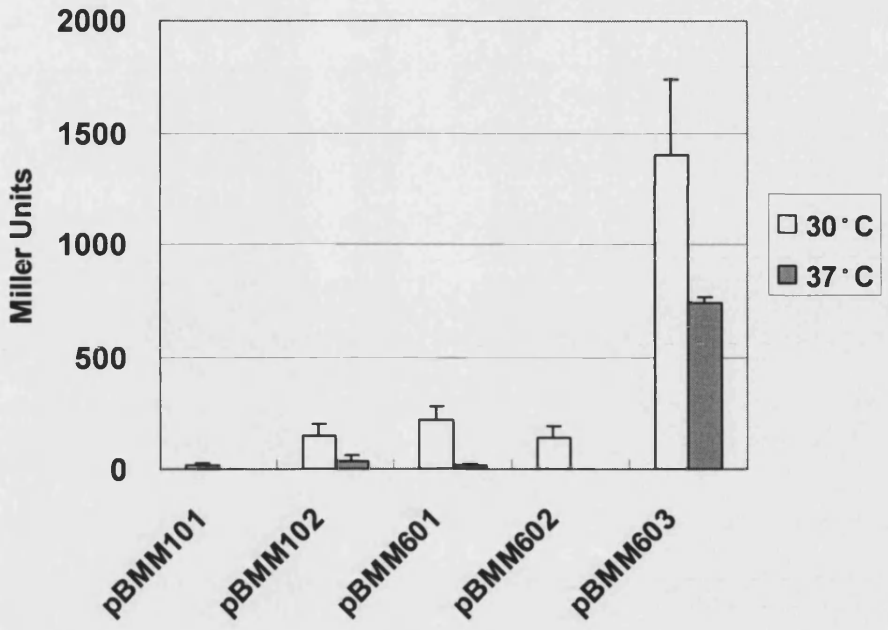

Figure 3.4. Induction of *cps-lacZ* expression by DjlA overproduction at 30°C and 37°C. PSG1038 (*rcsC52*::Tn10 *cpsB-lacZ*)/pPSG961-31 (P_{araBAD}-*djlA*$^+$) was transformed with plasmid encoding RcsC proteins from different *Enterobacteriaceae*, pBMM101 (vector), pBMM102, pBMM601, pBMM602, and pBMM603 (encoding $RcsC_{K12}$, $RcsC_{O157}$, $RcsC_{LT2}$ and $RcsC_{YP}$, respectively). Cells were cultured overnight at 30°C (white column) and 37°C (grey column) in LB broth in the presence of 0.2% L-arabinose. To determine the level of *cpsB-lacZ* expression, cells were harvested and assayed for β-galactosidase activity. The results shown are the mean of three independent biological replicates, and the error bars represent standard deviations.

3.2.2.3 Synergistic effect between DjlA overproduction and growth on solid surface

It has been previously shown that the RcsC sensor kinase responded to growth on a solid surface and was transiently activated by transferring growing cells from a liquid culture onto a solid surface (Ferrieres and Clarke, 2003). Therefore, both DjlA overproduction and solid surface may be considered as signals for RcsC activation. Moreover, it had been previously observed that RcsC appeared more sensitive to DjlA overproduction when cells were cultured on agar plates rather than in broth i.e. the level of *cpsB-lacZ* expression is significantly higher in cells growing on agar plates compared to the same cells growing in liquid cultures (Clarke, personal communication). Therefore the level of *cpsB-lacZ* expression observed with both signals is higher than the activity observed with each signal individually i.e. these signals appear synergistic. This suggests that the solid surface signal and DjlA overproduction maybe sensed independently by RcsC. To determine if the cloned RcsC homologues were capable of this synergy, bacteria were grown on either an agar plate or in liquid culture at 30°C in the presence of 0.2% (w/v) arabinose. Under these conditions, the level of *cpsB-lacZ* expression in bacteria grown on LB agar (i.e. solid) was twice that of bacteria grown in liquid culture when $RcsC_{K12}$ or $RcsC_{O157}$ was produced in the cells. There is also a synergy observed in cells that are producing $RcsC_{YP}$ although *cpsB-lacZ* expression is only increased by 32% when cells are grown on solid surface. However, the level of *cpsB-lacZ* expression in cells producing $RcsC_{LT2}$ is the same regardless of whether the cells are cultured in liquid culture or on LB agar, suggesting that the solid surface signal is not perceived by the $RcsC_{LT2}$ homologue (Fig. 3.5).

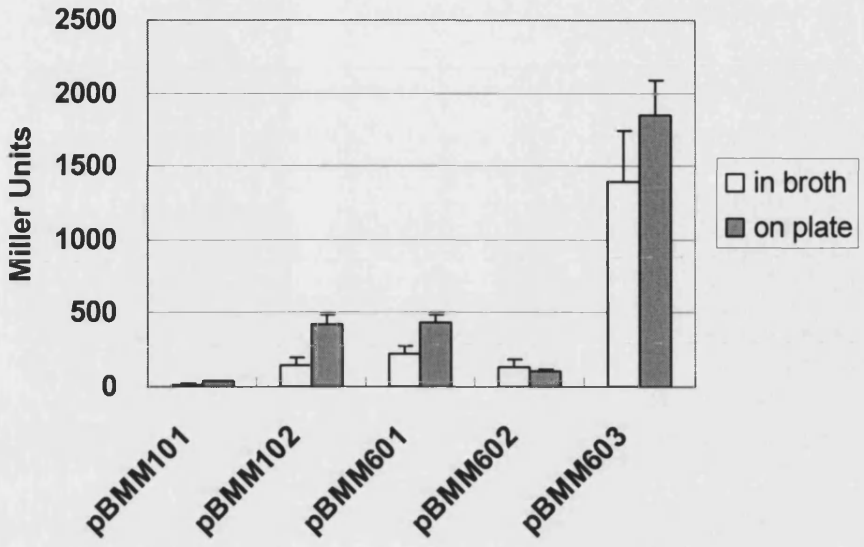

Figure 3.5. Synergistic effect of DjlA overproduction and growth on a solid surface. PSG1038 (*rcsC52*::Tn10 *cpsB-lacZ*)/pPSG961-31 (P_{araBAD}-*djlA*$^+$) was transformed with plasmid pBMM101 (vector), pBMM102, pBMM601, pBMM602, and pBMM603 (encoding $RcsC_{K12}$, $RcsC_{O157}$, $RcsC_{LT2}$ and $RcsC_{YP}$, respectively). Cells were cultured overnight at 30°C in LB broth (white column) and on LB agar plates (grey column) in the presence of 0.2% (w/v) L-arabinose. To determine the level of *cpsB-lacZ* expression, cells were harvested and assayed for β-galactosidase activity. The results shown are the mean of three independent biological replicates, and the error bars represent standard deviations.

3.2.2.4 RcsC proteins from other *Enterobacteriaceae* complement the *rcsC137* allele

Many sensor proteins have been shown to have both kinase and phosphatase activity and there is significant evidence to suggest that this is also the case for RcsC (Clarke *et al.*, 2002). The *E. coli* strain SG20907 has been shown to carry an allele of *rcsC*, *rcsC137*, that encodes a constitutively (i.e. signal-independent) active protein. The *rcsC137* mutation has been shown to be a point mutation in the receiver domain (A888V) of RcsC (Brill *et al.*, 1988; Majdalani *et al.*, 2005). Therefore the presence of *rcsC137* in the cell leads to a constitutively high level of *cpsB-lacZ* expression. The constitutive activity of RcsC137 can be complemented by the expression of a wild-type *rcsC* gene *in trans* and the dominant negative phenotype of the wild-type allele has led to the suggestion that RcsC137 has lost its phosphatase activity (Brill *et al.*, 1988). Therefore, the *rcsC* homologues were tested for phosphatase activity by measuring their ability to complement the *rcsC137* allele. Strain SG20907 was transformed with pBMM101, pBMM102, pBMM601, pBMM602 and pBMM603 and as expected, in cells transformed with pBMM101, i.e. the plasmid vector only, there is a high level of *cpsB-lacZ* expression (see Fig. 3.6). However, the level of *cpsB-lacZ* expression is reduced 10-fold when either $rcsC_{K12}$ or $rcsC_{O157}$ was expressed *in trans* (see Figure 3.6). Interestingly, the expression of $rcsC_{LT2}$ or $rcsC_{YP}$ *in trans* reduced *cpsB-lacZ* expression to an almost undetectable level (Fig. 3.6). Therefore all of the *rcsC* homologues are capable of complementing the *rcsC137* mutation suggesting that these genes encode proteins with phosphatase activity.

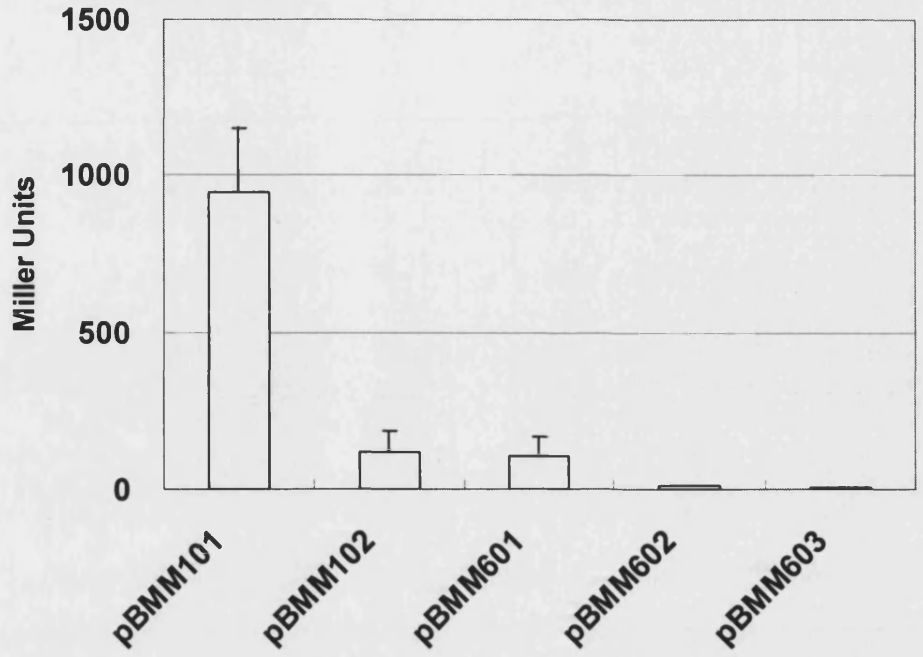

Figure 3.6. Complementation of the *rcsC137* allelle by RcsC homologues from the *Enterobacteriaceae*. SG20907 (*rcsC137 cpsB-lacZ*) was transformed with pBMM101 (vector), pBMM102, pBMM601, pBMM602, and pBMM603 (encoding $RcsC_{K12}$, $RcsC_{O157}$, $RcsC_{LT2}$ and $RcsC_{YP}$, respectively). Cells were cultured overnight at 30°C on LB agar plates and assayed for β-galactosidase activity. The results shown are the mean of three independent biological replicates, and the error bars represent standard deviations.

3.2.2.5 Complementation of biofilm formation in *rcsC* minus background

RcsC has been previously shown to be required for normal biofilm formation in *E. coli* K-12 (Ferrieres and Clarke, 2003). To test whether the different RcsC homologues could facilitate biofilm development, BMM520 (a $rcsC^-$ derivative of ZK2686), was transformed with the different *rcsC*-containing plasmids and incubated at 30°C, for 48 hours, without shaking in the well of a PVC microtitre plate. Planktonic bacteria were removed and crystal violet was used to determine the extent of biofilm formation (see Fig. 3.7). It is clear that biofilm formation in BMM520 can be complemented by $RcsC_{K12}$, $RcsC_{O157}$, and, at least partially, by

$RcsC_{LT2}$. However, cells carrying pBMM603, producing the $RcsC_{YP}$ homologue, formed even less biofilm than the BMM520 parental strain. Therefore, the $RcsC_{YP}$ protein was not only unable to support biofilm formation, but also appeared to have a further negative effect in biofilm formation.

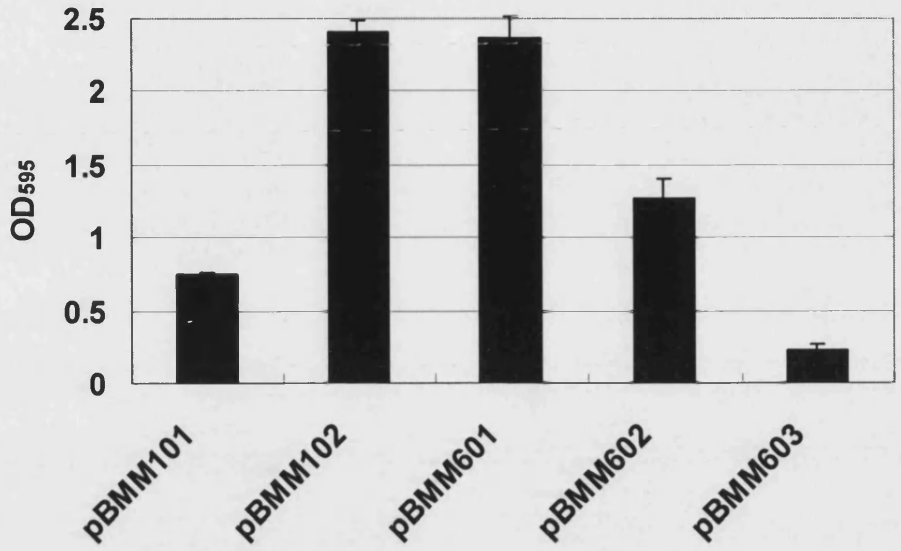

Figure 3.7. Complementation of biofilm formation of an *E. coli rcsC* mutant BMM520 (*rcsC52*::Tn10) by *rcsC* genes from other *Enterobacteriaceae*. BMM520 was transformed with pBMM101 (vector), pBMM102, pBMM601, pBMM602, and pBMM603 (encoding $RcsC_{K12}$, $RcsC_{O157}$, $RcsC_{LT2}$ and $RcsC_{YP}$, respectively). Cells were cultured overnight at 30°C in LB broth for 48 h. Biofilm formation was visualised by crystal violet staining. Crystal violet was then dissolved in ethanol and quantified by the absorbance of 595 nm. The results shown are the mean of three independent biological replicates, and the error bars represent standard deviations.

3.2.3 The functional analysis of RcsC chimeras of $RcsC_{K12}$ and $RcsC_{YP}$

3.2.3.1 Construction of chimeric RcsC proteins

The $RcsC_{YP}$ protein responded differently to input signals (i.e. DjlA and solid surface) than the other RcsC homologues; therefore it is possible that the biofilm defect of $RcsC_{YP}$ might be due to the fact that the input domain did not sense or interact with the environment in the same way as $RcsC_{K12}$. As shown in the alignment of four RcsC proteins (Fig. 3.1), the N-terminal region is the most divergent between the different RcsC homologues and it is thought that this region incorporates the signal input region. The full length $RcsC_{K12}$ and $RcsC_{YP}$ have 58.2% residue identity, and the identity of N-terminal regions and C-terminal regions are 52.8% and 63.9% respectively.

To investigate the importance of the input region during biofilm formation, the N-terminal regions of $RcsC_{K12}$ and $RcsC_{YP}$ were swapped to generate two chimeric proteins (see Figure 3.8). The recombinant plasmids were generated by taking advantage of a naturally occurring *Cla*I site (ATCGAT) in the $rcsC_{K12}$ sequence. Although $rcsC_{YP}$ does not have a *Cla*I site, the sequence at the corresponding site (TTCATG) encoded identical amino acids (Ser455 and Met456) as in $rcsC_{K12}$. PCR primer pairs were designed to introduce the *Cla*I site into $rcsC_{YP}$ during amplification of the 1.4kb fragment of DNA encoding the input domain of $RcsC_{Yp}$ and this was cloned into the *Nco*I-*Cla*I digested pBMM102 (see Materials and Methods). $RcsC_{YP\text{-}K12}$ is encoded by plasmid pBMM631 and is composed of the N-terminal part (Met1-Ser455) of $RcsC_{YP}$ and the C-terminal part of $RcsC_{K12}$. On the other hand, $RcsC_{K12\text{-}YP}$, encoded by pBMM639, is composed of N-terminal $RcsC_{K12}$ (Met1-Ser455) and the C-terminal part of $RcsC_{YP}$.

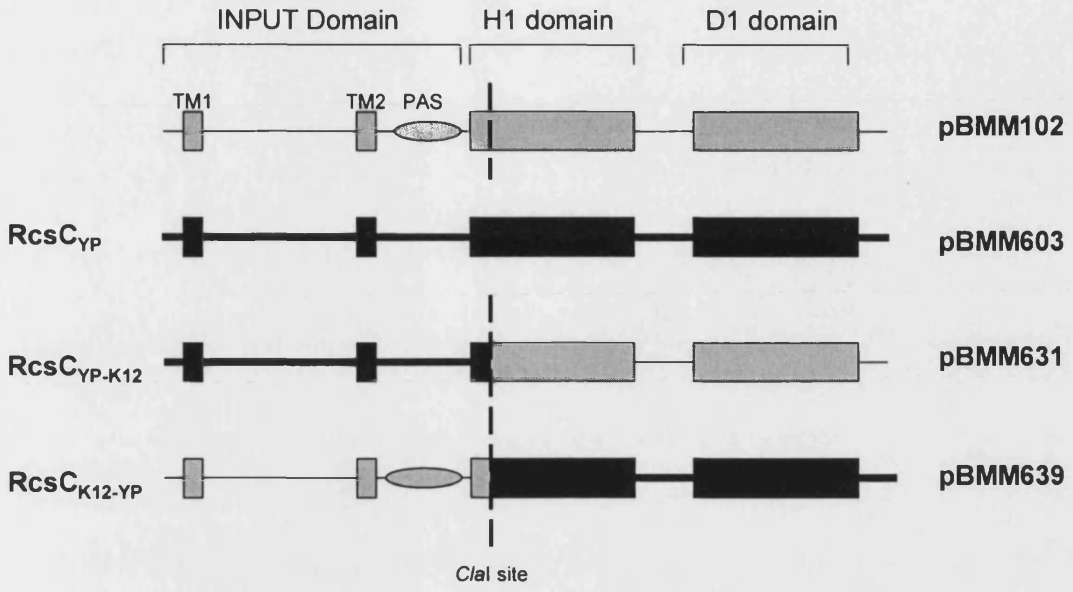

Figure 3.8. The modular architecture of RcsC chimeric proteins. RcsC$_{K12}$ is depicted in grey and RcsC$_{YP}$ in black. The input domain spans the cytoplasmic membrane and contains two transmembrane domains (TM1 and TM1). The *Cla*I site is indicated by a dashed line. The chimeric protein RcsC$_{YP-K12}$ consists of the input domain of Rcs$_{YP}$ and signalling domain of the RcsC$_{K12}$, encoded in pBMM631. In contrast, RcsC$_{YP-K12}$ consists of the input domain of Rcs$_{K12}$ and signalling domain of the RcsC$_{YP}$.

3.2.3.2 Biofilm formation ability with the chimeric proteins

To test for the ability of the chimeric RcsC proteins to support biofilm formation the plasmids were introduced into BMM520 and the cells were cultured in PVC microtiter plates as described in Materials and Methods. As expected cells producing RcsC$_{K12}$ from pBMM102 formed increased levels of biofilm compared to BMM520 whilst cells producing RcsC$_{YP}$ from pBMM603 formed less biofilm than BMM520 (see Figure 3.9). Interestingly, swapping the input domain of RcsC$_{YP}$ with that of RcsC$_{K12}$ restored biofilm formation. Therefore cells producing RcsC$_{K12-YP}$, encoded by pBMM639, did form increased levels of biofilm compared to BMM520. This suggests that the inability of RcsC$_{YP}$ to support biofilm formation in BMM520 is due to lack of an activity associated with the input domain (i.e. the N-terminal 455 amino acids). Moreover, when the input domain

of $RcsC_{K12}$ is replaced with the same domain from $RcsC_{YP}$ the ability to support biofilm formation in BMM520 is lost. Therefore, the input domain of $RcsC_{K12}$ is important during biofilm formation and it appears that $RcsC_{YP}$ is not interacting with the environment in the same way as $RcsC_{K12}$ during biofilm formation.

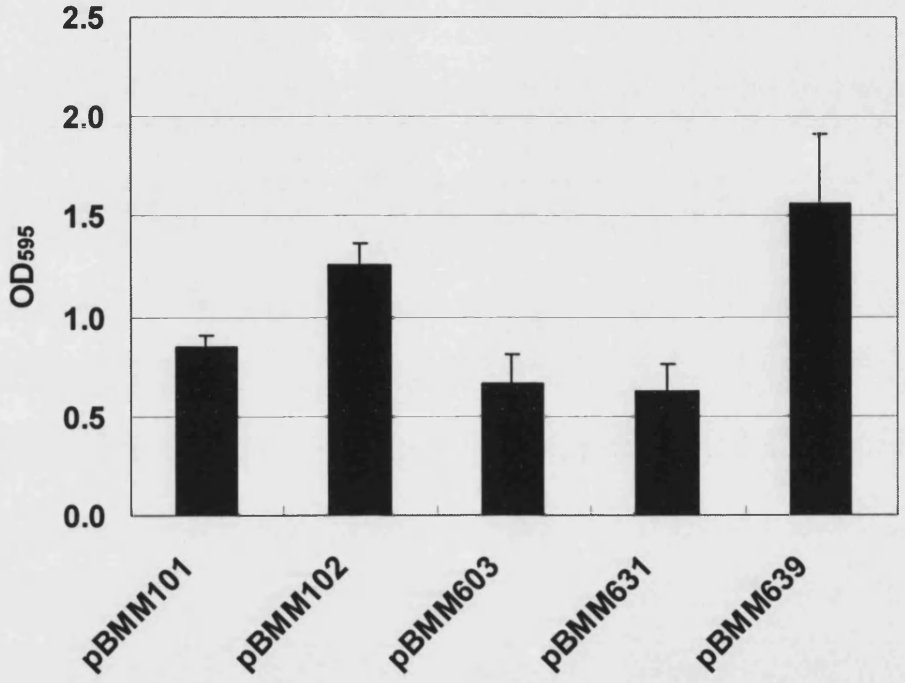

Figure 3.9. The N-terminal region of RcsC is important in biofilm formation. BMM520 (*rcsC52*::Tn10) was transformed with plasmid pBMM101 or derivatives carrying different *rcsC* alleles, pBMM102, pBMM603, pBMM631, and pBMM639 (encoding $RcsC_{K12}$, $RcsC_{YP}$, $RcsC_{YP\text{-}K12}$ and $RcsC_{K12\text{-}YP}$ respectively). Cells were cultured overnight at 30°C in LB broth for 48 h. Biofilm formation was visualised by crystal violet staining. Crystal violet was then dissolved in ethanol and quantified by the absorbance of 595 nm. The results shown are the mean of three independent biological replicates, and the error bars represent standard deviations.

3.2.3.3 The chimeric proteins respond to activation by DjlA

The ability of the chimeric proteins to respond to DjlA overproduction was also tested in strain PSG1038 (*rcsC52*::Tn10 *cpsB-lacZ*) containing pPSG961-31. In the absence of arabinose (i.e. DjlA is not overproduced), strains producing $RcsC_{YP}$ and $RcsC_{YP\text{-}K12}$ showed a low, but detectable level of *cpsB-lacZ* expression i.e. 57 Units and 150 Units respectively (see Fig. 3.10). On the other hand $RcsC_{K12}$ and $RcsC_{K12\text{-}YP}$ showed very low levels of *cpsB-lacZ* expression (10 Units and 7 Units respectively) suggesting that the activity observed with $RcsC_{YP}$ (see Fig. 3.2) is associated with the input domain of $RcsC_{YP}$. As expected, in the presence of arabinose (i.e. DjlA is overproduced), the chimeric proteins were responsive to DjlA overproduction and, in all cases, the level of *cpsB-lacZ* expression increased (see Fig. 3.10). However, the $RcsC_{K12\text{-}YP}$ chimera responded to DjlA overproduction at a level lower than $RcsC_{K12}$, as measured by lower levels of *cpsB-lacZ* expression (Fig. 3.10). In addition, *cpsB-lacZ* expression was higher in bacteria producing either $RcsC_{YP}$ or $RcsC_{YP\text{-}K12}$ compared to $RcsC_{K12}$ suggesting that the increased responsiveness to DjlA, originally observed with $RcsC_{YP}$ (see Fig. 3.3), is also associated with the input domain of $RcsC_{YP}$.

3.2.3.4 Phosphatase activity of $RcsC_{YP\text{-}K12}$ and $RcsC_{K12\text{-}YP}$

The phosphatase activity of the chimeric proteins was also tested in strain SG20907 (Brill *et al.*, 1988). As expected the level of *cpsB-lacZ* expression in SG20907 is reduced in the presence of either $RcsC_{K12}$ or $RcsC_{YP}$. Interestingly, both chimeric proteins were still able to reduce the level of *cpsB-lacZ* expression in the *rcsC137* background, but to a lesser extent than either $RcsC_{K12}$ or $RcsC_{YP}$ (Fig. 3.11). Although a certain amount of this observed decrease in apparent phosphatase activity might be explained by the basal kinase activity observed in $RcsC_{YP\text{-}K12}$ (see Fig. 3.10) these data do suggest that normal phosphatase activity might require both the the N-terminal and C-terminal regions of RcsC.

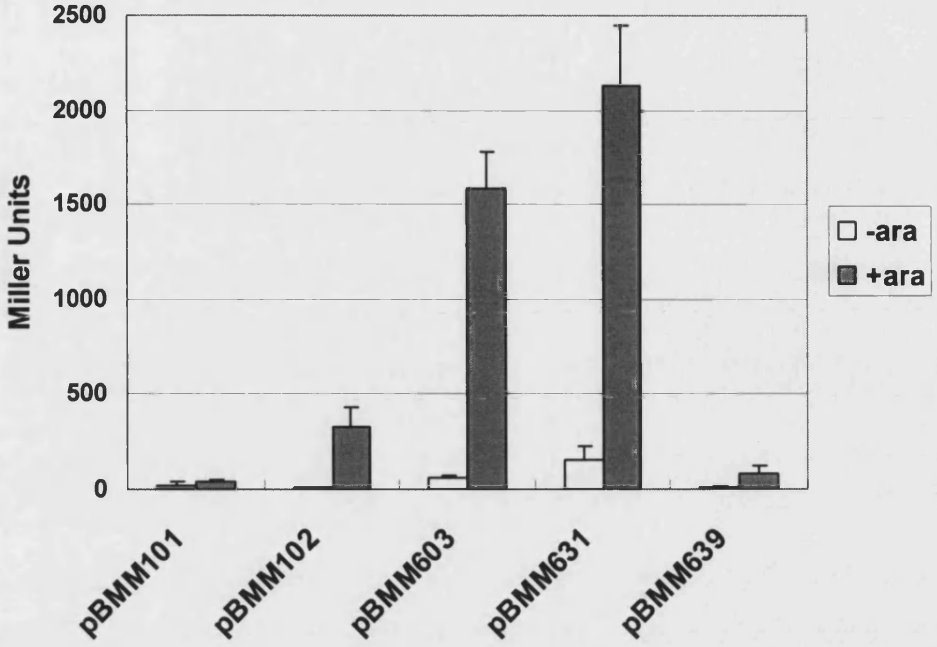

Figure 3.10. The chimeric RcsC proteins resond to DjlA overproduction. PSG1038 (*rcsC52*::Tn10 *cpsB-lacZ*)/pPSG961-31 (P_{araBAD}-*djlA*$^{+}$) was transformed with plasmid pBMM101 or derivatives carrying different *rcsC* alleles, pBMM102, pBMM603, pBMM631, and pBMM639 (encoding $RcsC_{K12}$, $RcsC_{YP}$, $RcsC_{YP\text{-}K12}$ and $RcsC_{K12\text{-}YP}$ respectively). Cells were cultured overnight at 30°C on LB agar plates in the absence (white column) or presence of 0.2% (w/v) L-arabinose (grey column). To determine the level of *cpsB-lacZ* expression, cells were harvested and assayed for β-galactosidase activity. The results shown are the mean of three independent biological replicates, and the error bars represent standard deviations.

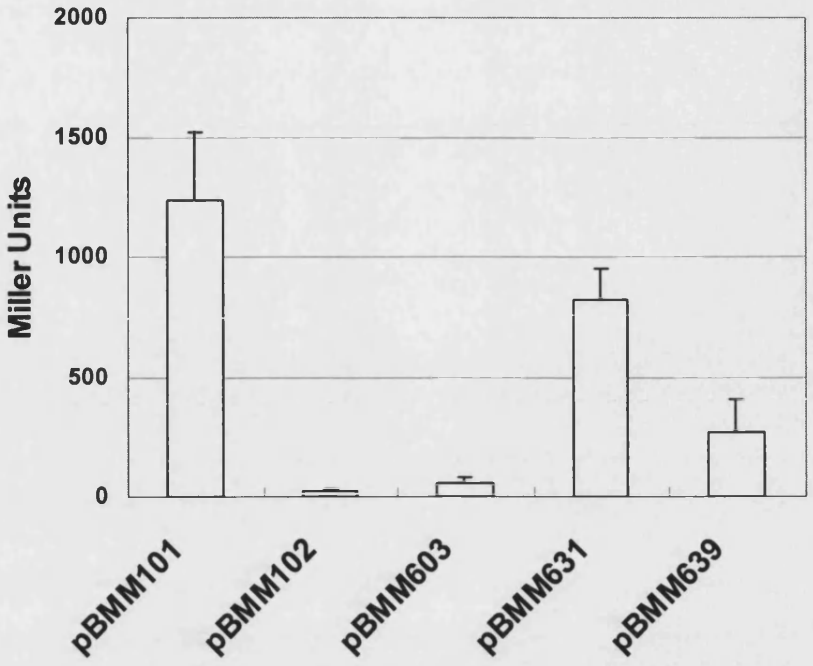

Figure 3.11. The chimeric RcsC proteins complement the *rcsC137* allele. SG20907 (*rcsC137 cpsB-lacZ*) was transformed with plasmid pBMM101 (vector) or derivatives carrying different *rcsC* alleles, pBMM102, pBMM603, pBMM631, and pBMM639 (encoding $RcsC_{K12}$, $RcsC_{YP}$, $RcsC_{YP\text{-}K12}$ and $RcsC_{K12\text{-}YP}$ respectively). Cells were cultured overnight at 30°C in LB agar plates and assayed for β-galactosidase activity. The results shown are the mean of three independent biological replicates, and the error bars represent standard deviations.

3.2.3.5 Activity on solid surface

Both $RcsC_{YP}$ and $RcsC_{YP\text{-}K12}$ are unable to support biofilm formation. Both proteins have a higher kinase activity upon activation and both of them still have some phosphatase activity. It is also noteworthy that both of these proteins have a higher basal level of activity, compared to other RcsC homologues, when cells were grown on a solid surface (see Figs. 3.3 and 3.10). However, when the activity of the different proteins was compared in broth and on plates, in the absence of the DjlA signal, it is clear that the basal activity of $RcsC_{YP\text{-}K12}$ is constitutive (i.e. signal independent) whilst the basal activity of $RcsC_{YP}$ requires

growth on a solid surface (Fig. 3.12). On the other hand, the $RcsC_{K12\text{-}YP}$ chimera, like $RcsC_{K12}$, does not have any basal activity and the level of *cpsB-lacZ* expression is very low regardless of whether the cells are grown in liquid or on solid media. This suggests that both N-terminus and the C-terminus are required for the normal function of RcsC, in this case response to solid surface.

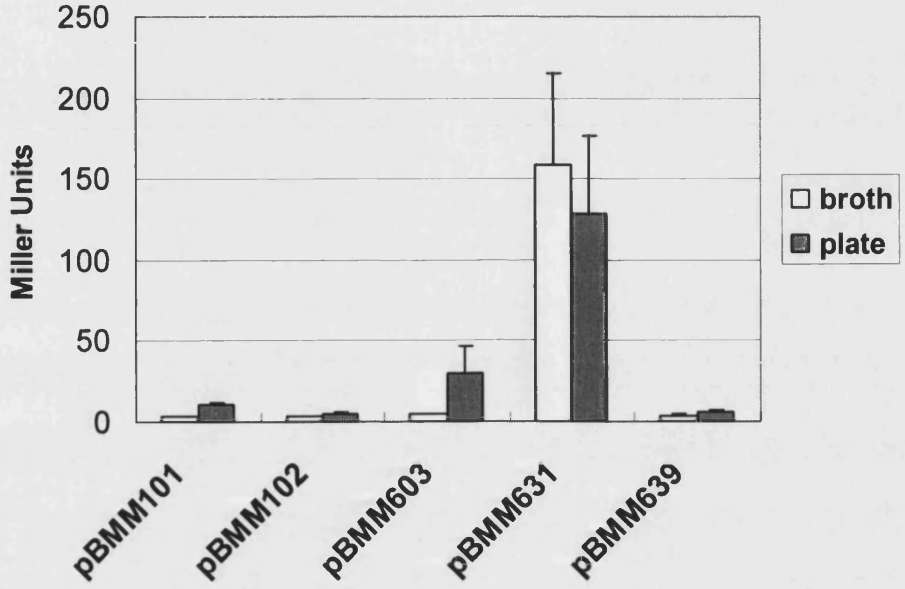

Figure 3.12. Activation by growth on a solid surface. PSG1038 (*rcsC52*::Tn10 *cpsB-lacZ*)/pPSG961-31 (P_{araBAD}-*djlA*$^+$) was transformed with with plasmid pBMM101 (vector) or derivatives carrying different *rcsC* alleles, pBMM102, pBMM603, pBMM631, and pBMM639 (encoding $RcsC_{K12}$, $RcsC_{YP}$, $RcsC_{YP\text{-}K12}$ and $RcsC_{K12\text{-}YP}$ respectively). Cells were cultured overnight at 30°C in LB broth (white column) and on LB agar plates (grey column) in the absence of 0.2% (w/v) L-arabinose. To determine the level of *cpsB-lacZ* expression, cells were harvested and assayed for β-galactosidase activity. The results shown are the mean of three independent biological replicates, and the error bars represent standard deviations. The difference of *cpsB-lacZ* expression was the activation by growth on solid surface.

3.3 Conclusion

In this study it was hoped to exploit the existing variation in *rcsC* alleles found in different, but closely related, species of *Enterobacteriaceae* to identify regions of RcsC that are important for the normal functioning of this signaling protein. Alignment of the amino acid sequences of RcsC from different *Enterobacteriaceae* showed the presence of highly conserved residues in domains required for signal transduction and the surrounding residues (Clarke *et al.*, 2002). However, there was also significant variation within these proteins, especially in the predicted perplasmic domain and the regions connecting the conserved domains. In order to assign potential functional differences to this variation we tested the activity of the RcsC homologues using a range of functionality tests. All of the proteins tested in this study exhibited, with varying degrees, both the kinase and phosphatase activities associated with RcsC.

Although it was not possible to detect all of the RcsC homologues using immunoblotting, it is clear that the different proteins are produced in the cells as various activities could be detected (see Figs. 3.3-3.7). However, it was not possible to determine the levels of each RcsC homologue produced under the conditions used in this study. The $RcsC_{K12}$ and $RcsC_{O157}$ proteins can be detected by RcsC-specific antibody only when expression is induced by the addition of IPTG. Nonetheless these experiments established that IPTG was not required in order to get appropriate levels of *rcsC* expression. Moreover as all of the *rcsC* genes in this study were expressed under the control of the same P_{trc} promoter it is likely that all genes are expressed at the same level.

It is worth highlighting the altered signaling observed with the $RcsC_{YP}$ homologue. This protein exhibited very high activity when activated by DjlA overproduction and, even in the absence of any signal, $RcsC_{YP}$ was capable of driving significant levels of *cpsB-lacZ* expression (see Fig 3.3) on LB agar plates. $RcsC_{YP}$ also complemented the *rcsC137* allele suggesting that the increased activity was not due to a compromised phosphatase activity. It is possible that the increased activity of $RcsC_{YP}$ is due to an increased or altered sensitivity to signals via the input domain. Indeed work described in this Chapter shows that

the N-terminal region of $RcsC_{YP}$ is responsible for the hyperactivation of this protein in response to DjlA overproduction (see Fig. 3.10). Interestingly, the *rcsD* gene in *Yersinia pestis* is a pseudogene by frameshift and therefore the Rcs phosphorelay in *Yersinia pestis* might have evolved to have different interactions and/or work differently to the phosphorelay in *E. coli* (Parkhill *et al.*, 2001).

DjlA overproduction and growth on a surface in *E. coli* K-12 act in a synergistic manner with regard to activation of the Rcs phosphorelay (see Figures 3.4 and 3.5). This synergism is clearly seen in *rcsC* mutant strains complemented with plasmids producing $RcsC_{K12}$, $RcsC_{O157}$ and $RcsC_{YP}$ (see Fig. 3.5). However, this synergy was not observed in *rcsC* mutant cells producing $RcsC_{LT2}$. The Rcs phosphorelay is required for biofilm formation and it has been shown that a deletion in *rcsC* results in lower levels of biofilm formation in *E. coli* K-12 (Ferrieres and Clarke, 2003). In this study it has been shown that the biofilm defect in an *rcsC*⁻ strain (BMM520) can be complemented by the production of $RcsC_{K12}$, $RcsC_{O157}$, $RcsC_{LT2}$ and $RcsC_{K12\text{-}YP}$ but not by the production of either $RcsC_{YP}$ or $RcsC_{YP\text{-}K12}$. Although $RcsC_{LT2}$ complemented biofilm formation, the level of biofilm formed is less compared to that of the other RcsC homologues.

The activation of RcsC by a surface signal has been shown to be transient (Ferrieres and Clarke, 2003). However, in the absence of RcsC, or when $RcsC_{YP}$ or $RcsC_{YP\text{-}K12}$ is present, basal levels of *cpsB-lacZ* expression can be detected suggesting that, under these conditions, an elevated level of Rcs~P is present in the cells. The elevated level of Rcs~P, although not abundant enough to drive maximal *cps* genes, might be enough to inhibit the expression of flagellum genes or activate *rprA* expression. It has been shown that a mutation in *rcsC* resulted in a 10-fold induction of RprA and 2-fold increase in the level of RpoS (Majdalani *et al.*, 2002). The inhibition of motility or early accumulation of RpoS might be responsible for the defect in biofilm formation observed in the absence of RscC (Ferrieres, personal communication).

The importance of the input region of the RcsC protein has been well demonstrated by the chimeric proteins produced during this study. Moreover, the inability of $RcsC_{YP}$ and $RcsC_{YP\text{-}K12}$ to complement biofilm formation in BMM520

might be due to differences in signal perception by this RcsC homologue. Further analysis of the relationship between the input domain of RcsC and biofilm formation will be the objective of the following chapter.

Chapter 4
Mutational Analysis of the N-terminal Region of RcsC and Its Role in Biofilm Formation

4.1 Introduction

Biofilm formation is a complex developmental process that can be divided into several stages, from initial attachment to the surface to the maturation of the biofilm into a three dimensional structure. Each stage requires that a different subset of genes are expressed, and the RcsC phosphorelay is one of the regulatory pathways that is responsible for the temporal regulation of gene expression during biofilm development (Huang *et al.*, 2006; Prigent-Combaret *et al.*, 2000; Prigent-Combaret and Brombacher, 2001; Schembri *et al.*, 2003)

In the previous chapter it was shown that the N-terminal region of the RcsC protein was important for normal biofilm formation. The $RcsC_{YP}$ and the chimeric $RcsC_{YP\text{-}K12}$ protein do not support biofilm formation but possess enzymatic (i.e. kinase and phosphatase) activities, suggesting the N-terminal region of $RcsC_{K12}$ may be involved in biofilm formation by interacting with the environment, in other words, sensing the signals.The N-terminal region of RcsC can be further divided into several domains, including two TM domains, a periplasmic domain, and the linker region located between the second TM domain and the transmitter domain (see Figure 4.1). There are examples whereby the periplasmic domain of the sensor kinase is, in fact, the signal sensing region for extracellular signals e.g. PhoQ (Regelmann *et al.*, 2002) and VirR. Cytosolic sensing modules have also been integrated into some HKs, e.g. PAS domains, which monitor changes in light, redox potential, oxygen and small ligands (Taylor and Zhulin, 1999). Some 2CP use both extra- and intracellular sensing modules to perceive the signals.

The linker region is the domain that separates the input domain from the cytoplasmic signalling domains i.e. the transmitter domain and it is critical for proper signal transduction. It either modulates the kinase-phosphatase activity ratio, or it is directly involved in intracellular signal perception (Park *et al.*, 1998). Many linkers contain a HAMP domain or a P-linker (Aravind and Ponting, 1999; Whitfield and Roberts, 1999). RcsC is one of the 13 membrane-bound sensors in *E. coli* predicted to contain a HAMP linker distal to the second TM domain (Williams and Stewart, 1999).

In this Chapter, N-terminal domain deletion derivatives of RcsC were constructed and tested for their ability to complement biofilm formation in an *rcsC* mutant. In addition, the N-terminal region was subject to a random mutagenesis and the mutant library was screened for mutants that were unable to complement biofilm formation in the *rcsC*⁻ background. These studies revealed that the biofilm forming signals were not sensed through the periplasmic region and identified some residues in the linker region that are important during signal transduction.

4.2 Results

4.2.1 Construction of RcsC chimera and deletion mutants

Domain deletion variants were constructed using a PCR-based method as described in Materials and Methods. PCR primers were designed and used to amplify and construct the domain deletion RcsC mutants (see Figure 4.1). A variety of mutant derivatives were constructed including $RcsC_{\Delta PP}$ (deleted for the periplasmic region), $RcsC_{\Delta Linker}$ (deleted for the linker region), $RcsC_{\Delta PP\text{-}\Delta Linker}$ (deleted for the periplasmic region and the linker region but retaining the 2 TM domains) and $RcsC_{\Delta input}$ (deleted for the N-terminal 435 amino acids of RcsC including both of the TM domains, the periplasmic domain and the linker region). These mutant derivatives were encoded by pBMM617, pBMM620, pBMM618 and pBMM619, respectively. A chimeric EnvZ-RcsC protein, encoded in pBMM106, and a truncated cytoplasmic RcsC variant, $RcsC_{\Delta TM}$ (deleted for the N-terminal 319 amino acids of RcsC but retaining the linker region), encoded in pBMM107 were also used in this study (Clarke, unpublished data). The EnvZ-RcsC protein consists of the N-terminal 191 amino acids of EnvZ and the C-terminal regions (Met320 to Ser933) of RcsC (see Figure 4.1) and it has been shown that this chimeric protein activates the expression of *cpsB-lacZ* in response to signals sensed by EnvZ (Clarke, unpublished data). The $RcsC_{\Delta TM}$ protein consists of the C-terminal region of RcsC with the deletion of both the TM domains and the periplasmic region. Plasmid pBMM102, encoding $RcsC_{K12}$, was used in all assays as a wild type control.

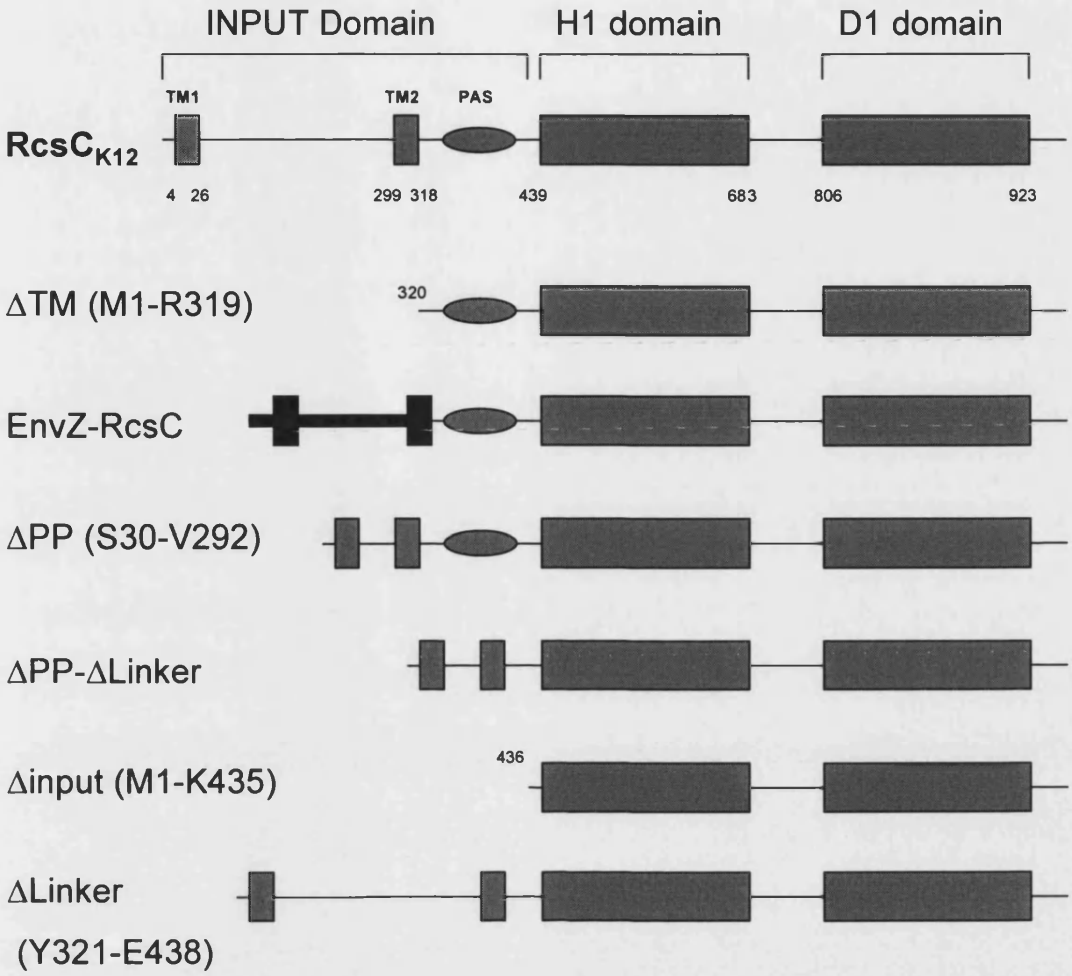

Figure 4.1. Schematic representation of structural organisation of RcsC derivatives used in this study. The RcsC$_{K12}$ was used as the wild type RcsC and is shown in the top figure. TM1 and TM2 show the putative TM regions. The numbers flanking the TM domains, H1 domain and D1 domain represent the predicted amino acid sequence limits of each domain based on *in silico* homology searches. Between the TM2 and the transmitter domain (R319-S439) is the linker region. A PAS domain is predicted between residues 341-409. EnvZ-RcsC consists of the N-terminal 191 a.a. of EnvZ and the C-terminal region of RcsC. RcsC$_{\Delta TM}$ is a protein deleted from M1 to R319. The periplasmic domain (S30–V292) was deleted in RcsC$_{\Delta PP}$. Both the periplasmic and linker region were deleted in RcsC$_{\Delta PP\text{-}\Delta Linker}$. RcsC$_{\Delta input}$ contains only the H1 and D1 domain, residues before M436 were deleted. The linker region (Y321 to E438) was deleted in RcsC$_{\Delta Linker}$.

4.2.2 The periplasmic region is not required for normal biofilm formation

The importance of the N-terminal region of RcsC in biofilm formation was illustrated in the previous chapter. The N-terminal region of RcsC can be further divided into several functional and structural domains (Figure 4.1). In order to investigate the roles of these domains, the RcsC variants were tested for their ability to complement biofilm formation in BMM520. As seen in Figure 4.2, of the six variants tested, only pBMM617, encoding $RcsC_{\Delta PP}$ supported biofilm formation to the same level as $RcsC_{K12}$, the wild-type protein. However, $RcsC_{\Delta Linker}$, $RcsC_{\Delta input}$, $RcsC_{\Delta PP\text{-}\Delta Linker}$, $RcsC_{\Delta TM}$ and the EnvZ-RcsC chimeric protein did not complement the biofilm defect observed in strain BMM520. Indeed, the other RcsC variants seemed to have a negative effect in biofilm formation, as cells carrying these proteins formed less biofilm than the *rcsC* mutant cells (Fig. 4.2).

4.2.3 The domain deletion RcsC variants do not respond to DjlA overproduction

The RcsC variants were then tested for their ability to respond to DjlA overproduction. The normal response to DjlA overproduction was dramatically altered in all six variants tested (see Fig. 4.3). As expected the level of *cpsB-lacZ* expression in cells producing $RcsC_{K12}$ increased from 5 to 218 Miller Units when DjlA was overproduced. However none of the mutants tested appeared to be significantly activated by DjlA and several mutants also exhibited altered basal levels of *cpsB-lacZ* expression (i.e., in the absence of DjlA overproduction) suggesting that the signaling properties of these proteins had been changed. In fact, the EnvZ-RcsC chimeric protein showed a decreased level of *cpsB-lacZ* expression when DjlA is overproduced (see Fig. 4.3). Interestingly although $RcsC_{\Delta PP}$ was capable of supporting biofilm formation, it did not respond to DjlA overproduction, suggesting that these inputs are sensed independently by RcsC.

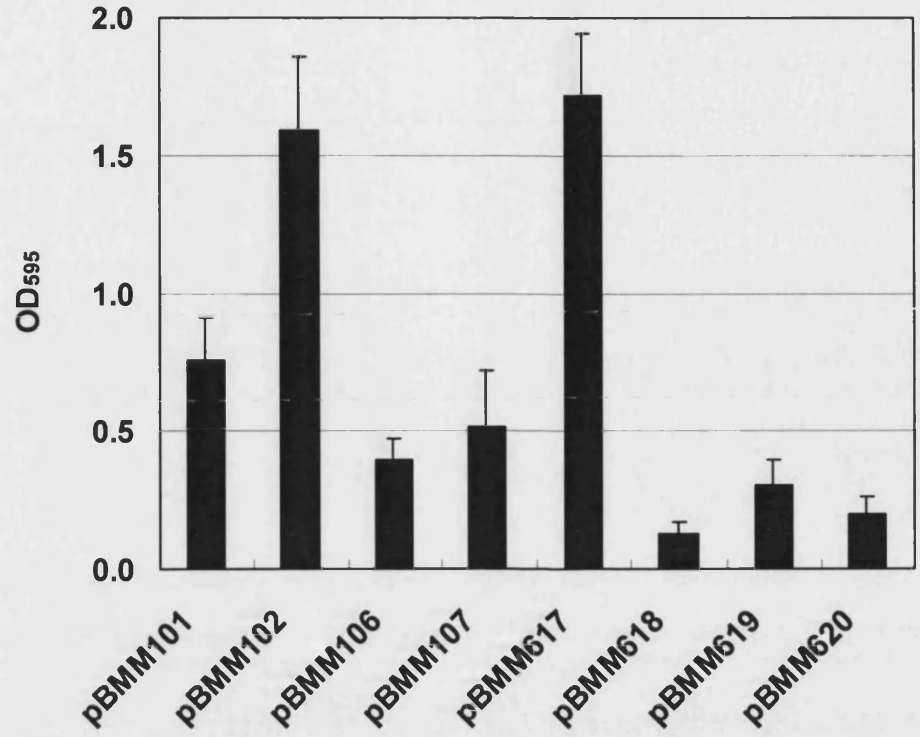

Figure 4.2. Complementation of biofilm formation in BMM520 by RcsC derivatives. BMM520 (*rcsC52*::Tn10) was transformed with plasmids encoding RcsC protein variants, including pBMM101 (vector), pBMM102 ($RcsC_{K12}$) pBMM106 (RcsC-EnvZ), pBMM107 ($RcsC_{\Delta TM}$), pBMM617 ($RcsC_{\Delta PP}$), pBMM618 ($RcsC_{\Delta PP\text{-}\Delta Linker}$), pBMM619 ($RcsC_{\Delta input}$), and pBMM620 ($RcsC_{\Delta Linker}$). Cells were cultured overnight at 30°C in LB broth for 48 h. Biofilm formation was visualised by crystal violet staining. Crystal violet was then dissolved in ethanol and quantified by the absorbance of 595 nm. The results shown are the mean of three independent biological replicates, and the error bars represent standard deviations.

4.2.4 The domain deletion RcsC variants complement the *rcsC137* allele

The RcsC variants were also tested for their ability to complement the constitutive activity of the *rcsC137* allele in strain SG20907 (Brill *et al.*, 1988). The Rcs phosphorelay is constitutively activated in SG20907 and a high level of *cpsB-lacZ* expression was observed (see Fig. 4.4). However, the level of *cpsB-*

lacZ expression is reduced by the presence of $RcsC_{K12}$, EnvZ-RcsC and $RcsC_{\Delta TM}$ suggesting that these variants have phosphatase activity (Fig. 4.4). However, the other deletion mutants were unable to complement the *rcsC137* allele, suggesting that they do not possess phophatase activity or were unable to interact with RcsC137.

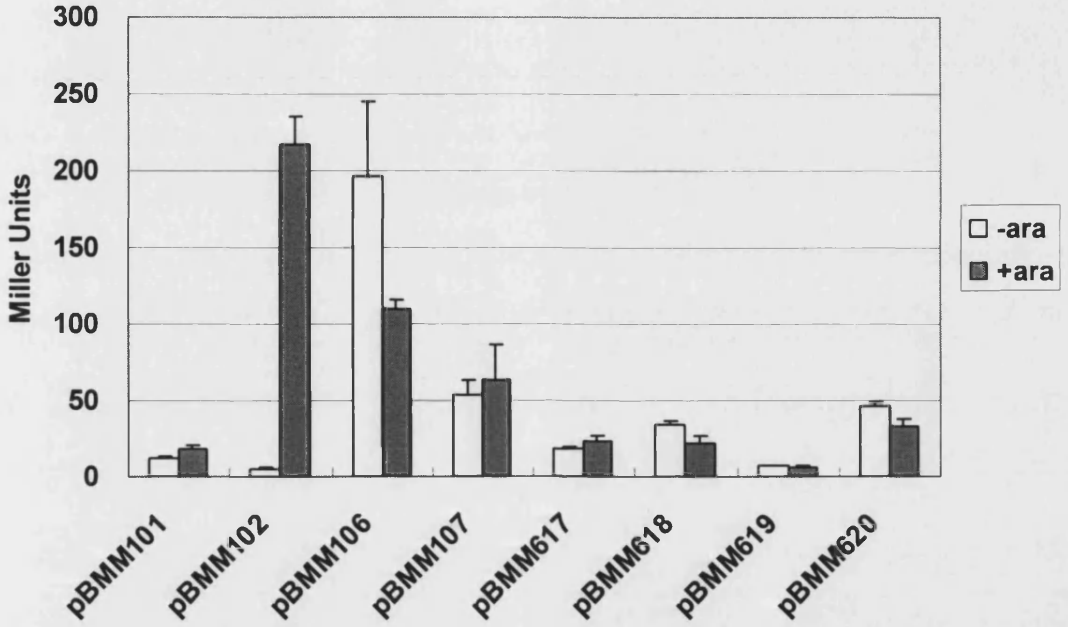

Figure 4.3. RcsC derivatives complement the induction of *cpsB-lacZ* expression by DjlA overproduction. PSG1038 (*rcsC52*::Tn10 *cpsB-lacZ*) carrying a DjlA overproducing plasmid pPSG961-31 was transformed with pBMM106 (RcsC-EnvZ), pBMM107 ($RcsC_{\Delta TM}$), pBMM617 ($RcsC_{\Delta PP}$), pBMM618 ($RcsC_{\Delta PP\text{-}\Delta Linker}$), pBMM619 ($RcsC_{\Delta input}$), and pBMM620 ($RcsC_{\Delta Linker}$). Cells were cultured overnight at 30°C on LB agar plates in the absence (white column) or presence of 0.2% L-arabinose (grey column). To determine the level of *cpsB-lacZ* expression, cells were harvested and assayed for β-galactosidase activity. The results shown are the mean of three independent biological replicates, and the error bars represent standard deviations.

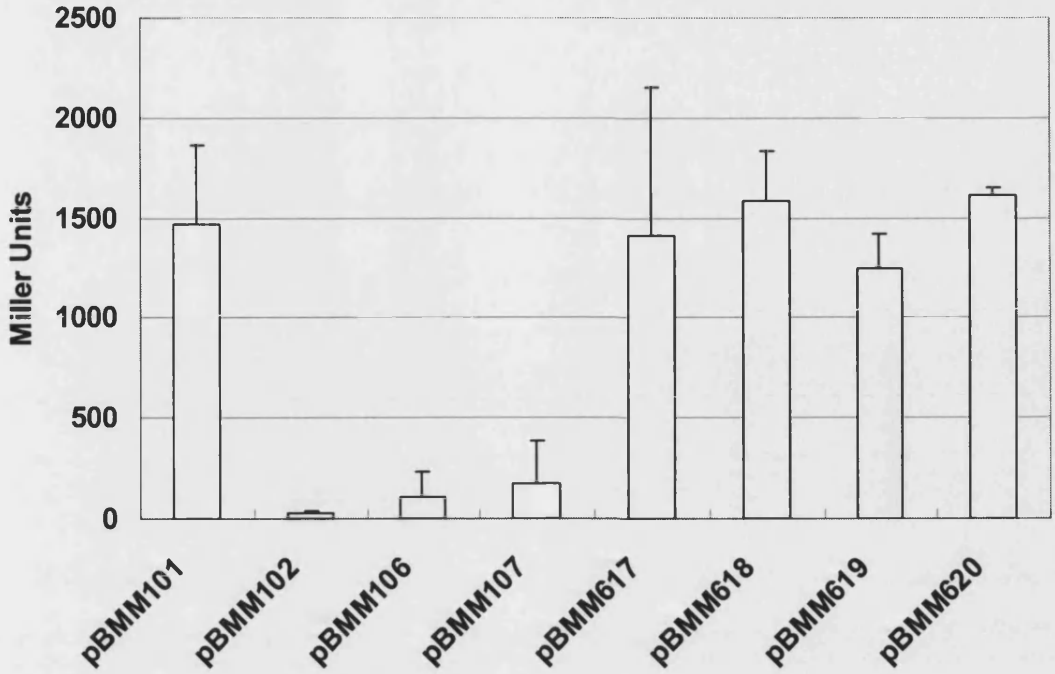

Figure 4.4. Complementation of the *rcsC137* allelle by RcsC derivatives. SG20907 (*rcsC137 cpsB-lacZ*) was transformed with plasmid pBMM101 (vector), pBMM106 (RcsC-EnvZ), pBMM107 ($RcsC_{\Delta TM}$), pBMM617 ($RcsC_{\Delta PP}$), pBMM618 ($RcsC_{\Delta PP\text{-}\Delta Linker}$), pBMM619 ($RcsC_{\Delta input}$), and pBMM620 ($RcsC_{\Delta Linker}$) Cells were cultured overnight at 30°C in LB agar plates and assayed for β-galactosidase activity. The results shown are the mean of three independent biological replicates, and the error bars represent standard deviations.

4.2.5 Deletion of *gmd* gene did not repress the biofilm-defective phenotype

Some of the RcsC deletion mutants (especially RcsC-EnvZ and $RcsC_{\Delta TM}$) had a high basal level of *cps-lacZ* expression without DjlA induction (Fig. 4.3). Although colanic acid production has been reported to be required for biofilm maturation in *E. coli* (Danese *et al.*, 2000), other studies showed that production of colanic acid could interfere with biofilm formation by inhibiting attachment (Hanna *et al.*, 2003; Schembri *et al.*, 2004). In addition, in *Vibrio vulnificus*, capsular polysaccharide production inhibits biofilm formation (Joseph and Wright, 2004). In order to determine whether the expression of polysaccharides

is responsible for the biofilm defect in the microtitre plate assay, an *rcsC gmd* double mutant, called BMM555 (Ferriere, unpublished data), was used. The *gmd* mutation did not restore biofilm formation in any of the RcsC variants tested (Fig. 4.5), suggesting that other gene(s) regulated by the Rcs phosphorelay may be responsible for the defect.

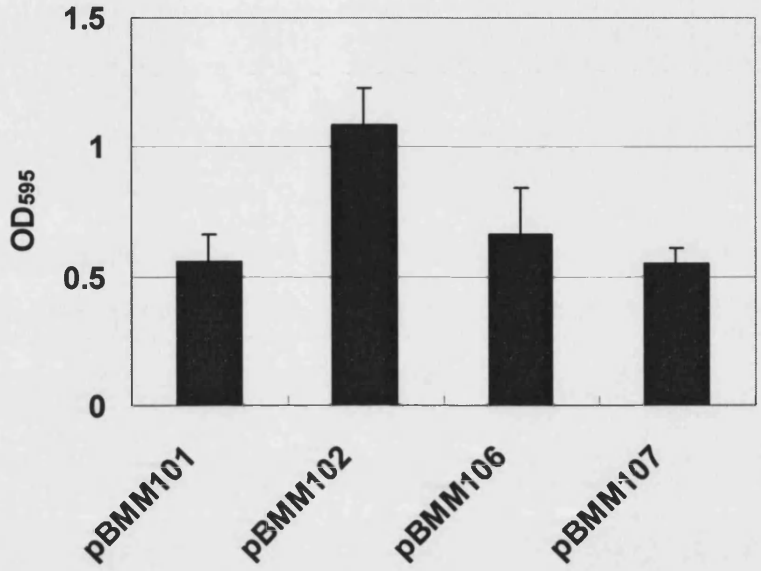

Figure 4.5. Biofilm formation of *E. coli* strain BMM555 (*rcsC*⁻*gmd*⁻) harbouring plasmid pBMM101 (vector), pBMM102 ($RcsC_{K12}$), pBMM106 (EnvZ-RcsC) and pBMM107 ($RcsC_{\Delta TM}$). Cells were cultured overnight at 30°C in LB broth for 48 h. Biofilm formation was visualised by crystal violet staining. The results shown are the mean of three independent biological replicates, and the error bars represent standard deviations.

4.2.6 Immunoblotting of the RcsC variants

There were some RcsC variants tested in our study that could be classified as non-functional i.e. not responding to DjlA signal and not complementing the phosphatase activity of *rcsC137*. This null phenotype could be due to low protein levels in the cell. To determine whether altered protein levels might be responsible for the phenotype, Western blotting was carried out using both RcsC-specific antibody and *c-myc* antibody. The production of $RcsC_{\Delta PP}$ and

$RcsC_{\Delta input}$ was detected in the present of IPTG (Fig. 4.6). Although $RcsC_{\Delta Linker}$ and $Rcs_{\Delta PP\text{-}\Delta Linker}$ could not be detected by Western blotting, these proteins had a negative effect on biofilm formation suggesting they were produced but likely to be less stable than both $RcsC_{\Delta PP}$ and $RcsC_{\Delta input}$.

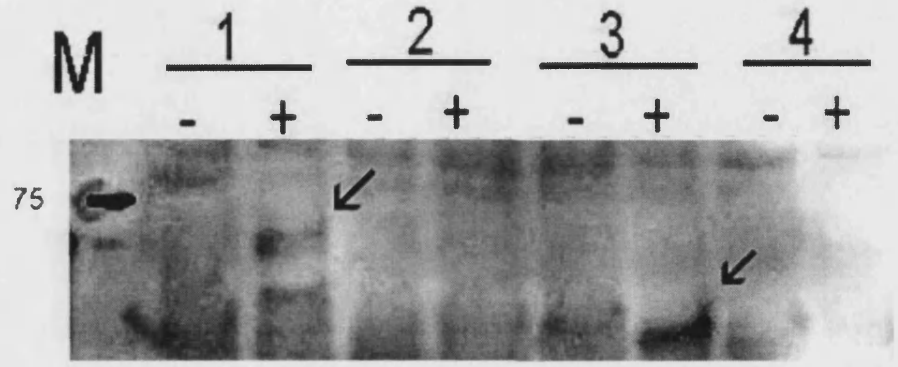

Figure 4.6. Detection of RcsC deletion mutants by immunoblotting. BMM520 (*rcsC52*::Tn10), carrying plasmid pBMM617, pBMM618, pBMM619, pBMM620 (encoding $RcsC_{\Delta PP}$, $RcsC_{\Delta PP\text{-}\Delta Linker}$, $RcsC_{\Delta input}$ and $RcsC_{\Delta Linker}$, Lane 1-4 respectively) were cultured overnight at 37°C in LB broth supplemented with or without (indicated by +/-) 5 mM IPTG and collected by centrifugation. 0.4 OD_{600} equivalents were analysed by sodium dodecyl sulphate-polyacrylamide gel electrophoresis and immunoblotted with the antibody against RcsC peptide. Black arrows indicate the truncated protein detected.

4.2.7 Mutagenesis of input region

The previous chapter had suggested that the input domain of RcsC was important during biofilm formation. The domain deletion study of RcsC suggested that the periplasmic region was not required for biofilm formation, but the linker region might play an important role in signal perception by RcsC. In parallel with the domain deletion approach, a random mutagenesis approach was also carried out to identify specific residues that are involved in biofilm formation. Taking advantage of the naturally occurring *Cla*I restriction site present in *rcsC* gene of *E. coli* K-12, the N-terminal region of the *rcsC* gene was amplified by PCR using the GeneMorph PCR Mutagenesis Kit (Fig. 4.7). The fragments were restricted with *Nco*I and *Cla*I, ligated with pBMM102 restricted

with *Nco*I-*Cla*I and introduced into BMM520. Mutants that did not restore biofilm formation were identified and these biofilm defective mutants were checked by immunoblotting to confirm that the full-length RcsC protein was produced.

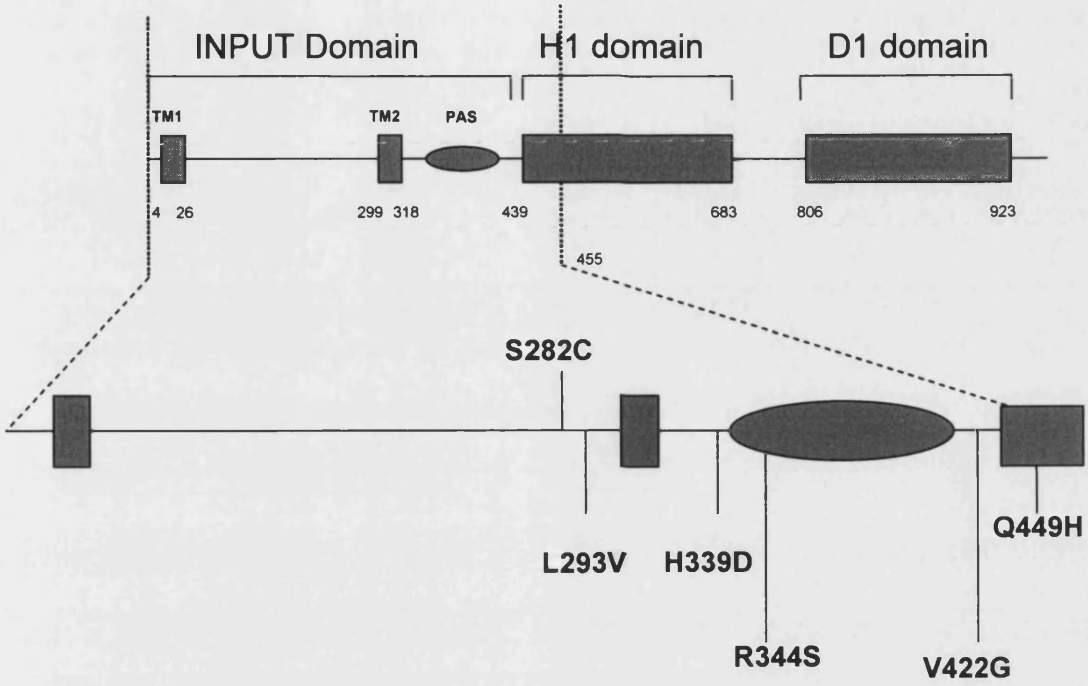

Figure 4.7. Schematic representation of single amino acid mutation derivatives in the RcsC input domain. Wild-type RcsC is shown on the top the structure. The numbers flanking the domains, H1 domain and D1 domain represent the predicted amino acid sequence limits of each domain based on *in silico* homology searches. In addition, a PAS fold is predicted between residue 341-409.The region between the dashed lines was subject to mutagenesis, and the positions of single amino acid substitution mutants used for further examination are presented.

In total, 1848 mutants were screened and 309 biofilm deficient clones were identified. Of these 309 biofilm-defective mutants, 30 were confirmed to produce full-length RcsC by immunoblotting (data not shown). These 30 mutants were sequenced and 25 unique biofilm-minus mutants (a frequency of 1.3%) were

finally identified. The locations of the mutations are listed in Table 4.1. It is clear that most of the mutants carry multiple mutations and the location of the mutations was spread over the region of *rcsC* tested i.e. input domain and linker region. However, it is worth noting that 22 out of the 25 mutants have at least one mutation in the linker region. In total 6 mutants with single amino acid substitutions were identified and these mutants were used for further analysis. The plasmids carrying these mutants were designated pBMM621 to pBMM626. The production of full-length RcsC protein and the inhibition of biofilm formation were confirmed for each of these single amino acid mutants (Figs. 4.8 and 4.9). However the proteins encoded by pBMM622 and pBMM626 were not consistently detected by immunoblotting, even after induction with IPTG, suggesting that these proteins were not stable in the cell.

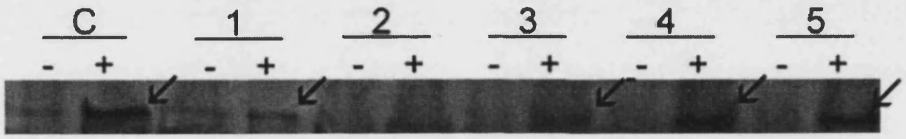

Figure 4.8. Immunodetection of mutant derivatives of *rcsC* expressed in BMM520. The -/+ indicate the presence of IPTG. Control lane: pBMM102 (*rcsC*$^{+}$), Lane 1-5: pBMM621- pBMM625 (encoding RcsC with mutations of Q449H, S282C, L293V, H339D, and R344S respectively). The RcsC proteins have a MW of 100 kD and were detected by the anti-RcsC peptide antibodies.

Mutant	nucleotide change	amino acid change	Location of mutation
1	g1347t	Q449H	H1
2	c120t, c631t, g663t, a844t	**S282C**	PP
3	c877g	L293V	PP
4	c891t, c1015g, g1113a	**H339D**	Linker
5	t618a, c1030a	**R344S**	Linker
6	t1265g	V422G	Linker
7	c1158g, g1193t	L386R, V398F	Linker (2)
8	t1223g, g1330a	L408R, A444T	Linker, H1
9	t478a, g1058a	H159Q, **G353D**	PP, Linker
10	g704a, a 1016g	G235D, **H339R**	PP, Linker
11	g890a, t1229a	R297H, **I410N**	PP, Linker
12	g633c, t1243c, g1284a	Q211H, S415P	PP, Linker
13	g210t, c263t, a 1102c	P88L, N368H	PP, Linker
14	g566a, g1013a, c1157t	G189E, E338K	PP, Linker
15	g157c, c453t, g1073c	V53L, **R358P**	PP, Linker
16	g850t, g1015c, g1087a,g1305a	V284L, V363I	PP, Linker
17	g24a, t35a, t1067a, c1217t	I13N, I356N, T406I	TM, Linker (2)
18	g733a,g884a,a1310t	E245K, R295H, E437V	PP (2), Linker
19	c328t, t828c, g881c, 91059a, c1087a, c1109t	L276P, E294Q,**G353D**	PP (2), Linker
20	g29c, g1031a, g1274a	W10S, **R344H**, C425Y	TM, Linker (2)
21	c251a, t410a, c555t, c958t, g1058a, g1296a	P84H, L137H,M320L, **G353D**	PP (2), Linker (2)
22	c71t, a203g, a337t, a588g, c1076a, t1223a	**A24V**, E68G,M113L, T359N, L408Q	TM, PP (2), Linker (2)
23	g289c. T1045c, g1057c, a1060t, c1112g	A97P, S349P, **G353R**, I354F, A371G	PP, Linker(4)
24	t390a, c419t, a504t, a844t, g1031t, g1073a, t1229a	F130L, A140V, **S282C, R344L, R358H, I410N**	PP(3), Linker(3)
25	c71t, t346c, g565a, c725g, g747t, c1015t, t1025c	**A24V**,W116R, G189R, T242S, K249N, **H339Y**, F342S	TM, PP (4), Linker (2)

Table 4.1 List of mutants identified in mutagensis study. Mutants 1 to 6 were identified as single amino acid substitution and were chosen for further analysis as pBMM621-6. Texts in bold indicate mutations found in multiple clones. The locaton of mutation is present as TM (transmembrane domain), H1 (transmitter domain), PP (periplasmic region) and Linker. The number of mutations is shown in brackets

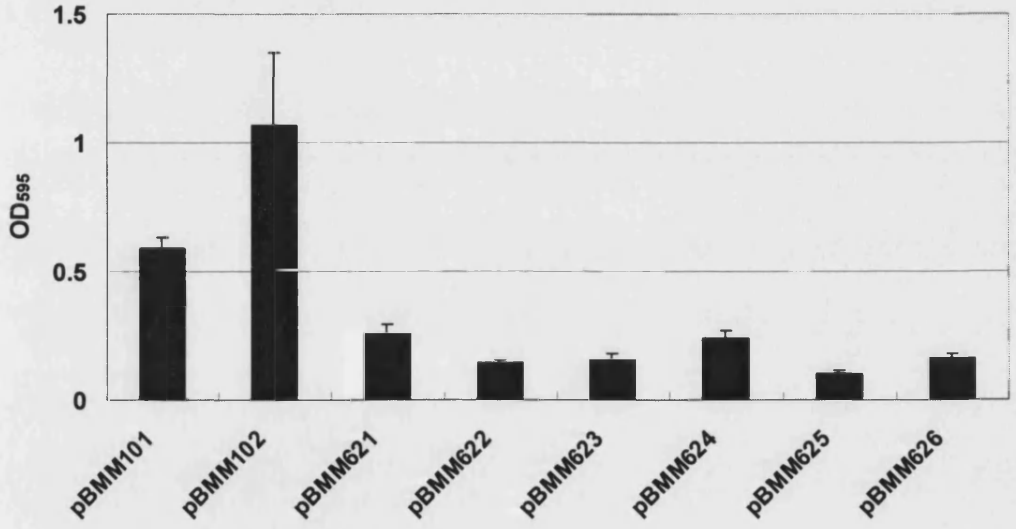

Figure 4.9. Complementation of biofilm formation in BMM520 by RcsC derivatives. BMM520 (*rcsC52*::Tn10) was transformed with plasmids pBMM101 (vector), pBMM102 (*rcsC*$^{+}$), and pBMM621-626 (encoding RcsC with mutations of Q449H, S282C, L293V, H339D, R344S and V422G, respectively). Cells were cultured overnight at 30°C in LB broth for 48 h. Biofilm formation was visualised by crystal violet staining. Crystal violet was then dissolved in ethanol and quantified by the absorbance of 595 nm. The results shown are the mean of three independent biological replicates, and the error bars represent standard deviations.

4.2.8 The DjlA response and phosphatase activities were not correlated to the biofilm deficiency

The RcsC mutants encoded by pBMM621-pBMM626 were tested for their ability to respond to DjlA activation. $RcsC_{Q449H}$, encoded by pBMM621, responded to DjlA in the same way as wild type RcsC. Although $RcsC_{L293V}$, $RcsC_{H339D}$ and $RcsC_{R344S}$, encoded by pBMM623, pBMM624 and pBMM625 respectively, responded to DjlA activation, in the absence of activation signal, expression of the reporter gene was still observed, indicating that these mutants are constitutively active. Indeed strains carrying pBMM624 and pBMM625 appeared to be mucoid when grown on LB agar plates at 30°C. Finally $RcsC_{S282C}$ and $RcsC_{V422G}$, encoded by pBMM622 and pBMM626 respectively, were not activated by DjlA (Fig. 4.10). This may be due to the fact that these proteins are unstable and do not accumulate in the cell (see Fig. 4.8), although they still have negative effect on biofilm formation.

The phosphatase activity of the different RcsC mutants was also determined by whether these mutants could complement the constitutive activity of the *rcsC137* allele. $RcsC_{S282C}$ and $RcsC_{V422G}$, encoded by pBMM622 and pBMM626 respectively, had little or no phosphatase activity (see Fig. 4.11). Although this could be explained by the fact that these proteins are not stable in the cell, the inhibitory effect of these RcsC mutants in biofilm formation implied even if the proteins are unstable, they still have some activities. Interestingly although $RcsC_{H339D}$ which is encoded by pBMM624, appears to have a constitutive kinase activity (see Fig. 4.10) this mutant is as good as the wild-type in its ability to complement the constitutive activity of *rcsC137* allele. Finally $RcsC_{R344S}$, $RcsC_{Q449H}$, $RcsC_{H339D}$ and $RcsC_{R344S}$ can all partially complement the constitutive activity of the *rcsC137* allele (Fig. 4.11).

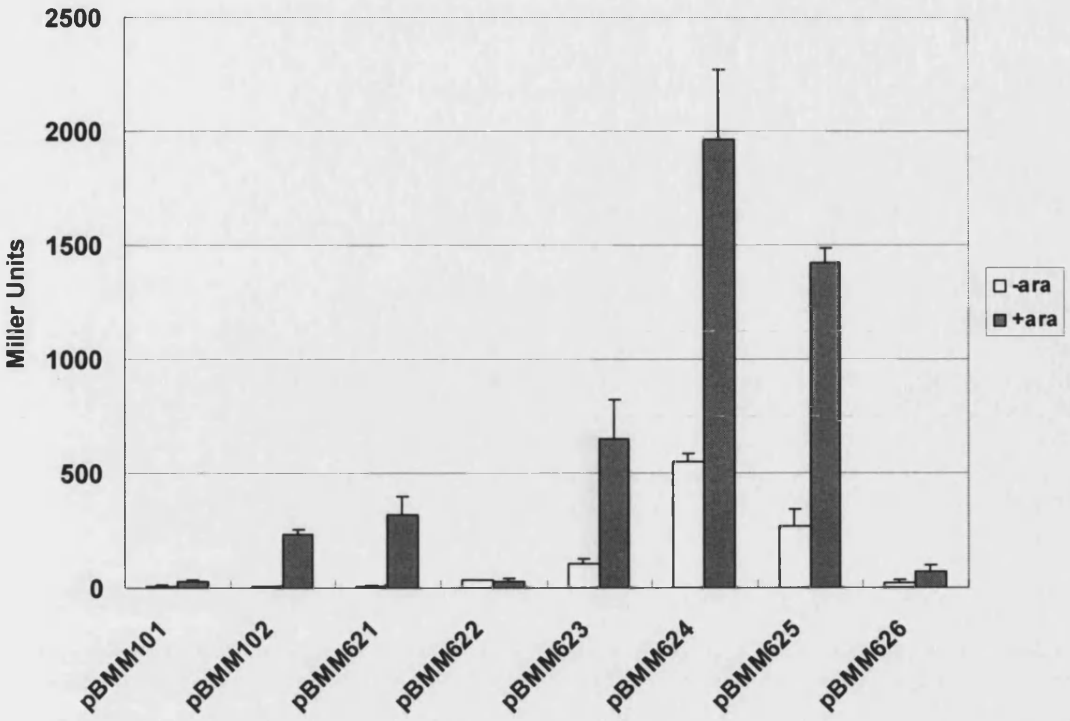

Figure 4.10. The response of RcsC mutant proteins to DjlA overproduction. PSG1038 (*rcsC52*::Tn10 *cpsB-lacZ*) carrying a DjlA overproducing plasmid pPSG961-31 was transformed with pBMM101 (vector), pBMM102 (*rcsC*$^{+}$), and pBMM621-626 (encoding RcsC with mutations of Q449H, S282C, L293V, H339D, R344S and V422G, respectively). Cells were cultured overnight at 30°C on LB agar plates in the absence (white column) or presence of 0.2% (w/v) L-arabinose (grey column). To determine the level of *cpsB-lacZ* expression, cells were harvested and assayed for β-galactosidase activity. The results shown are the mean of three independent biological replicates, and the error bars represent standard deviations.

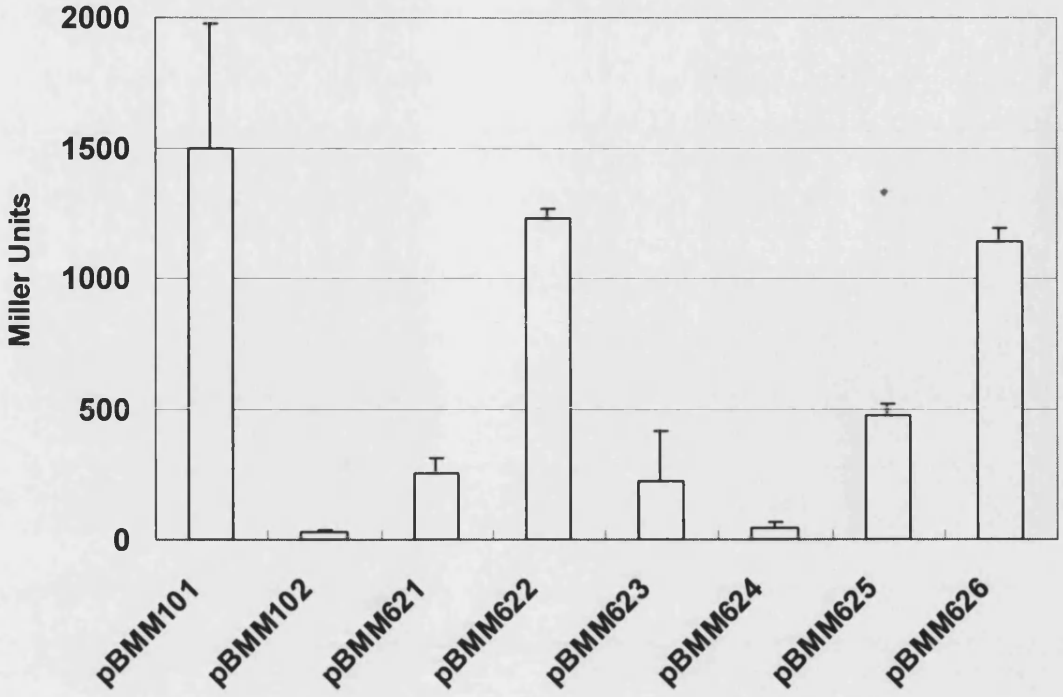

Figure 4.11. Complementation of *rcsC137* by RcsC derivatives. SG20907 (*rcsC137 cpsB-lacZ*) was transformed with pBMM101 (vector), pBMM102 (*rcsC*$^{+}$), and pBMM621-626 (encoding RcsC with mutations of Q449H, S282C, L293V, H339D, R344S and V422G, respectively). Cells were cultured overnight at 30°C in LB agar plates and assayed for β-galactosidase activity. The results shown are the mean of three independent biological replicates, and the error bars represent standard deviations.

4.2.9 The Q region

The $RcsC_{Q449H}$ mutant is unable to support biofilm formation but can respond to DjlA overproduction and complement the *rcsC137* allele. Therefore, it was reasoned that this mutant was competent for signalling but was unable to recognise an appropriate signal generated during biofilm formation. The Q449 residue is located at the beginning of the transmitter domain and upon closer examination of the $RcsC_{K12}$ amino acid sequence it is clear that there are several, equally spaced glutamine (Q) residues in this region. This Q-domain is well conserved in the various RcsC homologues except in $RcsC_{YP}$ (Fig. 4.12A). Interestingly, in the previous chapter, it was shown that the $RcsC_{YP}$ homologue was unable to restore biofilm formation in BMM520 and this was localised to a defect in the N-terminal region, including the potential Q domain. Furthermore, this region is predicted to be alpha helical in structure, and when presented as a helical wheel, it is clear that all of the Q residues fall on the same side of the helix (Fig. 4.12B). This asymmetry is striking and may be important for signal sensing and transduction. In addition, a chimeric $RcsC_{K12(Q449H)\text{-}YP}$ protein, encoded by pBMM642 did not support biofilm formation (Fig. 4.13), confirming the Q449H is the cause of aberrant biofilm.

To gain insight into the role of this region and, specifically, the Q residues, it was decided to carry out some site-directed mutagenesis using the pBMM641 plasmid, encoding $RcsC_{YP}$. $RcsC_{YP}$ contains a threonine residue at the Q2 position and it was decided to test whether a Thr to Gln mutation ($RcsC_{YP(T->Q)}$) would restore the ability to support biofilm formation. The substitution of Thr to Gln in $RcsC_{YP}$ did not restore biofilm formation (see Fig. 4.13), suggesting that there are other factors influence the activity of $RcsC_{YP}$ in biofilm.

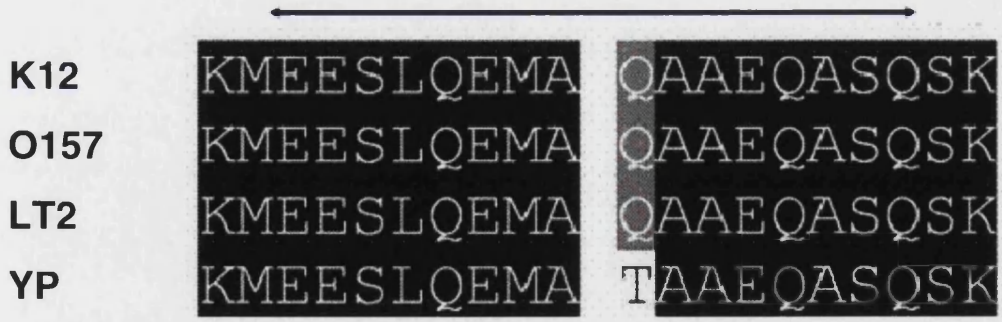

(A)

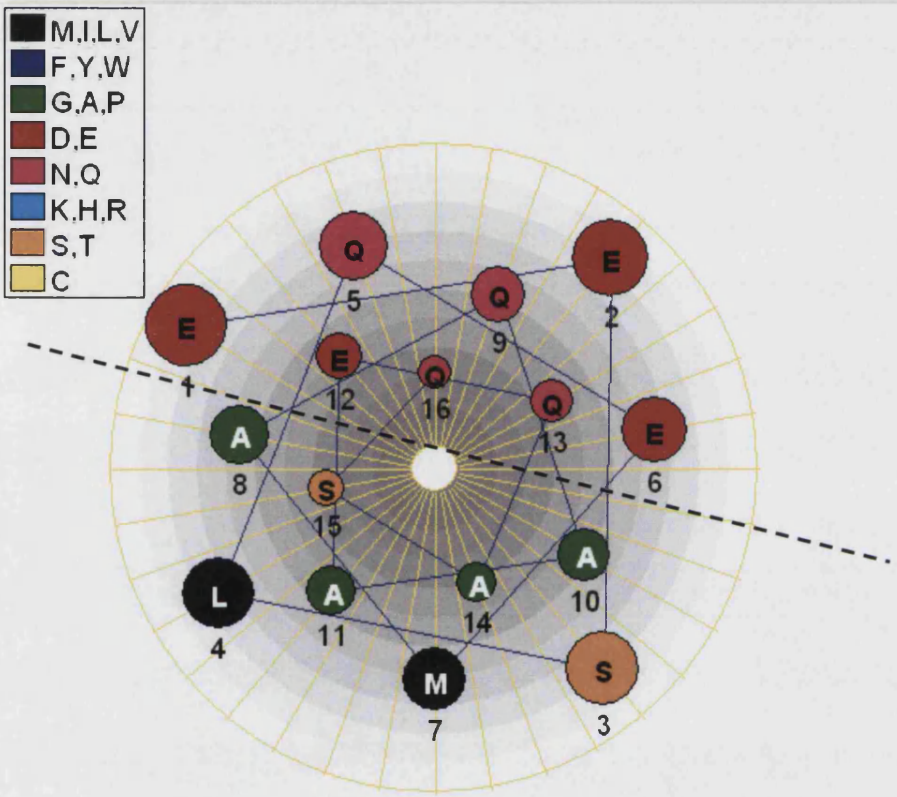

(B)

Figure 4.12. (A) Sequence alignment of the Q domain from *E. coli* K-12 (K12), *Salmonella typhimurium* serovar LT2 (LT2), and *Yersinia pestis* (YP). (B) Helical wheel representation of the Q domain from *E. coli* K-12 using PROTEAN software from DNASTAR (DNASTAR, Madison, WI). The asymmetry of the helix is indicated by a dashed line.

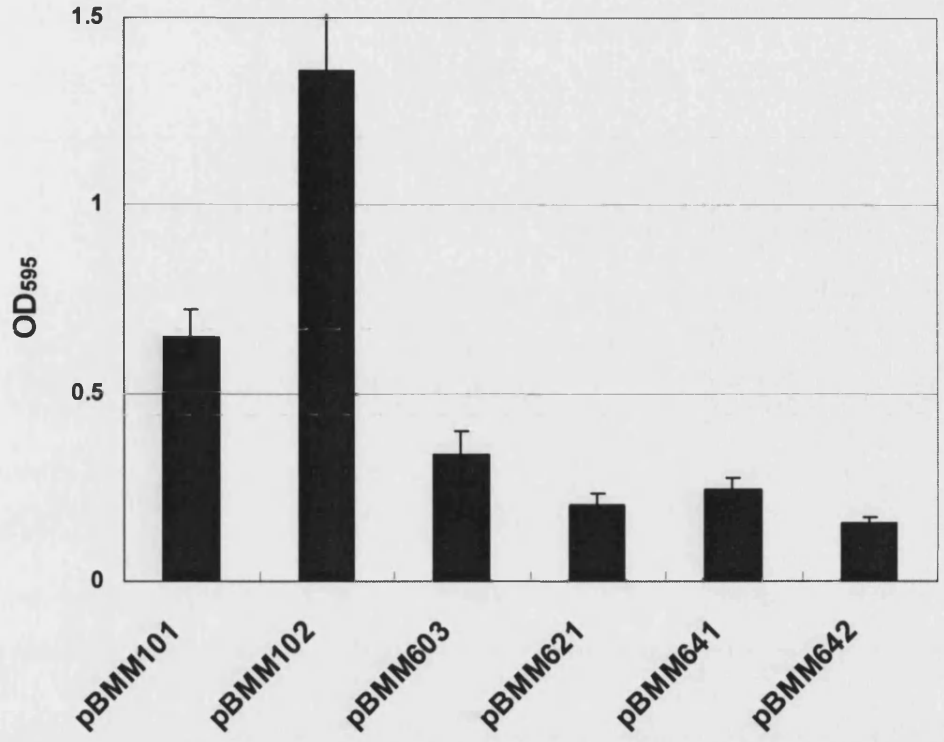

Figure 4.13. Biofilm formation of *E. coli* strains BMM520 (*rcsC*::Tn10) harbouring plasmid pBMM101 (vector), pBMM102 ($RcsC_{K12}$), pBMM603 ($RcsC_{YP}$), pBMM621 ($RcsC_{Q449H}$) pBMM641 ($RcsC_{K12(Q449H)-YP}$) or pBMM642 ($RcsC_{YP(T->Q)}$). Cells were cultured overnight at 30°C in LB broth for 48 h. Biofilm formation was visualised by crystal violet staining. Crystal violet was then dissolved in ethanol and quantified by the absorbance of 595 nm. The results shown are the mean of three independent biological replicates, and the error bars represent standard deviations.

4.3 Conclusion

4.3.1 The periplasmic region is not required for biofilm formation

Although the periplasmic domain is a part of the extracellular signal sensing region of other HKs, the $RcsC_{\Delta PP}$ deletion mutant supported biofilm formation suggesting that this mutant was able to respond to signals that may be generated during biofilm formation. However, the deletion of the periplasmic domain abrogated the response to DjlA overproduction suggesting that, although the periplasmic domain is not required for biofilm formation, it might be

involved in the perception of the DjlA signal. The signal that triggers biofilm formation development is not clear. However it does not appear to be sensed by the periplasmic domain suggesting that an intracellular signal may be involved in controlling the RcsC sensor activity during biofilm formation.

Although the deletion of the entire periplasmic domain did not affect biofilm formation a single mutation in the periplasmic region ($RcsC_{L293V}$) does impair biofilm formation. The periplasmic domain might be a ligand-recognition domain and the residue might be important for this recognition. Alternatively, this residue is close to TM2 and the substitution may change the conformation of the TM domain resulting in the movement of the intracellular signalling modules. This is reminiscent of the periplasmic domain of EnvZ, in which the deletion or replacement of the whole periplasmic domain did not affect its ability in osmosensing (Leonardo and Forst, 1996). However, mutations in a conserved region within the periplasmic domain (Pro41 to Glu53) of EnvZ, called the I box, impaired osmosensing suggesting that the periplasmic region is important during osmosensing by EnvZ (Waukau and Forst, 1999). In the *Salmonella* PhoQ sensor, a single amino acid substitution at T48 in the periplamic domain altered the activity of the sensor toward its cognate RR partner, PhoP (Sanowar *et al.*, 2003). Different amino acid substitutions at this position had the opposite effect on the activity of PhoQ. For example, T48V and T48I substitutions resulted in a PhoQ protein with decreased phosphatase activity that constitutively activated PhoP. In contrast, the T48L substitution resulted in a PhoQ protein with decreased autokinase activity and increased phosphatase activity. Therefore T48 appears to contribute to a conformational switch between the kinase and phosphatase state of PhoQ (Sanowar *et al.*, 2003) It is possible that L293 may play a similar role in RcsC as the I box region of EnvZ or T48 of PhoQ, although this still needs to be examined further.

4.3.2 The role of linker region

The various deletion mutants of RcsC suggested that the periplasmic region is not essential for biofilm formation. The deletion of the linker region not only abolished biofilm formation, but also had an impact on the protein activity and stability, suggesting that the linker region plays a important role in both protein

structure and activity. Mutations in the linker region of BarA result in impaired kinase activity and a net dephosphorylating activity by interfering with the conformational changes associated with signalling (Tomenius *et al.*, 2005). Although the linker-region deleted variants ($RcsC_{\Delta Linker}$, $RcsC_{\Delta PP\text{-}\Delta Linker}$ and $RcsC_{\Delta input}$) did not respond to DjlA and did not complement the *rcsC137* allele, it remains unknown if these proteins possess either kinase or phosphatase activity. The lack of a response to DjlA might simply reflect a defect in signal perception and not kinase activity. In addition, the inability to complement *rcsC137* could be explained by either the lack of phosphatase activity or altered interaction between the RcsC137 and the deletion mutants.

Two clones identified in this study resulted in a constitutively active RcsC protein and both mutations were located in the linker region, H339D and R344S. Interestingly a E338K substitution in RcsC has already been shown to induce mucoidy in *E. coli* (Clavel *et al.*, 1996). Similarly, mutations in the linker region of RcsC in *Salmonella* also showed constitutive activation of Rcs phosphorelay (Garcia-Calderon *et al.*, 2005).

4.3.3 The clustered glutamine residues in the linker region might be important in the biofilm formation

Random mutagenesis identified a biofilm defective mutant with a Q449H substitution in $RcsC_{K12}$. This mutant was able to respond to DjlA overproduction and complemented the constitutive activity of the *rcsC137* allele suggesting that the $RcsC_{Q449H}$ mutant is signaling-competent. Further analysis of this region in $RcsC_{K12}$ revealed the presence of several equally-spaced Q residues that fall on the same side of the helix when this region is presented in a helical wheel (Fig. 4.12B). In addition, $RcsC_{YP}$ did not support biofilm formation and had the second Q residue replaced by T. Therefore the occurrence and apparent non-random distribution of Q residues correlates with biofilm formation. However reconstruction of the Q domain in $RcsC_{YP}$ did not restore its ability to complement biofilm formation in BMM520 suggesting that the presence of the Q domain may be required, but is not sufficient, for biofilm signal sensing.

The linker region of RcsC is predicted to contain type a P linker (or HAMP linker) distal to the second TM domain, (Williams and Stewart, 1999) followed by a PAS fold. The Q domain is between the PAS fold and the transmitter (H1) domain, and its secondary structure is predicted to be α-helix. The striking asymmetry of the helix might suggest a role in signal transduction. In KdpD, a putative turgor sensor, substitutions in the clustered arginine residues adjacent to TM4 (see Fig. 1.5) modulated the ratio of kinase to phosphatase activity (Jung and Altendorf, 1998) The region was suggested to function as an electrostatic switch to modulate the kinase to phosphatase activity. The Q domain of RcsC might play a similar regulatory role (see Fig. 4.12).

Chapter 5
Characterisation of *Photorhabdus rcs* Mutants

5.1 Introduction

Photorhabdus luminescens is a Gram-negative bacterium that belongs to the family *Enterobacteriaceae*. It is the only known terrestrial bioluminescent bacteria, although the physiological role of bioluminescence is still unclear. It has a mutualistic relationship with entomophagous nematodes of the family *Heterorhabditiae* where *Photorhabus* colonises the gut of the infective juvenile (IJ) nematodes. Within the nematode gut, *Photorhabdus* appear to be encapsulated in a biofilm-like structure (ffrench-Constant *et al.*, 2003). The IJs live in the soil, where they seek potential insect hosts. After the IJs enter the insect host, *Photorhabus* are regurgitated from the nematode into the insect hemolymph where the bacteria can grow exponentially. During growth the bacteria avoid the insect immune response and within 48-72 h the insect dies of septicemia. Concomitant with insect death *Photorhabdus* have attained a high cell density in the larvae and the bacteria produce a range of hydrolytic enzymes and antibiotics that facilitate the conversion of the insect cadaver into a nutrient soup that is required for nematode growth and development. The IJ recovers to a self-fertile hermaphrodite stage that lays eggs and the nematode undergoes 2-3 generations of reproduction, feeding on the bacterial biomass. When resources within the insect cadaver become limiting, the nematodes develop into IJs, repackage *Photorhabus* in their guts and emerge from the insect cadaver in search of a new host (Fig. 5.1) (ffrench-Constant *et al.*, 2003).

Photorhabus produce various extracellular enzymes, pigments and antibiotics, which are related to their ability to support nematode development or pathogenicity to insects. It is expected that the transition between symbiosis and pathogenicity will be regulated by changes in gene expression. Recently HexA was identified as a repressor of symbiosis, and inactivation of *hexA* resulted in the de-repression of symbiosis factor production (Joyce and Clarke, 2003). However it also appears that HexA is required for pathogenicity as the *hexA* mutant was severely attenuated in virulence against the insect larvae. Therefore, pathogenicity and symbiosis are reciprocally regulated by HexA.

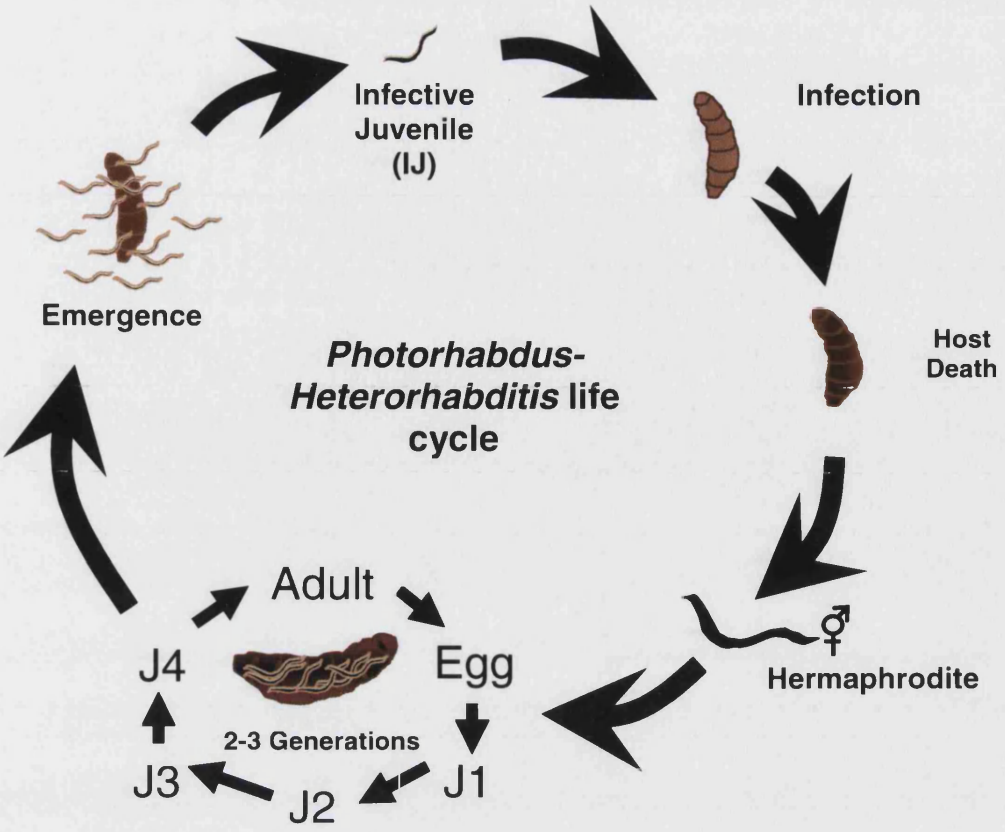

Figure 5.1. Life cycle of *Photorhabdus-Heterorhabditis*.

Two-component pathways are also likely to play an important role in controlling pathogenicity and symbiosis. The genome of *P. lumimescens* TT01 was complete sequenced and nineteen two-component regulatory systems were found in the genome (Duchaud *et al.*, 2003). The PhoPQ two-component pathway has been shown to be required for pathogenicity in *Photorhabdus*. A mutaion in *phoP* resulted in a complete loss of virulence in an insect model (Derzelle *et al.*, 2004).

The complex life cycle of *Photorhabus* makes it a valuable model for studying symbiosis and pathogenicity, not only in terms of signal transduction and gene regulation, but also the contribution of biofilm formation in the two distinct lifestyles. The Rcs phosphorelay was shown to be involved in biofilm formation and pathogenicity in other *Enterobacteriacea* (Arricau *et al.*, 1998; Ferrieres and

Clarke, 2003; Tierrez and Garcia-del Portillo, 2004; Tobe *et al.*, 2005; Venecia and Young, 2005). Homologues of the Rcs phosphorelay can be found in the TT01 genome and in this study, the *rcsB* and *rcsC* genes were individually knocked out in *Photorhabus*, and the effect of the Rcs phosphorelay on biofilm formation and other phenotypes was tested.

5.2 Results

5.2.1 Identification of the Rcs phosphorelay in *P. luminescens*

The organisation of the *P. luminescens rcs* locus is similar to that of other *Enterobacteriacea* (See Fig. 1.11). The sizes of the predicted RcsB response regulator (*plu3048*, 217 residues), RcsC sensor (*plu3049*, 938 residues) and the RcsD HPt containing protein (*plu3047*, 896 residues) are similar to the size of their counterparts in *E. coli*, and the sequences exhibit 78%, 49% and 33% identity at the amino acid level. The *rcsC* of *P. luminescens* is directly adjacent to *gyrA,* as in *Y. pestis,* unlike the organisation in *E. coli* and *Salmonella* in which the *gyrA* gene and the *rcs* locus are separated by a series of genes (Fig. 1.11). The *rcsC* gene of *P. luminescens* TT01 has been cloned and $RcsC_{TT01}$ did not support biofilm formation in BMM520 (data not shown).

5.2.2 The *rcsC* and *rcsB* genes are disrupted in BMM601 and BMM602

In order to investigate the role of the Rcs phosphorelay in *P. luminescens* TT01, *rcsC* and *rcsB* mutant strains were generated by allelic exchange with knockout plasmids pBMM630 and pBMM633 respectively. The rifampicin resistant *P. luminescens* TT01 (TT01-rif) was conjugated with *E. coli* S-17 carrying either pBMM630 or pBMM633. Exconjugants were obtained and selected as described in Material and Methods (Fig. 2.3). The presence of the *rcsC* and *rcsB* mutations was confirmed by PCR and sequencing. The resulting strains, BMM601 and BMM602, respectively, were stored at -80°C.

5.2.3. BMM601 and BMM602 are deficient in biofilm formation

The RcsC sensor kinase is required for normal biofilm formation in *E. coli* K-12 (Ferrieres and Clarke, 2003). In order to gain insight into the contribution of the Rcs phosphorelay in the formation of biofilm in *Photorabdus*, the biofilm forming

ability of *rcsC* and *rcsB* mutant strains were examined in both a microtitre plate and a flowcell chamber.

5.2.3.1 Static microtitre plate assay

Photorabdus strains were tested for their ability to form biofilms on the wells of polypropylene (PP) microtitre plates. The cells were incubated at 30°C, without shaking, for 48 h, and crystal violet was used to determine the extent of biofilm formation (as described in Materials and Methods). No difference was observed in the growth rates of BMM601, BMM602 and TT01 when the cells were grown in liquid broth (data not shown). All strains could form a biofilm under these conditions although quantification of the CV staining revealed that BMM601 (Δ*rcsC*) formed similar level of biofilm as wild type, but BMM602 (Δ*rcsB*) formed less biofilm than wild type or BMM601 (See Fig. 5.2) The differences are significant by paired t-test as p=0.014 and 0.009 respectively. Therefore, this suggests that *rcsB* is required for normal biofilm formation in *Photorhabdus*.

5.2.3.2 BMM602 form less biofilm in flowcell system

The dynamics and developmental stages during biofilm formation were studied in a flow chamber system using confocal scanning laser microscopy (CSLM). This allows the temporal examination of biofilm formation *in situ*. BMM601, BMM602 and TT01 were fluorescent tagged using the plasmid pSU2007, which carries genes encoding GFP and kanamycin resistance (Martinez and de la Cruz, 1988). The *Photorabdus* strains were injected into channels in a flowcell chamber that was prepared as described in Materials and Methods and the biofilm formed by the bacteria on the glass surface was monitored by CSLM at four time points, 12 h, 21 h, 36 h and 61 h (Fig. 5.3).

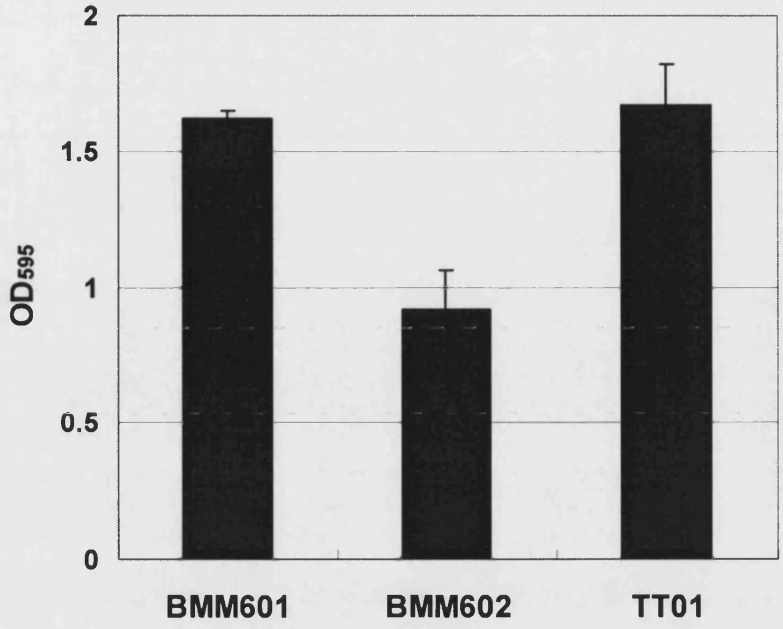

Figure 5.2. Biofilm formation of BMM601, BMM602 and TT01. All strains were grown overnight in LB broth at 30°C, diluted to an OD_{600}=0.05 and incubated at 30°C, without shaking, in PP wells. After 48 h, the extent of biofilm formation was assessed by staining the wells with 0.1% CV. The amount of CV staining (and therefore biofilm formation) was quantified by absorbance at 595 nm. The results shown are the mean of three independent biological replicates, and the error bars represent the standard deviation.

All strains are capable of attaching to the glass surface of the chamber and forming a biofilm, however, 12 h post-inoculation, both BMM601 and BMM602 had noticeably less cells attached to the surface, indicating there is a positive role for both RcsB and RcsC during biofilm formation. Moreover, compared to TT01, BMM601 and BMM602 formed unusual long chains of cells, suggesting that normal cell division during biofilm formation was affected by mutations in the Rcs phosphorelay. At 21 h post-inoculation, both mutant strains covered less area on the glass, suggesting that BMM601 and BMM602 were either less efficient at attaching to the surface or that the cells were easily dispersed after attachment. The depth of the biofilm also appeared lower in BMM601 and BMM602 until 36 h post-inoculation. Moreover, compared to the smooth and homogeneous wild type biofilm formed by TT01, biofilms formed by BMM601 and BMM602 appeared more clumpy with open areas devoid of cells interspersed with bacteria-covered areas (see Fig. 5.3). However, after 61 hours of incubation in the flow chamber, differences between the mutant strains and TT01 were not apparent. At all stages up to 36 h, the defect in biofilm formation in BMM602 was more severe than observed in BMM601.

The biofilm phenotype in flowcells suggests that BMM601 and BMM602 can form a biofilm on the glass surface after prolonged incubation. However, in the initial steps of biofilm formation, both mutant strains were noticeably less efficient than TT01 in attaching to the glass and this defect in attachment might be responsible for the delayed biofilm formation.

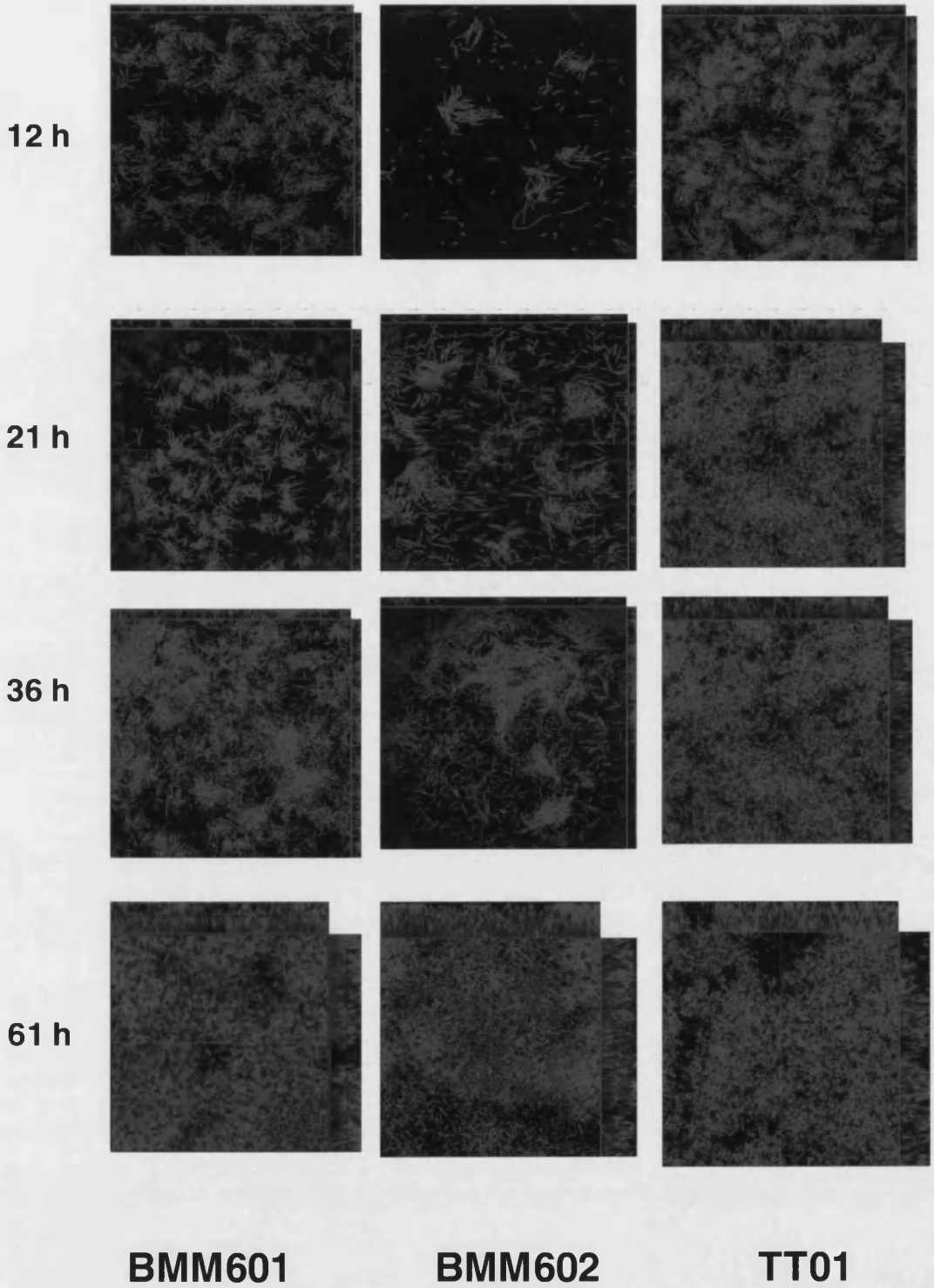

Figure 5.3. Confocal laser scanning microscopy of biofilms formed by BMM601 (Δ*rcsC*), BMM602 (Δ*rcsB*) and TT01. Each individual strain was grown under flow in modified FAB medium supplemented with 2% LB. Experiments were done in triplicate, and the data shown are from one representative experiment.

5.2.3.3 Activation of Rcs phosphorelay prevented biofilm formation

It has been shown that the overproduction of RcsB results in the up-regulation of Rcs-regulated genes, in the absence of any signal (Brill *et al.*, 1988). Therefore, RcsB overproduction can be used to mimic activation of the Rcs phosphorelay. To investigate the effect of activating the Rcs phosphorelay in *Photorhabdus*, the *rcsB* gene was cloned into an arabinose-inducing plasmid, pBAD24 (Guzman *et al.*, 1995), resulted in plasmid pBMM640. Both pBMM640 and pBAD24 were electroporated into TT01 and these strains were tested for biofilm formation in the presence and absence of arabinose. As expected, in the absence of induction i.e. growth in the absence of arabinose, TT01 with either pBMM640 or pBAD24 formed similar amounts of biofilm in the wells of PP microtiter plates (see Fig. 5.4). The arabinose had no significant effect on TT01 bearing pBAD24. However, in the presence of arabinose, there was a significant reduction in the formation of biofilm by TT01/pBMM640 compared to TT01/pBAD24 ($p=0.012$) (Fig. 5.4). Therefore the promiscuous activation of the Rcs phosphorelay reduced the biofilm forming ability of TT01.

5.2.4 The Biofilm formation phenotype is not due to loss of motility

Photorhabdus are motile bacteria with peritrichous flagella and swimming motility can be observed on a semisolid LB plate (0.3% [w/v] agar) (Ffrench-Constant *et al.*, 2000). In *E. coli* it has been shown that the Rcs phosphorelay represses motility by repressing the expression of the *flhDC* operon (Francez-Charlot *et al.*, 2003). Therefore, in *E. coli*, mutants in *rcsB* produce slightly elevated levels of flagella compare to the wild-type and have slightly increased rates of motility. Flagella are important during the early stages of biofilm formation in *E. coli* and to determine if the Rcs phosphorelay may play a similar role in motility regulation in *Photorhabdus* the mutant strains were examined for motility as described in Materials and Methods. After 48 h on motility plate, a colony formed at the site of initial inoculation and motile cells could be seen to form a halo around this colony. The motility of bacteria was determined by measuring the diameters of the halos formed after 64 hours of inoculation. The relative motility of each strain was compared to TT01 and presented as a percentage (i.e. [halo of mutant/halo wild-type] x 100) (see Fig. 5.5). The

BMM602 (*ΔrcsB*) was slightly but significantly more motile than both TT01 (p=0.031) and BMM601 (p=0.044), suggesting that, as is the case in *E. coli*, the Rcs phosphorelay represses motility in *P. luminescens*. The significance of this slightly increased rate of motility for biofilm formation remains to be established.

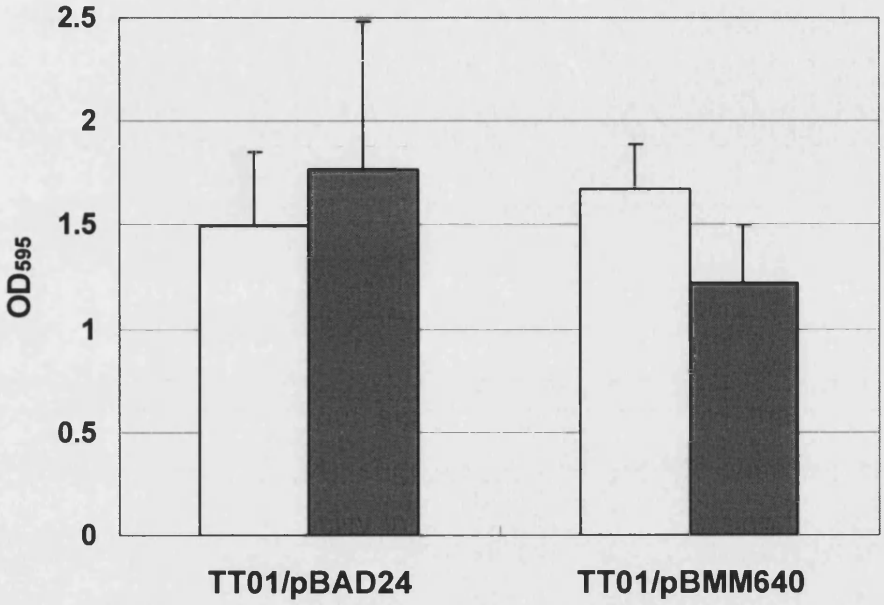

Figure 5.4. Overproduction of RcsB impairs biofilm formation in *Photorhabdus*. TT01 carrying pBAD24 and pBMM640 (encoding $RcsB_{TT01}$) were grown overnight at 30°C in LB broth at 30°C, diluted to an OD_{600}=0.05 and incubated at 30°C, without shaking, in PP wells in LB broth (white columns) and LB with 0.2% (w/v) arabinose (grey columns). After 48 h, the extent of biofilm formation was assessed by staining the wells with 0.1% CV. The amount of CV staining was quantified by absorbance at OD_{595}. The results shown are the mean of three independent experiments, and the error bars represent the standard deviation.

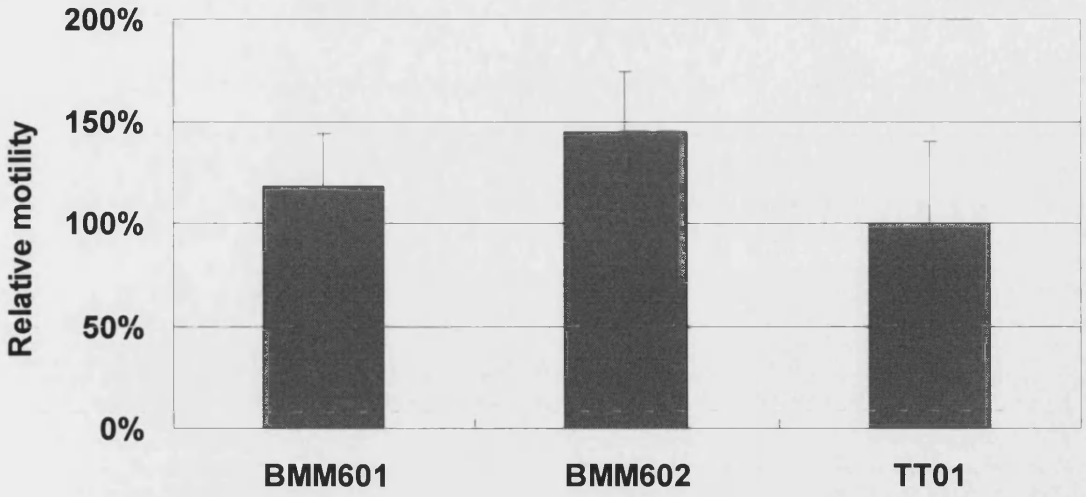

Figure 5.5. The relative motility of BMM601 (*ΔrcsC*), BMM602 (*ΔrcsB*) and TT01 on motility agar. The results shown are the mean of seven independent experiments, and the error bars represent the standard deviation.

5.2.5 BMM602 and BMM601 support nematode growth and development

In order to determine the role of the Rcs phosphorelay during symbiosis in *Photorhabdus,* it was decided to analyse nematode growth and development using an *in vitro* symbiosis assay (see Materials and Methods). Therefore BMM601, BMM602 and TT01 were grown on lipid agar plates for 72 h at 30ºC and approximately 60 surface sterile IJs were added to each plate (see Materials and Methods). The IJs developed to hermaphrodites on all sets of plates, the hermaphrodites laid eggs at the same time, the eggs hatched into J1 larvae. These larvae developed through the normal larval stages (J1-J4) into adult males and females. Sexual reproduction continued for 2-3 generations until, after 3 weeks of incubation, the developing J1 nematode larvae enter an alternative J3 stage, called the infective juvenile. The IJs migrated to the lid of the Petri dish and were collected for further analysis. No differences in the timing of nematode development were observed when comparing nematodes grown on wild-type TT01 with nematodes grown on BMM601 or BMM602 (data not shown).

5.2.5.1 BMM601 is slightly impaired in IJ yield

The number of IJs collected from the *in vitro* symbiosis plates was counted and this can be used as a quantitative measure of symbiosis. The average number of IJs collected from BMM601 plates was less than the number collected from TT01 or BMM602 plates, suggesting that the *ΔrcsC* mutant maybe affected in symbiosis (Fig. 5.6). However, the difference *in vitro* symbiosis assays might not reflect IJ development and yield *in vivo*, therefore, *in vivo* symbiosis were performed using insect larvae infected with nematodes.

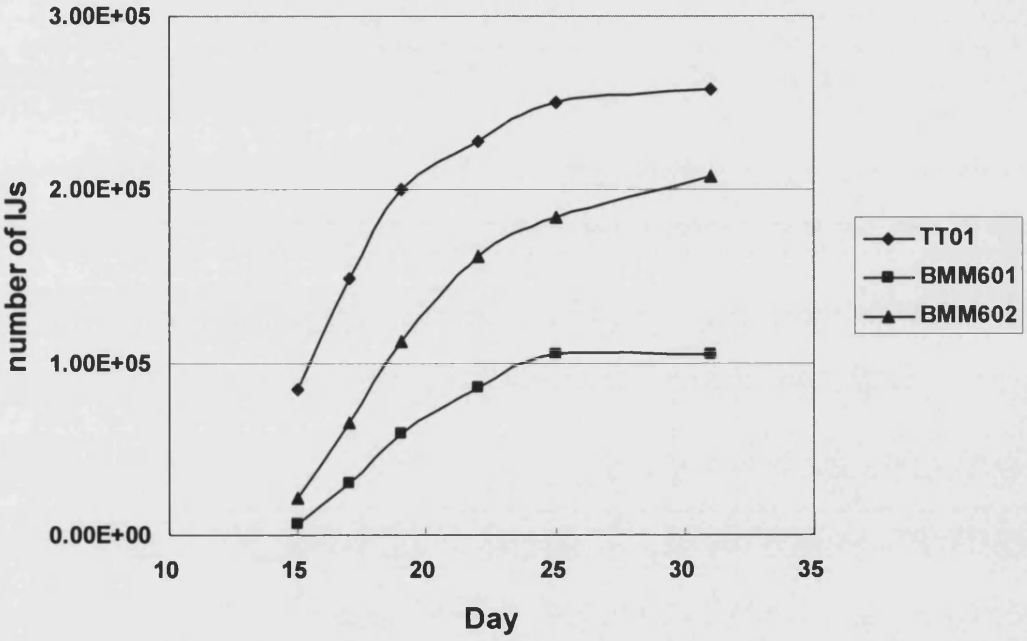

Figure 5.6. IJ recovery from symbiosis plates of BMM601 (*ΔrcsC*), BMM602 (*ΔrcsB*) and TT01. IJs were collected from the lid of symbiosis plate and counted between 15 to 31 days after the IJ were added to the symbiosis plates. The result showed here was the average of 4 plates for each strain tested. Nematode started to emerge from 13 days after inoculation on the symbiosis plates. (Diamond: TT01, square: BMM601 and triangle: BMM602)

5.2.5.2 BMM601 and BMM602 support IJ recovery from insect cadavers

In order to test analyse the *in vivo* life cycle of the IJs containing the different mutant strains of TT01, surface-sterilised IJs collected from the *in vitro*

symbiosis assays were used to infect insect larvae (as described in Materials and Methods). Once dead the insects were set up in White traps so that the new generation of IJs could be collected and quantified. There was no difference in either the time of IJ emergence or IJ yield per insect infected with IJs carrying either TT01, BMM601 or BMM602 (see Fig. 5.7). Therefore the Rcs phosphorelay does not appear to be important for the *in vivo* interaction between *Photorhabdus*, the nematode and the insect.

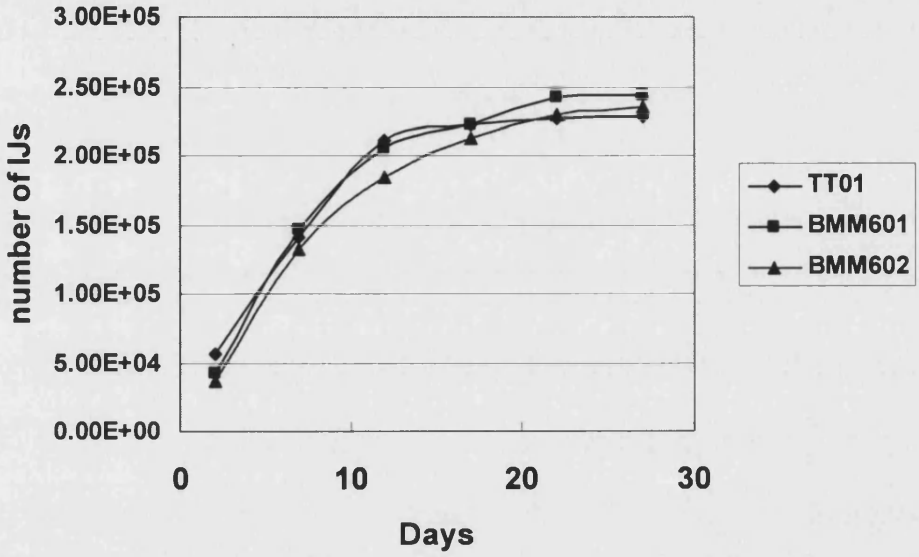

Figure 5.7. IJ yield per insect. IJs. Insects killed by IJs packaging with TT01, BMM601 (Δ*rcsC*) BMM602 (Δ*rcsB*) were placed in White trap 10 days after death. IJs started to emerge 2 days after the White trap setup. The results showed were the average of four independent White trap plates for each strain.

5.2.6 The BMM601 and BMM602 were retained by nematodes

In order to determine the effect of the Rcs phosphorelay on the ability of TT01 to colonize the nematode, 10 individual IJs were picked out from the pool of IJs grown on each strain and the nematodes were crushed to release the bacteria. The level of bacterial retention was determined by enumerating the CFUs on LB/Rif agar plates and the results are presented as a Box and Whisker plot (Fig. 5.8). Neither the Mann-Whitney U-Test nor the Mood's Median test revealed any significance in the level of the different bacteria within the nematode, leading to the conclusion that the level of bacterial retention is not affected by deletion of

either *rcsC* or *rcsB*. However the median level of colonisation was 101, 190 and 48 CFU/IJ for TT01, BMM601 and BMM602, respectively, and the lack of significance may simply reflect the low sample size (n=10) used in these analyses.

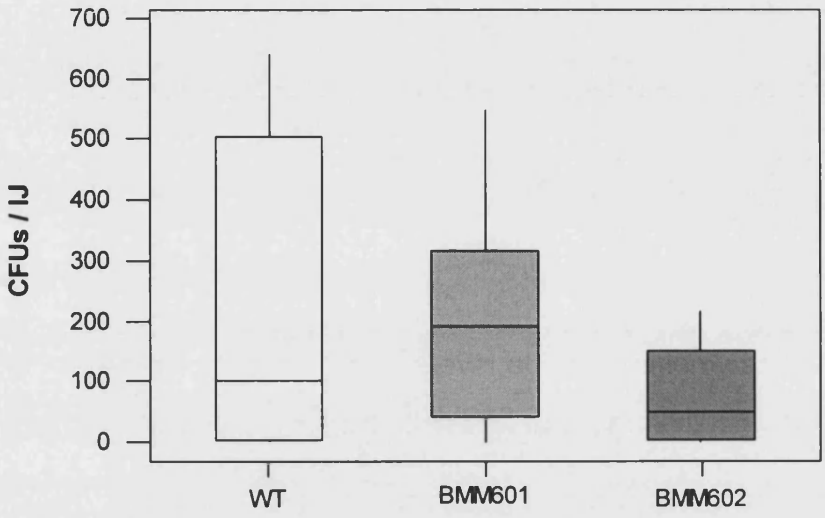

Figure 5.8. Bacterial retention in IJs packaging with TT01, BMM601 (Δ*rcsC*) BMM602 (Δ*rcsB*). 10 individual IJs were picked out from the pool of IJs collected for each strain, and crushed to obtain the CFU per IJ.

5.2.7 Pathogenicity and several phenotypic traits were not affected in BMM601 and BMM602

To assess whether the disruption of Rcs phosphorelay had other effects on the standard phenotypes of *Photorhabdus* TT01, BMM601 and BMM602 were examined for pigmentation, dye uptake, antibiotics production and secretion of extracellular enzymes were using selective media. BMM601 and BMM602 were shown to be like wild type in all characteristics tested (Table 5.1).

BMM601 and BMM602 were as virulent as the wild type strain toward *G. mellonella* either by direct injection of a bacterial suspension or by infection by IJs containing the mutant bacteria and all insect larvae were dead within 48 h,

suggesting that Rcs phosphorelay is not an important regulator of *Photorhabdus* virulence.

Phenotype/ Strain		BMM601	BMM 602	TT01
Pigmentation		Yellow/brown	Yellow/brown	Yellow/brown
Siderophore production		+	+	+
Antibiotic production		+	+	+
Protease production		+	+	+
Lipase production		+	+	+
Catalase production		+	+	+
Dye adsorption	MacConkey	+	+	+
	EMB	+	+	+
	NBTA	+	+	+
Motility		+	+	+
Colony Morphology		Convex, mucoid	Convex, mucoid	Convex, mucoid
Bioluminescence		+	+	+

Table 5.1 Phenotypic tests and the results for BMM601 (*ΔrcsC*), BMM602 (*ΔrcsB*) and TT01. + indicates a positive result

5.2.8 The bioluminescence of *Photorhabdus rcsC* and *rcsB* mutants

Although the physiological roles of bioluminescence remain to be determined, previous studies identified a mutation in *rcsD* as being hyper-bioluminescent (Susan Joyce, Univeristy of Bath, personal communication). To assess whether the disruption of Rcs phosphorelay of *Photorhabdus* has effects on bioluminescence, the growth and bioluminescence were monitored using a luminometer over time. There was no difference of growth rate of BMM601, BMM602 and TT01 and all three strains reached stationary phase after ten hours of incubation. Bioluminescence was maximum soon after entering stationary phase, and although all strains produced bioluminescence, and the timing of peak light production was similar, the relative luminescence unit (RLU) of BMM602 appeared to be lower than TT01 and BMM601 (Fig 5.8). This might suggest that the Rcs phosphorelay positively regulates bioluminescence.

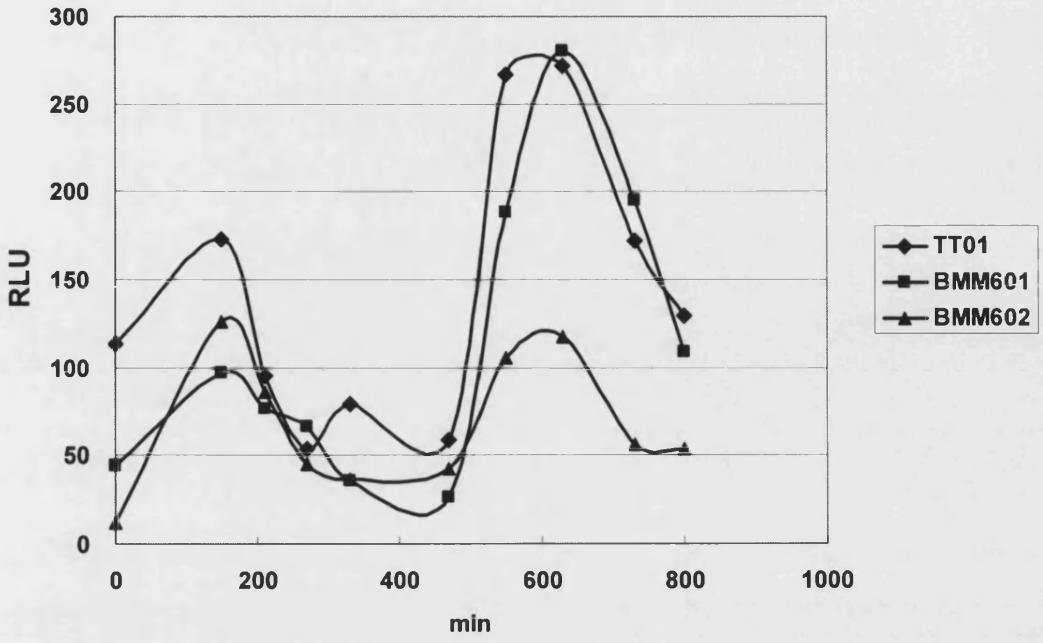

Figure 5.9. Bioluminescence of *Photorhabdus*. BMM601, BMM602 and TT01 cells from overnight culture were diluted to an OD_{600}=0.05 by inoculation into LB. Cells were incubated at 30°C with shaking. Growth rate was monitored by OD_{600}, and bioluminescence was measured using a Tecan luminometer.

5.3 Conclusion

The disruption of the Rcs phosphorelay does not significantly affect either symbiosis or pathogenicity in *Photorhabdus*. Nevertheless, biofilm formation of *Photorhabdus* was impaired by mutations in Rcs phosphorelay. Although mutations in either *rcsC* or *rcsB* result in aberrant biofilm formation, the mutation in *rcsB* has a more significant effect. Interestingly, both the mutation and overproduction of RcsB can cause a biofilm defect in the microtiter plate assay.

In the flowcell chamber system, mutations in either *rcsB* or *rcsC* affected biofilm development. In the early hours of flowcell biofilm study, both *rcsB* and *rcsC* mutants had noticeably less cells attached to the surface, suggesting a defect in

attachment. The mutations in the Rcs phosphorelay might affect surface composition and therefore prevent cells from attaching to a surface. Moreover, long chains of undivided cells were observed in both mutants, suggesting cell division was affected by mutations in the Rcs phosphorelay in *Photorhabdus*. The RcsC phosphorelay in *E. coli* regulates the cell division gene, *ftsZ* (Carballes *et al.*, 1999). However, after prolonged incubation, both mutant strains can reach the same maturation status as wild type, suggesting the defect may happen during the early stages of biofilm formation and may be overcome at higher cell densities.

The contribution of biofilm formation during both the virulence and symbiosis stages remains obscure. Within the nematode gut, *Photorhabdus* are encapsulated in a biofilm-like structure (ffrench-Constant *et al.*, 2003). Moreover the disruption of the *rcs* genes in *Photorhabdus* impaired biofilm formation although there was no obvious effect on pathogenicity or symbiosis, suggesting that the importance of biofilm formation was not significant in the tripartite bacteria-nematode-insect interaction. However, since the *rcsC* and *rcsB* mutations appear to act at an early stage in the flow chamber biofilm experiment, we can not rule out the possibility that the the Rcs phosphorelay has some minor effect on pathogenicity and symbiosis due to the disturbance at an early stage of biofilm formation. Both *rcsC* and *rcsB* mutations can form normal biofilm after prolonged incubation, suggesting that the outcome of biofilm-related function is not affected.

Chapter 6
General Discussion

The Rcs phosphorelay is a unique and complex signalling network found throughout the *Enterobacteriaceae* (Huang *et al.*, 2006; Majdalani and Gottesman, 2005). The aim of this study was to elucidate (a) the mechanism of RcsC function and (b) the role of the Rcs phosphorelay in *Enterobacteriaceae* with regard to biofilm formation. To this end, it was decided to undertake both comparative and mutagenesis studies of RcsC. In the comparative analysis, this study confirmed that both the Rcs phosphorelay and the function of RcsC are conserved in the *Enterobacteriaceae.* However, the differences in how RcsC from different species could complement biofilm formation in an *E. coli rcsC* mutant implied that RcsC from different species might sense and respond to different environmental signals. The genetic manipulation of the input domain of RcsC gave insight into the mechanism of RcsC function in *E. coli* and, in this study, separate sensing domains were identified.

The signal inputs of the Rcs phosphorelay

Work carried out in this study has revealed that there are at least three signals perceived independently by RcsC, i.e. DjlA overproduction, growth on a solid surface and an, as yet, unidentified signal during biofilm formation. DjlA overproduction has been used for the conditional activation of the Rcs phosphorelay in previous studies (Clarke *et al.*, 2002) whilst growth on a solid surface can be seen as a physiological signal to activate the Rcs phosphorelay (Ferrieres and Clarke, 2003). In this study, it was shown that growth on a surface (i.e. agar) appeared to be synergistic to DjlA overproduction (Fig. 3.5), implying that DjlA and solid surface act as independent signals on RcsC. In addition, by comparing $RcsC_{YP}$ and $RcsC_{\Delta PP}$, it is clear that a signal different from DjlA overproduction is perceived by RcsC during biofilm formation. $RcsC_{YP}$ was found to respond to DjlA yet this protein was unable to support biofilm formation. On the other hand, a periplasmic domain deletion $RcsC_{\Delta PP}$ did not respond to DjlA but did support biofilm formation. Therefore, the signal(s) perceived during biofilm formation is different from DjlA overproduction.

It might be argued that growth on a solid surface could be a signal related to biofilm formation. Previously it has been shown that the input signals of the Rcs phosphorelay can be categorised into two classes, according to their

dependence on RcsF (Majdalani and Gottesman, 2005). Most signals identified are RcsF-dependent, including the solid surface signal (Ferrierres, personal communication). However, the exception is DjlA overproduction which has been shown to be RcsF-independent (Majdalani *et al.*, 2005). Work in our lab has shown that biofilm formation is not affected by a mutation in *rcsF*, implying that signal perception during biofilm formation may also be RcsF-independent (Ferrierres, personal communication). Therefore, it appears that the signal perceived during biofilm formation is different from the signal perceived during growth on a surface. Biofilm formation is a complex developmental process, and multiple signals might be sensed at different stages. Therefore, a solid surface could be one, but not the only, signal perceived by RcsC during biofilm formation. Therefore, DjlA overproduction, growth on a solid surface and the biofilm signal are independently perceived by RcsC.

What is the nature of the signals during biofilm formation?

Although the nature of the signal generated during biofilm formation remains to be determined, this study revealed that several regions of RcsC were important for sensing this signal. Firstly, membrane localisation of RcsC appeared to be important. This was demonstrated by the fact that $RcsC_{\Delta TM}$ and $RcsC_{\Delta INPUT}$ did not support biofilm formation. However, although EnvZ-RcsC is anchored to the inner membrane, this chimera showed the same phenotype as $RcsC_{\Delta TM}$, implying that anchoring to the inner membrane is not sufficient for biofilm formation. Therefore, the nature of the TMs also appears to be important for RcsC function. Several biofilm-deficient mutants identified in the mutagenesis study contain mutations that are in or close to the TMs. The TMs of HKs are thought to undergo some movements during signal transduction and these movements can modulate the activity of the HK (Leonardo and Forst, 1996). Mutations in residues near the TMs might therefore affect how the TMs interact resulting in conformational changes in the intracellular signalling modules that will affect the activity of the RcsC protein. On the other hand, it is also possible that the TMs might be directly involved in signal perception (Kwon *et al.*, 2000).

The periplasmic domain has been shown to be important in signal sensing in several HKs (Chamnongpol *et al.*, 2003; Chang and Winans, 1992) and the

results presented here suggest that this domain plays a similar role in RcsC. In effect, the periplasmic domain of RcsC is required to respond to DjlA overproduction. Interestingly, however, deletion of this domain does not affect the ability of RcsC to support biofilm formation, suggesting that the periplasmic domain is not involved in sensing the signal during biofilm formation.

The linker region of RcsC is important for biofilm formation, as 22 out of 25 biofilm-deficient mutants identified in this study have at least one mutation localised in the linker region. The linker region of RcsC is predicted to consist of a HAMP linker and a PAS fold, and both are predicted to be domains involved in signal transduction (Hefti *et al.*, 2004; Williams and Stewart, 1999). Mutations in the linker region of RcsC appear to affect the ratio of kinase to phosphatase activity as two mutations H339D and R344S, resulted in a constitutively active RcsC. These mutations are similar to the E338K substitution identified in RcsC that also induced mucoidy in *E. coli* (Clavel *et al.*, 1996). In addition, mutations in the linker region of RcsC in *Salmonella* were also shown to constitutively activate the Rcs phosphorelay (Garcia-Calderon *et al.*, 2005). Furthermore, this study has shown that the deletion of the linker region of RcsC not only abolished biofilm formation but also had a significant impact on protein stability suggesting that the linker region plays an important role in both the structure and activity of RcsC.

One of the point mutations in the linker region, $RcsC_{Q449H}$, was of particular interest. This mutant failed to support biofilm formation but was able to respond to DjlA overproduction and also complemented the constitutive activity of the *rcsC137* allele suggesting that the $RcsC_{Q449H}$ mutant was enzymatically active. Further analysis of RcsC identified a conserved domain in the linker region that contained several equally spaced Q residues that, when presented as a helical wheel, fall on the same side of the predicted α-helix (Fig. 4.12B). The striking asymmetry of these Q residues strongly implies a role in signal transduction and it is proposed that this domain, called the Q domain, is a novel domain involved in signal transduction by the Rcs phosphorelay. Strikingly, $RcsC_{YP}$, a protein that does not restore biofilm formation in the *E. coli rcsC* mutant background, has an incomplete Q domain (i.e. the second Q residue is replaced by T) suggesting

that this domain might be involved in signal perception during biofilm formation. However, reconstruction of the Q domain in $RcsC_{YP}$ did not restore its ability to complement biofilm formation in BMM520, suggesting that although an intact Q domain may be necessary for biofilm formation, it is not sufficient.

During biofilm formation, it is expected that the cell surface will undergo significant changes (Van Houdt and Michiels, 2005), and it has been reported that there is significant alteration in expression of genes involved in peptidoglygan during biofilm formation in *E. coli* (Schembri *et al.*, 2003). The biosynthesis of peptidoglycan requires the lipid carrier Un-PP, and the cycling of Un-PP and Un-P across the cell membrane (El Ghachi *et al.*, 2005; Huang *et al.*, 2006). The ratio of Un-PP/Un-P can potentially serve as an intracellular signal reflecting the status of cell envelope composition, and it has been suggested to be a signal sensed by RcsC during biofilm formation (Huang *et al.*, 2006). In support of this, as shown in this study, regions adjacent to the cell membrane, i.e., TMs and the linker region are involved in perception of the biofilm signal.

RcsC activities in biofilm formation

Previous studies have suggested that the development of a biofilm is under the temporal control of the Rcs phosphorelay (Ferrieres and Clarke, 2003; Pruss *et al.*, 2006). Furthermore it has been shown that both the lack of RcsC activity and a constitutive (locked-on kinase) RcsC activity can impair biofilm formation (Ferrieres and Clarke, 2003; Vianney *et al.*, 2005) and this study has confirmed these results. It has also been reported that a *Salmonella rcsC* mutant is attenuated for systemic infection and, in addition, the constitutive activation of the Rcs phosphorelay also caused loss of virulence in *Salmonella* (Detweiler *et al.*, 2003; Garcia-Calderon *et al.*, 2005; Mouslim *et al.*, 2004). Therefore, there are parallels in the role of the Rcs phosphorelay during virulence in *Salmonella* and during biofilm formation in *E. coli* (Huang *et al.*, 2006; Tierrez and Garcia-del Portillo, 2005). In *E. coli*, in the absence of RcsC, RcsB is phosphorylated by other phosphate donors (Fredericks *et al.*, 2006; Shin and Park, 1995) and the deletion of *rcsC* was shown to result in an increased level of *rprA* expression, presumably due to an increased level of RcsB~P (Majdalani *et al.*, 2002). The Rcs phosphorelay has also been shown to negatively regulate genes involved in

cell adhesion and motility and therefore the low level of RcsB~P might be enough to inhibit the expression of flagella and cell adhesins thus preventing cells from attaching to a surface and forming a biofilm (Ferrieres and Clarke, 2003; Francez-Charlot *et al.*, 2003). Therefore, the phosphatase activity of RcsC could be important to ensure that there are very low levels of RcsB~P during the early stages of biofilm formation.

If the absence of RcsC phosphatase activity (and thus increased levels of RcsB~P) is responsible for the biofilm defect it is possible that the deletion of certain genes regulated by the Rcs phosphorelay would restore biofilm formation. Previous studies have shown that colanic acid production could interfere with biofilm formation by inhibiting cellular attachment (Hanna *et al.*, 2003; Schembri *et al.*, 2004). Therefore we disrupted the *gmd* gene in the *cps* operon to inhibit colanic acid production. However, this mutation failed to restore biofilm formation in an *rcsC* mutant (Fig. 4.5), suggesting that other genes in the Rcs regulon might be responsible for the defect in biofilm formation. However, the production of colanic acid is required during the maturation stage of biofilm formation suggesting that the kinase activity of RcsC is important during the later stages of biofilm formation (Danese *et al.*, 2000; Ferrieres and Clarke, 2003; Huang *et al.*, 2006). Therefore, the lack of RcsC kinase activity would also be expected to result in a defect in biofilm formation. Therefore it is likely that both phosphatase and kinase activity of RcsC are required for normal biofilm formation in *E. coli* and mutations affecting either the enzymatic or sensing function of RcsC can deteriorate biofilm formation (this study and Ferrieres and Clarke, 2003).

The phosphatase activity of RcsC and the *rcsC137* allele

Data from our laboratory suggests that the absence of RcsC phosphatase activity is the likely cause of the biofilm formation defect observed in *rcsC* mutant cells (Ferrieres, unpublished data). Therefore, it could be argued that the restoration of biofilm formation could be used as an assay to localise the domains involved in phosphatase activity in RcsC. In this way, it can be concluded from previous studies that functional H1 and D1 domains are required for phosphatase activity of RcsC (Ferrieres and Clarke, 2003). This study has further shown that the input domain of RcsC plays an important role in

controlling the activity of this protein and phosphatase activity does not require the periplasmic domain but does require both the TMs and the linker domain of RcsC.

Until now complementation of *rcsC137*, a constitutively activated (locked-on kinase) allele of *rcsC* has been used to assay for RcsC phosphatase activity (Clarke *et al.*, 2002). The constitutive activity of the *rcsC137* allele was thought to be due to the loss of phosphatase activity (primarily because the mutation was recessive to the wild-type *rcsC* gene) although it is now clear that this allele is not simply a loss-of-function mutation. If the *rcsC137* allele was simply a loss of phosphatase activity one might expect to see the same affect on gene expression as seen with an *rcsC* deletion mutant and this is clearly not the case (Majdalani and Gottesman, 2005). Moreover, *rcsC* mutants that restored biofilm formation did not always complement the *rcsC137* allele indicating that there is not a strict correlation between restoration of biofilm formation and complementation of the *rcsC137* allele. Finally, $rcsC_{H339D}$ and $rcsC_{R344S}$ were identified in this study and these alleles encode proteins with a locked-on kinase activity yet both alleles complement the *rcs137* allele, suggesting that the phosphatase activity can be restored by the interaction between two constitutive alleles. These results suggest that the "locked-on kinase" phenotype of the *rcsC137* allele is more complex than previously thought.

VirA, a sensor kinase that regulates expression of the *vir* genes in *Agrobacterium tumefaciens*, has a similar domain structure to RcsC i.e. both proteins are hybrid kinases containing both an H1 and a D1 domain. The removal of the D1 domain of VirA results in high basal activity suggesting that the D1 domain negatively regulates the kinase activity (Chang and Winans, 1992). The D1 domain of VirA is not directly involved in the phosphorelay but rather competes with the D1 domain of the VirB response regulator for phosphoryl groups donated by the H1 domain of VirA (Chang *et al.*, 1996). VirA is assembled as a dimer and studies have shown that the D1 domain of VirA inhibited the kinase activity of the opposite subunit in the dimer and mutations interfering with this interaction prevented the inhibitory effect (Brencic *et al.*, 2004). Therefore, it is possible that the mutation in *rcsC137* does not affect the

phosphatase activity of RcsC but rather changes the conformation of the D1 domain resulting in the loss of some inhibitory effect. Moreover, if RcsC functions as a dimer and the inhibitory effect is intermolecular (as seen with VirA) then it would be possible to restore the inhibitory effect through the intermolecular complementation of two constitutive alleles.

The biofilm defect observed in an *rcsC* null mutant, which does not have phosphatase activity, or a locked-on kinase mutant can be explained by the elevated level of RcsB~P (Ferrieres, unpublished data). Therefore it is clear that the level of RcsB~P is important during biofilm formation. It is noteworthy that many of the biofilm-deficient RcsC mutants identified in this study actually result in lower levels of biofilm formation than the *rcsC* mutant, suggesting that these mutations are actually gain-of-function mutations rather than loss-of-function. One possibility is that these mutants have a locked-on phosphatase activity. This would prevent the cell from producing the appropriate level of RcsB~P thus contributing to the repression of biofilm formation observed in these mutants.

The biological role of the Rcs phosphorelay in the *Enterobacteriaceae*

Yersinia and *Photorhabdus* are relatively phylogenetically distant from *E. coli* and it is not surprising that there are differences in the Rcs phosphorelay between these bacteria. The diversity lies not only in amino acid sequence but also in gene organisation around the *rcs* locus and and it is likely that the bacteria have adapted the conserved Rcs phosphorelay for sensing different signals (Huang *et al.*, 2006). In support of this, this study has shown that both $RcsC_{YP}$ and $RcsC_{TT01}$ did not complement biofilm formation in the *E. coli rcsC mutant* (Fig. 3.7 and data not shown). In *E. coli*, RcsC is required for biofilm formation but a mutation in *rcsB* does not affect biofilm formation (Ferrieres, unpublished data). In contrast, in *Photorhabdus,* the disruption of the *rcsC* gene does not affect biofilm formation but the mutation in *rcsB* impaired biofilm formation in the microtitre plate assay (Fig. 5.2). The Rcs phosphorelay appears to be important in the later stages of biofilm formation in *E. coli* and in *Salmonella* for the persistence within host macrophages (Tierrez and Garcia-del Portillo, 2005). In contrast, the Rcs phosphorelay is required during the early stages of *Yersinia* pathogenicity and during the early stages of biofilm formation

in *Photorhabdus* (Venecia and Young, 2005).

It has been shown that *Photorhabdus* are encapsulated in a biofilm-like structure within the nematode gut and it has been suggested that biofilm formation by *Photorhabdus* might play an important role during the bacteria-nematode interaction (ffrench-Constant *et al.*, 2003). Previous studies have shown that the level of bacterial colonisation in the nematode was significantly reduced in a biofilm-deficient *Photorhabdus pbgPE* mutant (Bennett and Clarke, 2005). However in this study it has been shown that the *Photorhabdus rcsB* mutant, which is deficient in biofilm formation (although not as significantly as the *pbgPE* mutant) did support nematode development and could colonise the nematode. However, the level of bacteria colonising each nematode does appear to be lower in the *rcsB* mutant, although more samples are required to test the difference statistically (Fig. 5.7). Therefore, it is possible that the *rcsB* mutant is less able to colonise the nematode and this may be due to the defect in biofilm formation observed in this mutant.

This study set out to gain insight into the role and mechanism of signal perception by RcsC, the HK of the Rcs phosphorelay. In this study, I have successfully identified several regions of RcsC that can affect the function of the RcsC protein and are involved in signal perception, including the periplasmic domain (required for responding to DjlA overproduction) and the Q domain. Furthermore, comparisons between the RcsC homologues from different *Enterobacteriaceae* led to the conclusion that, although these proteins are homologous in sequence and function, different RcsC proteins have evolved in different ways and may have adapted to respond to different environmental signals, reflecting the different life styles of the bacteria.

References

Achtman, M., Zurth, K., Morelli, G., Torrea, G., Guiyoule, A., and Carniel, E. (1999) *Yersinia pestis*, the cause of plague, is a recently emerged clone of *Yersinia pseudotuberculosis*. *Proc Natl Acad Sci U S A* **96**: 14043-14048.

Aravind, L., and Ponting, C.P. (1999) The cytoplasmic helical linker domain of receptor histidine kinase and methyl-accepting proteins is common to many prokaryotic signalling proteins. *FEMS Microbiol Lett* **176**: 111-116.

Arricau, N., Hermant, D., Waxin, H., Ecobichon, C., Duffey, P.S., and Popoff, M.Y. (1998) The RcsB-RcsC regulatory system of *Salmonella typhi* differentially modulates the expression of invasion proteins, flagellin and Vi antigen in response to osmolarity. *Mol Microbiol* **29**: 835-850.

Ashby, M.K. (2004) Survey of the number of two-component response regulator genes in the complete and annotated genome sequences of prokaryotes. *FEMS Microbiol Lett* **231**: 277-281.

Baker, M.D., Wolanin, P.M., and Stock, J.B. (2006) Signal transduction in bacterial chemotaxis. *Bioessays* **28**: 9-22.

Belas, R., Schneider, R., and Melch, M. (1998) Characterization of *Proteus mirabilis* precocious swarming mutants: identification of *rsbA*, encoding a regulator of swarming behavior. *J Bacteriol* **180**: 6126-6139.

Bennett, H.P., and Clarke, D.J. (2005) The *pbgPE* operon in *Photorhabdus luminescens* is required for pathogenicity and symbiosis. *J Bacteriol* **187**: 77-84.

Bentley, S.D., Chater, K.F., Cerdeno-Tarraga, A.M., Challis, G.L., Thomson, N.R., James, K.D., Harris, D.E., Quail, M.A., Kieser, H., Harper, D., Bateman, A., Brown, S., Chandra, G., Chen, C.W., Collins, M., Cronin, A., Fraser, A., Goble, A., Hidalgo, J., Hornsby, T., Howarth, S., Huang, C.H., Kieser, T., Larke, L., Murphy, L., Oliver, K., O'Neil, S., Rabbinowitsch, E., Rajandream, M.A., Rutherford, K., Rutter, S., Seeger, K., Saunders, D., Sharp, S., Squares, R., Squares, S., Taylor, K., Warren, T., Wietzorrek, A., Woodward, J., Barrell, B.G., Parkhill, J., and Hopwood, D.A. (2002) Complete genome sequence of the model actinomycete *Streptomyces coelicolor* A3(2). *Nature* **417**: 141-147.

Bernard, S., Clarke, D.J., Chen, M.X., Holland, I.B., and Jacq, A. (1998) Increased sensitivity of *E. coli* to novobiocin, EDTA and the

anticalmodulin drug W7 following overproduction of DjlA requires a functional transmembrane domain. *Mol Gen Genet* **259**: 645-655.

Bijlsma, J.J., and Groisman, E.A. (2005) The PhoP/PhoQ system controls the intramacrophage type three secretion system of *Salmonella enterica*. *Mol Microbiol* **57**: 85-96.

Bock, A., and Gross, R. (2002) The unorthodox histidine kinases BvgS and EvgS are responsive to the oxidation status of a quinone electron carrier. *Eur J Biochem* **269**: 3479-3484.

Brencic, A., Xia, Q., and Winans, S.C. (2004) VirA of *Agrobacterium tumefaciens* is an intradimer transphosphorylase and can actively block *vir* gene expression in the absence of phenolic signals. *Mol Microbiol* **52**: 1349-1362.

Brill, J.A., Quinlan-Walshe, C., and Gottesman, S. (1988) Fine-structure mapping and identification of two regulators of capsule synthesis in *Escherichia coli* K-12. *J Bacteriol* **170**: 2599-2611.

Cano, D.A., Dominguez-Bernal, G., Tierrez, A., Garcia-Del Portillo, F., and Casadesus, J. (2002) Regulation of capsule synthesis and cell motility in *Salmonella enterica* by the essential gene *igaA*. *Genetics* **162**: 1513-1523.

Carballes, F., Bertrand, C., Bouche, J.P., and Cam, K. (1999) Regulation of *Escherichia coli* cell division genes *ftsA* and *ftsZ* by the two-component system *rcsC-rcsB*. *Mol Microbiol* **34**: 442-450.

Castanie-Cornet, M.P., Cam, K., and Jacq, A. (2006) RcsF is an outer membrane lipoprotein involved in the RcsCDB phosphorelay signaling pathway in *Escherichia coli*. *J Bacteriol* **188**: 4264-4270.

Chain, P.S., Carniel, E., Larimer, F.W., Lamerdin, J., Stoutland, P.O., Regala, W.M., Georgescu, A.M., Vergez, L.M., Land, M.L., Motin, V.L., Brubaker, R.R., Fowler, J., Hinnebusch, J., Marceau, M., Medigue, C., Simonet, M., Chenal-Francisque, V., Souza, B., Dacheux, D., Elliott, J.M., Derbise, A., Hauser, L.J., and Garcia, E. (2004) Insights into the evolution of *Yersinia pestis* through whole-genome comparison with *Yersinia pseudotuberculosis*. *Proc Natl Acad Sci U S A* **101**: 13826-13831.

Chamnongpol, S., Cromie, M., and Groisman, E.A. (2003) Mg^{2+} sensing by the Mg^{2+} sensor PhoQ of *Salmonella enterica*. *J Mol Biol* **325**: 795-807.

Chang, C.H., and Winans, S.C. (1992) Functional roles assigned to the periplasmic, linker, and receiver domains of the *Agrobacterium tumefaciens* VirA protein. *J Bacteriol* **174**: 7033-7039.

Chang, C.H., Zhu, J., and Winans, S.C. (1996) Pleiotropic phenotypes caused by genetic ablation of the receiver module of the *Agrobacterium tumefaciens* VirA protein. *J Bacteriol* **178**: 4710-4716.

Clarke, D.J., Holland, I.B., and Jacq, A. (1997) Point mutations in the transmembrane domain of DjlA, a membrane-linked DnaJ-like protein, abolish its function in promoting colanic acid production via the Rcs signal transduction pathway. *Mol Microbiol* **25**: 933-944.

Clarke, D.J., Joyce, S.A., Toutain, C.M., Jacq, A., and Holland, I.B. (2002) Genetic analysis of the RcsC sensor kinase from *Escherichia coli* K-12. *J Bacteriol* **184**: 1204-1208.

Clavel, T., Lazzaroni, J.C., Vianney, A., and Portalier, R. (1996) Expression of the *tolQRA* genes of *Escherichia coli* K-12 is controlled by the RcsC sensor protein involved in capsule synthesis. *Mol Microbiol* **19**: 19-25.

Conter, A., Sturny, R., Gutierrez, C., and Cam, K. (2002) The RcsCB His-Asp phosphorelay system is essential to overcome chlorpromazine-induced stress in *Escherichia coli. J Bacteriol* **184**: 2850-2853.

Costa, C.S., and Anton, D.N. (2001) Role of the *ftsA1p* promoter in the resistance of mucoid mutants of *Salmonella enterica* to mecillinam: characterization of a new type of mucoid mutant. *FEMS Microbiol Lett* **200**: 201-205.

Danese, P.N., Pratt, L.A., and Kolter, R. (2000) Exopolysaccharide production is required for development of *Escherichia coli* K-12 biofilm architecture. *J Bacteriol* **182**: 3593-3596.

Derzelle, S., Turlin, E., Duchaud, E., Pages, S., Kunst, F., Givaudan, A., and Danchin, A. (2004) The PhoP-PhoQ two-component regulatory system of Photorhabdus luminescens is essential for virulence in insects. *J Bacteriol* **186**: 1270-1279.

Detweiler, C.S., Monack, D.M., Brodsky, I.E., Mathew, H., and Falkow, S. (2003) *virK*, *somA* and *rcsC* are important for systemic *Salmonella enterica* serovar Typhimurium infection and cationic peptide resistance. *Mol Microbiol* **48**: 385-400.

Dominguez-Bernal, G., Pucciarelli, M.G., Ramos-Morales, F., Garcia-Quintanilla, M., Cano, D.A., Casadesus, J., and Garcia-del Portillo, F. (2004) Repression of the RcsC-YojN-RcsB phosphorelay by the IgaA protein is a requisite for *Salmonella* virulence. *Mol Microbiol* **53**: 1437-1449.

Duchaud, E., Rusniok, C., Frangeul, L., Buchrieser, C., Givaudan, A., Taourit, S., Bocs, S., Boursaux-Eude, C., Chandler, M., Charles, J.F., Dassa, E., Derose, R., Derzelle, S., Freyssinet, G., Gaudriault, S., Medigue, C., Lanois, A., Powell, K., Siguier, P., Vincent, R., Wingate, V., Zouine, M., Glaser, P., Boemare, N., Danchin, A., and Kunst, F. (2003) The genome sequence of the entomopathogenic bacterium *Photorhabdus luminescens*. *Nat Biotechnol* **21**: 1307-1313.

Dunphy, G.B., and Chadwick, J.S. (1989) Effects of selected carbohydrates and the contribution of the prophenoloxidase cascade system to the adhesion of strains of *Pseudomonas aeruginosa* and *Proteus mirabilis* to hemocytes of nonimmune larval Galleria mellonella. *Can J Microbiol* **35**: 524-527.

Dutta, R., Qin, L., and Inouye, M. (1999) Histidine kinases: diversity of domain organization. *Mol Microbiol* **34**: 633-640.

Ebel, W., and Trempy, J.E. (1999) *Escherichia coli* RcsA, a positive activator of colanic acid capsular polysaccharide synthesis, functions to activate its own expression. *J Bacteriol* **181**: 577-584.

El-Kazzaz, W., Morita, T., Tagami, H., Inada, T., and Aiba, H. (2004) Metabolic block at early stages of the glycolytic pathway activates the Rcs phosphorelay system via increased synthesis of dTDP-glucose in *Escherichia coli*. *Mol Microbiol* **51**: 1117-1128.

El Ghachi, M., Bouhss, A., Blanot, D., and Mengin-Lecreulx, D. (2004) The *bacA* gene of Escherichia coli encodes an undecaprenyl pyrophosphate phosphatase activity. *J Biol Chem* **279**: 30106-30113.

El Ghachi, M., Derbise, A., Bouhss, A., and Mengin-Lecreulx, D. (2005) Identification of multiple genes encoding membrane proteins with undecaprenyl pyrophosphate phosphatase (UppP) activity in *Escherichia coli*. *J Biol Chem* **280**: 18689-18695.

Ferrieres, L., and Clarke, D.J. (2003) The RcsC sensor kinase is required for normal biofilm formation in *Escherichia coli* K-12 and controls the

expression of a regulon in response to growth on a solid surface. *Mol Microbiol* **50**: 1665-1682.

Ferrieres, L., Francez-Charlot, A., Gouzy, J., Rouille, S., and Kahn, D. (2004) FixJ-regulated genes evolved through promoter duplication in *Sinorhizobium meliloti*. *Microbiology* **150**: 2335-2345.

ffrench-Constant, R., Waterfield, N., Daborn, P., Joyce, S., Bennett, H., Au, C., Dowling, A., Boundy, S., Reynolds, S., and Clarke, D. (2003) *Photorhabdus*: towards a functional genomic analysis of a symbiont and pathogen. *FEMS Microbiol Rev* **26**: 433-456.

Ffrench-Constant, R.H., Waterfield, N., Burland, V., Perna, N.T., Daborn, P.J., Bowen, D., and Blattner, F.R. (2000) A genomic sample sequence of the entomopathogenic bacterium *Photorhabdus luminescens* W14: potential implications for virulence. *Appl Environ Microbiol* **66**: 3310-3329.

Foultier, B., Troisfontaines, P., Muller, S., Opperdoes, F.R., and Cornelis, G.R. (2002) Characterization of the *ysa* pathogenicity locus in the chromosome of *Yersinia enterocolitica* and phylogeny analysis of type III secretion systems. *J Mol Evol* **55**: 37-51.

Francez-Charlot, A., Laugel, B., Van Gemert, A., Dubarry, N., Wiorowski, F., Castanie-Cornet, M.P., Gutierrez, C., and Cam, K. (2003) RcsCDB His-Asp phosphorelay system negatively regulates the *flhDC* operon in Escherichia coli. *Mol Microbiol* **49**: 823-832.

Fredericks, C.E., Shibata, S., Aizawa, S., Reimann, S.A., and Wolfe, A.J. (2006) Acetyl phosphate-sensitive regulation of flagellar biogenesis and capsular biosynthesis depends on the Rcs phosphorelay. *Mol Microbiol* **61**: 734-747.

Fujita, M., Gonzalez-Pastor, J.E., and Losick, R. (2005) High- and low-threshold genes in the Spo0A regulon of *Bacillus subtilis*. *J Bacteriol* **187**: 1357-1368.

Galperin, M.Y. (2006) Structural classification of bacterial response regulators: diversity of output domains and domain combinations. *J Bacteriol* **188**: 4169-4182.

Garcia-Calderon, C.B., Garcia-Quintanilla, M., Casadesus, J., and Ramos-Morales, F. (2005) Virulence attenuation in *Salmonella enterica rcsC*

mutants with constitutive activation of the Rcs system. *Microbiology* **151**: 579-588.

Gervais, F.G., and Drapeau, G.R. (1992) Identification, cloning, and characterization of *rcsF*, a new regulator gene for exopolysaccharide synthesis that suppresses the division mutation *ftsZ84* in *Escherichia coli* K-12. *J Bacteriol* **174**: 8016-8022.

Gong, W., Hao, B., Mansy, S.S., Gonzalez, G., Gilles-Gonzalez, M.A., and Chan, M.K. (1998) Structure of a biological oxygen sensor: a new mechanism for heme-driven signal transduction. *Proc Natl Acad Sci U S A* **95**: 15177-15182.

Gottesman, S., Trisler, P., and Torres-Cabassa, A. (1985) Regulation of capsular polysaccharide synthesis in *Escherichia coli* K-12: characterization of three regulatory genes. *J Bacteriol* **162**: 1111-1119.

Guiney, D.G. (2005) The role of host cell death in *Salmonella* infections. *Curr Top Microbiol Immunol* **289**: 131-150.

Gunn, J.S., Lim, K.B., Krueger, J., Kim, K., Guo, L., Hackett, M., and Miller, S.I. (1998) PmrA-PmrB-regulated genes necessary for 4-aminoarabinose lipid A modification and polymyxin resistance. *Mol Microbiol* **27**: 1171-1182.

Guzman, L.M., Belin, D., Carson, M.J., and Beckwith, J. (1995) Tight regulation, modulation, and high-level expression by vectors containing the arabinose P_{BAD} promoter. *J Bacteriol* **177**: 4121-4130.

Hagiwara, D., Sugiura, M., Oshima, T., Mori, H., Aiba, H., Yamashino, T., and Mizuno, T. (2003) Genome-wide analyses revealing a signaling network of the RcsC-YojN-RcsB phosphorelay system in *Escherichia coli*. *J Bacteriol* **185**: 5735-5746.

Hanna, A., Berg, M., Stout, V., and Razatos, A. (2003) Role of capsular colanic acid in adhesion of uropathogenic *Escherichia coli*. *Appl Environ Microbiol* **69**: 4474-4481.

Heermann, R., Fohrmann, A., Altendorf, K., and Jung, K. (2003) The transmembrane domains of the sensor kinase KdpD of *Escherichia coli* are not essential for sensing K^+ limitation. *Mol Microbiol* **47**: 839-848.

Hefti, M.H., Francoijs, K.J., de Vries, S.C., Dixon, R., and Vervoort, J. (2004) The PAS fold. A redefinition of the PAS domain based upon structural prediction. *Eur J Biochem* **271**: 1198-1208.

Huang, Y.H., Ferrieres, L., and Clarke, D.J. (2006) The role of the Rcs phosphorelay in *Enterobacteriaceae*. *Res Microbiol* **157**: 206-212.

Hulko, M., Berndt, F., Gruber, M., Linder, J.U., Truffault, V., Schultz, A., Martin, J., Schultz, J.E., Lupas, A.N., and Coles, M. (2006) The HAMP domain structure implies helix rotation in transmembrane signaling. *Cell* **126**: 929-940.

Ize, B., Stanley, N.R., Buchanan, G., and Palmer, T. (2003) Role of the *Escherichia coli* Tat pathway in outer membrane integrity. *Mol Microbiol* **48**: 1183-1193.

Ize, B., Porcelli, I., Lucchini, S., Hinton, J.C., Berks, B.C., and Palmer, T. (2004) Novel phenotypes of *Escherichia coli tat* mutants revealed by global gene expression and phenotypic analysis. *J Biol Chem* **279**: 47543-47554.

Joseph, L.A., and Wright, A.C. (2004) Expression of *Vibrio vulnificus* capsular polysaccharide inhibits biofilm formation. *J Bacteriol* **186**: 889-893.

Joyce, S.A., and Clarke, D.J. (2003) A *hexA* homologue from *Photorhabdus regulates* pathogenicity, symbiosis and phenotypic variation. *Mol Microbiol* **47**: 1445-1457.

Jung, K., and Altendorf, K. (1998) Individual substitutions of clustered arginine residues of the sensor kinase KdpD of *Escherichia coli* modulate the ratio of kinase to phosphatase activity. *J Biol Chem* **273**: 26415-26420.

Kaldalu, N., Mei, R., and Lewis, K. (2004) Killing by ampicillin and ofloxacin induces overlapping changes in *Escherichia coli* transcription profile. *Antimicrob Agents Chemother* **48**: 890-896.

Kaspar, S., Perozzo, R., Reinelt, S., Meyer, M., Pfister, K., Scapozza, L., and Bott, M. (1999) The periplasmic domain of the histidine autokinase CitA functions as a highly specific citrate receptor. *Mol Microbiol* **33**: 858-872.

Kelm, O., Kiecker, C., Geider, K., and Bernhard, F. (1997) Interaction of the regulator proteins RcsA and RcsB with the promoter of the operon for amylovoran biosynthesis in *Erwinia amylovora*. *Mol Gen Genet* **256**: 72-83.

Kuo, M.S., Chen, K.P., and Wu, W.F. (2004) Regulation of RcsA by the ClpYQ (HslUV) protease in *Escherichia coli*. *Microbiology* **150**: 437-446.

Kwon, O., Georgellis, D., Lynch, A.S., Boyd, D., and Lin, E.C. (2000) The ArcB sensor kinase of *Escherichia coli*: genetic exploration of the transmembrane region. *J Bacteriol* **182**: 2960-2966.

Leonardo, M.R., and Forst, S. (1996) Re-examination of the role of the periplasmic domain of EnvZ in sensing of osmolarity signals in *Escherichia coli*. *Mol Microbiol* **22**: 405-413.

Liaw, S.J., Lai, H.C., and Wang, W.B. (2004) Modulation of swarming and virulence by fatty acids through the RsbA protein in *Proteus mirabilis*. *Infect Immun* **72**: 6836-6845.

Majdalani, N., Hernandez, D., and Gottesman, S. (2002) Regulation and mode of action of the second small RNA activator of RpoS translation, RprA. *Mol Microbiol* **46**: 813-826.

Majdalani, N., and Gottesman, S. (2005) The Rcs Phosphorelay: A Complex Signal Transduction System. *Annu Rev Microbiol*.

Majdalani, N., Heck, M., Stout, V., and Gottesman, S. (2005) Role of RcsF in signaling to the Rcs phosphorelay pathway in *Escherichia coli*. *J Bacteriol* **187**: 6770-6778.

Martinez, E., and de la Cruz, F. (1988) Transposon Tn21 encodes a RecA-independent site-specific integration system. *Mol Gen Genet* **211**: 320-325.

Mendez-Ortiz, M.M., Hyodo, M., Hayakawa, Y., and Membrillo-Hernandez, J. (2006) Genome-wide transcriptional profile of *Escherichia coli* in response to high levels of the second messenger 3',5'-cyclic diguanylic acid. *J Biol Chem* **281**: 8090-8099.

Miller, J.H. (1972) *Experiments in Molecular Genetics*. Cold Spring Harbor, NY: Cold Spring Harbor Laboratory Press.

Minogue, T.D., Carlier, A.L., Koutsoudis, M.D., and von Bodman, S.B. (2005) The cell density-dependent expression of stewartan exopolysaccharide in *Pantoea stewartii* ssp. stewartii is a function of EsaR-mediated repression of the *rcsA* gene. *Mol Microbiol* **56**: 189-203.

Mireles, J.R., 2nd, Toguchi, A., and Harshey, R.M. (2001) *Salmonella enterica* serovar Typhimurium swarming mutants with altered biofilm-forming abilities: surfactin inhibits biofilm formation. *J Bacteriol* **183**: 5848-5854.

Mizuno, T. (1997) Compilation of all genes encoding two-component phosphotransfer signal transducers in the genome of *Escherichia coli*. *DNA Res* **4**: 161-168.

Mouslim, C., and Groisman, E.A. (2003) Control of the *Salmonella ugd* gene by three two-component regulatory systems. *Mol Microbiol* **47**: 335-344.

Mouslim, C., Latifi, T., and Groisman, E.A. (2003) Signal-dependent requirement for the co-activator protein RcsA in transcription of the RcsB-regulated *ugd* gene. *J Biol Chem* **278**: 50588-50595.

Mouslim, C., Delgado, M., and Groisman, E.A. (2004) Activation of the RcsC/YojN/RcsB phosphorelay system attenuates *Salmonella* virulence. *Mol Microbiol* **54**: 386-395.

Pappalardo, L., Janausch, I.G., Vijayan, V., Zientz, E., Junker, J., Peti, W., Zweckstetter, M., Unden, G., and Griesinger, C. (2003) The NMR structure of the sensory domain of the membranous two-component fumarate sensor (histidine protein kinase) DcuS of *Escherichia coli*. *J Biol Chem* **278**: 39185-39188.

Park, H., and Inouye, M. (1997) Mutational analysis of the linker region of EnvZ, an osmosensor in *Escherichia coli*. *J Bacteriol* **179**: 4382-4390.

Park, H., Saha, S.K., and Inouye, M. (1998) Two-domain reconstitution of a functional protein histidine kinase. *Proc Natl Acad Sci U S A* **95**: 6728-6732.

Parkhill, J., Wren, B.W., Thomson, N.R., Titball, R.W., Holden, M.T., Prentice, M.B., Sebaihia, M., James, K.D., Churcher, C., Mungall, K.L., Baker, S., Basham, D., Bentley, S.D., Brooks, K., Cerdeno-Tarraga, A.M., Chillingworth, T., Cronin, A., Davies, R.M., Davis, P., Dougan, G., Feltwell, T., Hamlin, N., Holroyd, S., Jagels, K., Karlyshev, A.V., Leather, S., Moule, S., Oyston, P.C., Quail, M., Rutherford, K., Simmonds, M., Skelton, J., Stevens, K., Whitehead, S., and Barrell, B.G. (2001) Genome sequence of *Yersinia pestis*, the causative agent of plague. *Nature* **413**: 523-527.

Perraud, A.-L., Kimmel, B., Weiss, V., and Gross, R. (1998) Specificity of the BvgAS and EvgAS phosphorelay is mediated by the C-terminal HPt domains of the sensor proteins. *Molecular Microbiology* **27**: 875.

Philippe, N., Alcaraz, J.P., Coursange, E., Geiselmann, J., and Schneider, D. (2004) Improvement of pCVD442, a suicide plasmid for gene allele exchange in bacteria. *Plasmid* **51**: 246-255.

Piggot, P.J., and Hilbert, D.W. (2004) Sporulation of *Bacillus subtilis*. *Curr Opin Microbiol* **7**: 579-586.

Prigent-Combaret, C., Prensier, G., Le Thi, T.T., Vidal, O., Lejeune, P., and Dorel, C. (2000) Developmental pathway for biofilm formation in curli-producing *Escherichia coli* strains: role of flagella, curli and colanic acid. *Environ Microbiol* **2**: 450-464.

Prigent-Combaret, C., and Brombacher, E. (2001) Complex Regulatory Network Controls Initial Adhesion and Biofilm Formation in Escheria coli *via* Regulation of the *csgD* Gene. *Journal of Bacteriololgy* **183**: 7213-7223.

Prouty, A.M., Van Velkinburgh, J.C., and Gunn, J.S. (2002) *Salmonella enterica* serovar Typhimurium resistance to bile: identification and characterization of the *tolQRA* cluster. *J Bacteriol* **184**: 1270-1276.

Pruss, B.M., Besemann, C., Denton, A., and Wolfe, A.J. (2006) A complex transcription network controls the early stages of biofilm development by *Escherichia coli*. *J Bacteriol* **188**: 3731-3739.

Raetz, C.R., and Whitfield, C. (2002) Lipopolysaccharide endotoxins. *Annu Rev Biochem* **71**: 635-700.

Raffa, R.G., and Raivio, T.L. (2002) A third envelope stress signal transduction pathway in *Escherichia coli*. *Mol Microbiol* **45**: 1599-1611.

Regelmann, A.G., Lesley, J.A., Mott, C., Stokes, L., and Waldburger, C.D. (2002) Mutational analysis of the Escherichia coli PhoQ sensor kinase: differences with the *Salmonella enterica* serovar Typhimurium PhoQ protein and in the mechanism of Mg^{2+} and Ca^{2+} sensing. *J Bacteriol* **184**: 5468-5478.

Reinelt, S., Hofmann, E., Gerharz, T., Bott, M., and Madden, D.R. (2003) The structure of the periplasmic ligand-binding domain of the sensor kinase CitA reveals the first extracellular PAS domain. *J Biol Chem* **278**: 39189-39196.

Robinson, V.L., Buckler, D.R., and Stock, A.M. (2000) A tale of two components: a novel kinase and a regulatory switch. *Nat Struct Biol* **7**: 626-633.

Rodrigue, A., Quentin, Y., Lazdunski, A., Mejean, V., and Foglino, M. (2000) Two-component systems in *Pseudomonas aeruginosa*: why so many? *Trends Microbiol* **8**: 498-504.

Sailer, F.C., Meberg, B.M., and Young, K.D. (2003) β-Lactam induction of colanic acid gene expression in *Escherichia coli*. *FEMS Microbiol Lett* **226**: 245-249.

Sanowar, S., Martel, A., and Moual, H.L. (2003) Mutational analysis of the residue at position 48 in the *Salmonella enterica* Serovar Typhimurium PhoQ sensor kinase. *J Bacteriol* **185**: 1935-1941.

Schembri, M.A., Kjaergaard, K., and Klemm, P. (2003) Global gene expression in *Escherichia coli* biofilms. *Mol Microbiol* **48**: 253-267.

Schembri, M.A., Dalsgaard, D., and Klemm, P. (2004) Capsule shields the function of short bacterial adhesins. *J Bacteriol* **186**: 1249-1257.

Sebaihia, M., Bentley, S., Thomson, N., Holden, M., and Parkhill, J. (2002) Genome giants. *Trends Microbiol* **10**: 309-310.

Shiba, Y., Yokoyama, Y., Aono, Y., Kiuchi, T., Kusaka, J., Matsumoto, K., and Hara, H. (2004) Activation of the Rcs signal transduction system is responsible for the thermosensitive growth defect of an *Escherichia coli* mutant lacking phosphatidylglycerol and cardiolipin. *J Bacteriol* **186**: 6526-6535.

Shiba, Y., Matsumoto, K., and Hara, H. (2006) DjlA negatively regulates the Rcs signal transduction system in *Escherichia coli*. *Genes Genet Syst* **81**: 51-56.

Shin, S., and Park, C. (1995) Modulation of flagellar expression in *Escherichia coli* by acetyl phosphate and the osmoregulator OmpR. *J Bacteriol* **177**: 4696-4702.

Sledjeski, D., and Gottesman, S. (1995) A small RNA acts as an antisilencer of the H-NS-silenced *rcsA* gene of *Escherichia coli*. *Proc Natl Acad Sci U S A* **92**: 2003-2007.

Sledjeski, D.D., and Gottesman, S. (1996) Osmotic shock induction of capsule synthesis in *Escherichia coli* K-12. *J Bacteriol* **178**: 1204-1206.

Stephenson, K., and Hoch, J.A. (2002) Evolution of signalling in the sporulation phosphorelay. *Mol Microbiol* **46**: 297-304.

Stock, A.M., Robinson, V.L., and Goudreau, P.N. (2000) Two-component signal transduction. *Annu Rev Biochem* **69**: 183-215.

Stout, V., and Gottesman, S. (1990) RcsB and RcsC: a two-component regulator of capsule synthesis in *Escherichia coli*. *J Bacteriol* **172**: 659-669.

Stout, V., Torres-Cabassa, A., Maurizi, M.R., Gutnick, D., and Gottesman, S. (1991) RcsA, an unstable positive regulator of capsular polysaccharide synthesis. *J Bacteriol* **173**: 1738-1747.

Szurmant, H., and Ordal, G.W. (2004) Diversity in chemotaxis mechanisms among the bacteria and archaea. *Microbiol Mol Biol Rev* **68**: 301-319.

Tabatabai, N., and Forst, S. (1995) Molecular analysis of the two-component genes, *ompR* and *envZ*, in the symbiotic bacterium *Xenorhabdus nematophilus*. *Mol Microbiol* **17**: 643-652.

Takeda, S., Fujisawa, Y., Matsubara, M., Aiba, H., and Mizuno, T. (2001) A novel feature of the multistep phosphorelay in *Escherichia coli*: a revised model of the RcsC --> YojN --> RcsB signalling pathway implicated in capsular synthesis and swarming behaviour. *Mol Microbiol* **40**: 440-450.

Tanaka, T., Saha, S.K., Tomomori, C., Ishima, R., Liu, D., Tong, K.I., Park, H., Dutta, R., Qin, L., Swindells, M.B., Yamazaki, T., Ono, A.M., Kainosho, M., Inouye, M., and Ikura, M. (1998) NMR structure of the histidine kinase domain of the *E. coli* osmosensor EnvZ. *Nature* **396**: 88-92.

Taylor, B.L., and Zhulin, I.B. (1999) PAS domains: internal sensors of oxygen, redox potential, and light. *Microbiol Mol Biol Rev* **63**: 479-506.

Tierrez, A., and Garcia-del Portillo, F. (2004) The *Salmonella* membrane protein IgaA modulates the activity of the RcsC-YojN-RcsB and PhoP-PhoQ regulons. *J Bacteriol* **186**: 7481-7489.

Tierrez, A., and Garcia-del Portillo, F. (2005) New concepts in *Salmonella* virulence: the importance of reducing the intracellular growth rate in the host. *Cell Microbiol* **7**: 901-909.

Tobe, T., Ando, H., Ishikawa, H., Abe, H., Tashiro, K., Hayashi, T., Kuhara, S., and Sugimoto, N. (2005) Dual regulatory pathways integrating the RcsC-RcsD-RcsB signalling system control enterohaemorrhagic *Escherichia coli* pathogenicity. *Mol Microbiol* **58**: 320-333.

Toguchi, A., Siano, M., Burkart, M., and Harshey, R.M. (2000) Genetics of swarming motility in *Salmonella enterica* serovar Typhimurium: critical role for lipopolysaccharide. *J Bacteriol* **182**: 6308-6321.

Tomenius, H., Pernestig, A.K., Mendez-Catala, C.F., Georgellis, D., Normark, S., and Melefors, O. (2005) Genetic and functional characterization of the *Escherichia coli* BarA-UvrY two-component system: point mutations in the HAMP linker of the BarA sensor give a dominant-negative phenotype. *J Bacteriol* **187**: 7317-7324.

Tomomori, C., Tanaka, T., Dutta, R., Park, H., Saha, S.K., Zhu, Y., Ishima, R., Liu, D., Tong, K.I., Kurokawa, H., Qian, H., Inouye, M., and Ikura, M. (1999) Solution structure of the homodimeric core domain of *Escherichia coli* histidine kinase EnvZ. *Nat Struct Biol* **6**: 729-734.

Van Houdt, R., and Michiels, C.W. (2005) Role of bacterial cell surface structures in *Escherichia coli* biofilm formation. *Res Microbiol* **156**: 626-633.

Venecia, K., and Young, G.M. (2005) Environmental regulation and virulence attributes of the Ysa type III secretion system of *Yersinia enterocolitica* biovar 1B. *Infect Immun* **73**: 5961-5977.

Vianney, A., Jubelin, G., Renault, S., Dorel, C., Lejeune, P., and Lazzaroni, J.C. (2005) *Escherichia coli tol* and *rcs* genes participate in the complex network affecting curli synthesis. *Microbiology* **151**: 2487-2497.

Virlogeux, I., Waxin, H., Ecobichon, C., Lee, J.O., and Popoff, M.Y. (1996) Characterization of the *rcsA* and *rcsB* genes from *Salmonella typhi*: *rcsB* through *tviA* is involved in regulation of Vi antigen synthesis. *J Bacteriol* **178**: 1691-1698.

Waukau, J., and Forst, S. (1999) Identification of a conserved N-terminal sequence involved in transmembrane signal transduction in EnvZ. *J Bacteriol* **181**: 5534-5538.

Wehland, M., and Bernhard, F. (2000) The RcsAB box. Characterization of a new operator essential for the regulation of exopolysaccharide biosynthesis in enteric bacteria. *J Biol Chem* **275**: 7013-7020.

White, G.F. (1927) A method for obtaining infective nematode larva from cultures. *Science* **66**: 302-303.

Whitfield, C., and Roberts, I.S. (1999) Structure, assembly and regulation of expression of capsules in Escherichia coli. *Mol Microbiol* **31**: 1307-1319.

Williams, S.B., and Stewart, V. (1999) Functional similarities among two-component sensors and methyl-accepting chemotaxis proteins suggest a role for linker region amphipathic helices in transmembrane signal transduction. *Mol Microbiol* **33**: 1093-1102.

Wolfe, A.J. (2005) The acetate switch. *Microbiol Mol Biol Rev* **69**: 12-50.

Zhang, W., and Shi, L. (2005) Distribution and evolution of multiple-step phosphorelay in prokaryotes: lateral domain recruitment involved in the formation of hybrid-type histidine kinases. *Microbiology* **151**: 2159-2173.

Zhu, Y., and Inouye, M. (2003) Analysis of the role of the EnvZ linker region in signal transduction using a chimeric Tar/EnvZ receptor protein, Tez1. *J Biol Chem* **278**: 22812-22819.